ANALYSIS AND OPTIMISATION OF PERFORMANCES OF ELECTRO DISCHARGE MACHINING OF ADVANCED ENGINEERING MATERIALS

Thesis Submitted By

SANDIP KUMAR CHAUDHURY

DOCTOR OF PHILOSOPHY (ENGINEERING)

PRODUCTION ENGINEERING DEPARTMENT
FACULTY COUNCIL OF ENGINEERING & TECHNOLOGY
JADAVPUR UNIVERSITY
KOLKATA-700 032
INDIA

2025

JADAVPUR UNIVERSITY
KOLKATA-700032

Index No. 290/18/E
Registration No. 1021816004

TITLE OF THE Ph. D. (Engg.) THESIS:

Analysis and Optimisation of Performances of Electro Discharge Machining of Advanced Engineering Materials

NAME, DESIGNATION & INSTITUTION OF THE SUPERVISORS:

Dr. BIJOY BHATTACHARYYA
Professor,
Production Engineering Department,
Jadavpur University,
Kolkata-700032, India.

Dr. BIPLAB RANJAN SARKAR
Professor,
Production Engineering Department,
Jadavpur University,
Kolkata-700032, India.

LIST OF PUBLICATIONS

International Journal:

1. Chaudhury, S.K., Sarkar, B.R., Bhattacharyya, B., Analysis and Optimisation of Performances of Electro Discharge Machining of Shape Memory Alloy (NITINOL), International Journal of Advanced Research in Engineering and Technology (IJARET), 16(3), pp. 95-110, 2025

International Conferences:

1. Chaudhury, S.K., Bhattacharyya, B., Sarkar, B. R., Upadhyay, R., Mishra, K., Electro Discharge Machining of Advanced Engineering Ceramics, Electro-Discharge Machining of Advanced Engineering Ceramics, 8th International and 29th All India Manufacturing Technology, Design and Research Conference, December 9 to 11, 2021
2. Chaudhury, S.K., Sarkar, B.R., Bhattacharyya, B., Faiyazuddin, M., Majumdar, S., Electro Discharge Machining of Shape Memory Alloy Material (NiTinol), 5th International Conference on Current Trends in Materials Science and Engineering, February 28 to March 1, 2025 (Scopus)

Book Chapter:

1. Chaudhury, S.K., Bhattacharyya, B., Sarkar, B. R., Upadhyay, R., Mishra, K., Electro Discharge Machining of Advanced Engineering Ceramics, Electro-Discharge Machining of Advanced Engineering Ceramics, Lecture Notes in Mechanical Engineering, Springer Nature Singapore Pte Ltd, PartF54, pp. 39-49, 2023 (Scopus)

PROFORMA-1

"Statement of Originality"

I, Sri Sandip Kumar Chaudhury registered on 28th May, 2018 do hereby declare that this thesis entitled "**ANALYSIS AND OPTIMISATION OF PERFORMANCES OF ELECTRO DISCHARGE MACHINING OF ADVANCED ENGINEERING MATERIALS**" contains literature survey and original research work done by the undersigned candidate as part of Doctoral studies.

All information in this thesis have been obtained and presented in accordance with existing academic rules and ethical conduct. I declare that, as required by these rules and conduct, I have fully cited and referred all materials and results that are not original to this work.

I also declare that I have checked this thesis as per the "Policy on Anti Plagiarism, Jadavpur University, 2019", and the level of similarity as checked by iThenticate software is 10%

Signature of Candidate:

Date:

Certified by Supervisor(s):

(Signature with date, seal)

Ex-Professor
Production Engineering Department
Jadavpur University
Kolkata - 700 032

Professor
Production Engineering Department
Jadavpur University
Kolkata - 700 032

JADAVPUR UNIVERSITY

FACULTY OF ENGINEERING AND TECHNOLOGY
DEPARTMENT OF PRODUCTION ENGINEERING

CERTIFICATE FROM THE SUPERVISORS

This is to certify that the thesis entitled **"ANALYSIS AND OPTIMISATION OF PERFORMANCES OF ELECTRO DISCHARGE MACHINING OF ADVANCED ENGINEERING MATERIALS"** *submitted by Sri Sandip Kumar Chaudhury, who got his name registered on 28th May, 2018 for the award of Ph.D. (Engg.) degree of Jadavpur University is absolutely based upon his own work under the supervision of Prof. Bijoy Bhattacharyya and Prof. Biplab Ranjan Sarkar and that neither his thesis nor any part of the thesis has been submitted for any degree/ diploma or any other academic award anywhere before.*

(Signature of the Supervisor
with date and official seal)
Ex-Professor
Production Engineering Department
Jadavpur University
Kolkata - 700 032

(Signature of the Supervisor
with date and official seal)
Professor
Production Engineering Department
Jadavpur University
Kolkata - 700 032

PREFACE

Machining of difficult-to-machine materials such as ceramics, various alloys of metals poses a new challenge in different fields. The ceramics are used in machine tool, aerospace, automotive, electrical and electronics sectors. Conventional machining processes like turning, milling grinding does not hold good to machine those difficult to machine materials.

Electro-discharge machining (EDM) process has been widely explored in various research domains, its application for machining on electrically non-conducting materials remains limited. There is a strong need of in-depth studies and experimental investigations into the process, particularly focusing on electro-discharge drilling of different advanced engineering materials. Significant research efforts and technical advancements are required to enhance this technology, widely accepted in modern manufacturing industries for machining of advanced engineering materials.

To accomplish machining problems during machining of advanced engineering materials, the objectives of the present investigation are given as below:

(i) To study the feasibility of machining electrically non-conducting materials such as ceramic materials by electro-discharge machining (EDM) process.

(ii) To study the influences of various process parameters such as peak-current, pulse on-time and flushing pressure etc. on material removal rate (MRR), tool wear rate (TWR) and overcut (OC) during machining of ceramic i.e. Alumina (Al_2O_3) by electro-discharge machining process.

(iii) To analyse the influences of input process parameters such as polarity, peak current, pulse on-time, spark time etc. on MRR and Taper angle during drilling on shape memory alloy such as Nitinol by electro-discharge machining (EDM) process based on Taguchi method.

(iv) To develop mathematical models to correlate various process parameters to different performance characteristics e.g. MRR and overcut during drilling on shape memory alloy such as Nitinol based on response surface methodology (RSM).

(v) To analyse the influences of many process parameters such as gap voltage, peak current, pulse on-time etc. on MRR, overcut based on the developed models during drilling on Nitinol by electro-discharge machining (EDM) process.

(vi) To search out the optimal machining conditions of EDM process for maximum MRR and minimum TWR and overcut during drilling operation on Alumina using multi-criteria decision methods (MCDM).

(vii) To find out the optimal parametric combinations of EDM process for maximum MRR and minimum taper angle during drilling operation on Nitinol based on Taguchi method as well as to search out the optimal machining conditions of EDM process for maximum MRR and minimum overcut during drilling operation on Nitinol based on the developed models by using distance optimality technique of RSM.

In-depth studies on electro-discharge machining of Alumina and NiTinol have been done in this present research work with assisted electrode and different design of experiments. The main emphasis is given to observe and analyze the effects of various process variables on machining characteristics during EDMing of Alumina and NiTinol and to find out the optimum parametric condition to achieve the desired machining characteristics.

The thesis is systematically divided into six chapters, with a brief summary of each chapter given below:

Chapter 1 provides an overview of electro-discharge machining processes, highlighting the various non-conventional machining processes. It outlines the applications of these technologies in various engineering fields and discusses both the mechanisms of material removal and limitations. Additionally, this chapter includes a literature review of previous research in the field, covering recent developments in EDM for machining of ceramics and other advanced engineering materials. The chapter also outlines different major research gap and objectives of the present investigation.

Chapter 2 focuses on fundamental characteristics of EDM process and material removal mechanism. It discusses different process parameters, machining performances and electrical circuits being used in EDM process.

Chapter 3 highlights the experimental setup EDM setup along with various subsystems. It highlights about the power supply and specifications of the experimental setup.

Chapter 4 discusses the investigation on the performances of EDM process during machining of electrically non-conducting ceramic materials such as Alumina (Al_2O_3). It highlights the mechanism of material removal when Alumina is machined with the help of assisted electrode method. It also includes the analyses of experimental result based on one factor at a time (OFAT) and the effects of different process parameters such as peak-current, gap-voltage, pulse-on time and flushing pressure on various machining criteria e.g. material removal rate

(MRR), tool wear rate (TWR) and overcut (OC). Further this chapter explores the optimal parametric combination for obtaining maximum MRR and minimum OC and TWR with the use of different multi-criteria decision making (MCDM) techniques such as MOOORA, SAW, TOPSIS etc.

Chapter 5 represents the experimentation on shape memory alloy (SMA) i.e. NiTinol for finding out the influence of various parameters based on two design of experiments (DOEs) i.e. Taguchi method and Response Surface Methodology (RSM). The first section of this chapter documents the effects of various process parameters on different machining characteristics such as MRR and taper angle and also the suitable parametric combination for obtaining maximum MRR and minimum taper angle. This section analyses ANOVA test results to find out the significant process parameters. Next section of this chapter includes the experimentation on NiTinol based on RSM. It discusses the effects of process parameters on MRR and overcut as well as the development of mathematical models in order to correlate the process parameters to machining criteria. This section also highlights the ANOVA test results, which is carried out to justify the goodness of development of mathematical models and explores the parametric combination for yielding optimal machining criteria during machining on NiTinol by EDM process.

Chapter 6 presents the general conclusions drawn based on the results and discussions derived from various experiments conducted throughout the investigation. It provides a comprehensive overview of the main findings and emphasizing how various process parameters affect the machining performance during machining of advanced engineering materials such as electrically non-conducting ceramic material i.e. Alumina and shape memory alloy NiTinol. Finally, suggestions for future scopes of research work are also included in this chapter.

It is anticipated that the current study's findings will provide fresh perspectives on process performance analysis for the efficient application of the electro-discharge machining (EDM) technique for cutting sophisticated engineering materials. Through a variety of experimental studies utilising several DOEs, including OFAT, Taguchi method, and RSM, the author has attempted to support the originality of the current research work. The author also attempts to examine how several machining parameters, such as polarity, peak current, pulse on-time, gap voltage, spark time, and dielectric flushi pressure, affect the EDM process while machining alumina and NiTinol. It is anticipated that the current research will give applied researchers

and manufacturers a better understanding of the various aspects of the electro-discharge machining (EDM) process. It will also give them guidance on how to choose the best parametric setting to achieve the goal of minimising overcut and maximising material removal when electro-discharge machining advanced engineering materials.

ACKNOWLEDGEMENT

The acknowledgement is an attempt to express feelings of gratitude towards people who were helpful to me in successfully completing my research work.

I owe deepest debt of gratitude to my joint-guides Ex-Professor Dr. Bijoy Bhattacharyya and Professor Dr. Biplab Ranjan Sarkar, Dept. of Production Engineering, Jadavpur University for their invaluable and untiring guidance, encouragement and supervision throughout this thesis work. Their effective skill, knowledge and experience have made it possible for me to successfully complete this thesis work within stipulated time. I am very much indebted to both of them and express my sincere gratitude to both of them.

My special thanks to Head of Production Engineering Department, for allowing me to carry out the research investigation with various facilities of the department. I would acknowledge the support received from Prof. Dr. Biswanath Doloi and would like to thank all the respected faculty members and non-teaching staff members of this department who directly or indirectly helped and encouraged me during this thesis work.

I am indebted to Institute of Engineering and Management, Founder President Late Dr. Satyajit Chakraborty, Madam Banani Chakraborty for their blessings and Director, Prof Dr. Satyajit Chakraborty to support me with constant encouragement to carry out the research work. I am grateful to all my colleagues in IEM, who have constantly encouraged me to complete the thesis work.

I would like to express my sincere thank specially to Mr. Sudip Santra for his immense help and also to Mr. Rohit Upadhyay, to carry out experiments with me. I would like to thank my dear students Mr.Md.Faiyazuddin, and Mr. Spandan Majumder of IEM, for helping me to carry out the experiments with me.

I am indebted to Mr. Apurba Mitra, Ms. Parshati Chaudhury and Mr. Tathagata Chattterjee, who helped me in all possible way to complete the thesis.

I am grateful to all my relatives and well-wishers to encourage me in every way to complete the research work.

Sandip Kumar Chaudhury

VITA

The author, Mr. Sandip Kumar Chaudhury, son of Late Nirmal Kumar Chaudhury and Late Suchitra Chaudhury, born on 20th February,1961 at Kolkata, West Bengal, India. He passed his Secondary Examination under West Bengal Board of Secondary Education in 1976 with First Division. Then he passed his Higher Secondary Examination in 1978 with First Division. He passed Bachelor of Production Engineering in 1982 with First Class (Hons.). Then he joined General Electric Co of India Ltd. From 1982 to 1986 (4.5 years) as Tooling Engineer. While in service he joined Jadavpur University in 1983 as a sponsored candidate and used to study in day time and worked in Evening or Night shifts. He passed Master of Production Engineering in 1985 with Gold medal for standing First in order of merit. He worked in Philips India Ltd from 1987 to 1989 (2.5 years) as Planning Officer in PMF Unit at Kolkata. He joined next in Siemens Ltd, Joka Works, Kolkata as Production Engineer (Quality Control) and used to design of Inspection Fixture etc.(1.5 years). In 1990, he got the opportunity to join Research & Development, as Deputy Manager in Mcnally Bharat Engineering Co.Ltd., Kumardhubi Works. He was involved in Product development activities like Crushers, Ball Mills, Vibrating Screens, Conveyors for material handling plants etc. He was promoted to the position of Manager and Sr. Manager (R&D) as he worked till 2000.(9.5 years).

In the year 2000 he changed his job and Joined in International Combustion (I) Ltd as Asst.General Manager Design in Kolkata and served till 2007 (7.5 years). He rejoined Mcnally Bharat Engineering Co Ltd as Deputy General Manager Projects and worked for 1.5 years till 2009. He served TIL Ltd, as Head, Design, Crushing and Screening and worked closely with foreign collaborators there (4.5 years). He joined M N Dastur & Co and worked in Material Handling Department as Addl.Chief Engineer till 2015.(1.5 years) He joined in Academics and presently he works as Assistant Professor Mechanical Engineering in Institute of Engineering & Management, Saltlake, Kolkata, from 2015.(9.5 years). He has written a Journal paper and two nos. International conference papers on his research work. One no conference paper is published in Book chapter also. He was awarded Best Oral Presentation in 5TH International Conference on Current Trends in Materials Science and Engineering.

I would like to dedicate my thesis to my mother Late Suchitra Chaudhury, whose blessings has helped me to complete the research work.

I am grateful to my wife Ms. Paramita Chaudhury, whose whole hearted support and understanding has encouraged me to complete the thesis work.

LIST OF THE FIGURES

LIST OF THE TABLES

Table of Contents

1. Introduction

1.1. Non-Conventional Machining Processes: An overview

In order to machine extremely hard materials that are nearly impossible to machine profitably using traditional methods, non-conventional machining techniques were first developed. In a traditional machining process, the material removal process begins when the cutting tool stresses the material past its yield point. For this to happen, the cutting tool's material must be harder than the work piece's. It is challenging to machine new materials with high strength to weight ratios, heat resistance, and hardness using the conventional method. Examples of these materials include Nimonic alloys and alloys containing alloying elements like tungsten, molybdenum, and columbium. These materials are very difficult and time-consuming to machine using the traditional method because the rate of material removal decreases as the amount of work increases, material hardness increases. Hence there is the need for development of non-conventional machining processes which utilizes other methods such as electro-discharge processes for the material removal. As a result, these processes are termed as Unconventional or non-conventional machining methods. Applications of the non-conventional machining processes are as follows:

Complex shapes which are difficult to machine by traditional methods and time consuming.

i) Besides complexity of the surface, high accuracy to be desired.

ii) For hard and brittle materials.

However, the non-conventional machining processes depend on the number of other factors such as the vaporization of the metal, electrolytic displacement, chemical reactions and mechanical erosion. Non –Conventional Machining Processes are used for 1. High Strength Alloys. 2. Complex Surfaces. 3. Higher accuracy and Surface Finish. 4. Difficult Geometries. 5. Automation

1.2. Various Non-Conventional Machining Processes

Non-conventional machining processes can be classified as per Energy types, mechanics of material removal, energy sources and process as follows

Table 1.1 Non-conventional machining processes

Energy type	Mechanics of material removal	Energy source	Process
Electrochemical	Ion displacement	Electric current	Electrochemical machining (ECM)
Mechanical	Plastic shear	Mechanical motion of tool/ job	Conventional machining
	Erosion	Mechanical/fluid motion	Abrasive jet machining (AJM)
			Ultrasonic machining (USM)
Chemical	Fusion and vaporization	Electric spark	Electric discharge machining
		High speed electrons	Electron beam machining (EBM)
	Corrosive reaction	Corrosive agent	Chemical machining (CHM)
Thermal		Powerful radiation	Laser beam machining (LBM)
		Ionized substance	Ion beam machining (IBM)
			Plasma arc machining (PAM)

1.2.1. Electro-Chemical Machining (ECM)

ECM uses electrochemical reactions to remove metal from a workpiece. The workpiece and the tools are connected to positive and negative terminals respectively. While designing an Electro-Chemical machining few important points to be taken care. These consist of the components' substance and rigidity. The high pressure of the electrolyte needed to maintain an adequate flow velocity through the narrow gap may cause very large forces to develop between the tool and workpiece surface, even though at first glance it seems like the machining force is

minimal because there is no physical contact between them. Therefore, the machine needs to be sufficiently robust to prevent any considerable tool deflection that could compromise the accuracy of the parts being machined. The design should account for the possibility of relative movement between the tool and the workpiece due to temperature changes.

1.2.2. Abrasive Jet Machining (AJM)

High-velocity abrasive particles are designed to strike the work material during Abrasive Jet Machining (AJM). The abrasive particle jet is transported by air or a carrier gas. A high velocity abrasive jet is produced when the air or carrier gas's pressure energy is transformed into its kinetic energy. A controlled nozzle allows the abrasive jet to be directed onto the work material, allowing for the desired impingement angle and distance between the nozzle and the work piece. Through brittle fracture of the work material and micro-cutting action, high velocity abrasive particles remove the substance.

Process physics:

(i) A gas stream accelerates fine particles (0.025 mm) and

(ii) directs the particles towards the machining focus.

(iii) The particles' impact on the surface results in a microfracture, and the gas transports the broken particles away.

(iv) Fragile and brittle materials function better.

In AJM, compressed air is used as the carrier gas after being compressed in an air compressor at a pressure of around 5 bar. N2 and CO2 are examples of gases that can be employed. In most cases, oxygen is not employed as a carrier gas. The desired operating pressure is initially achieved by passing carrier gas via a pressure regulator. After that, the gas is sent through an air dryer to eliminate any remaining water vapour. The mixture is sent through a number of filters to eliminate any oil vapour or particle matter. After that, the carrier gas moves inside the mixing chamber, a closed space. A metallic sieve allows abrasive particles from a hopper to enter the chamber. An electromagnetic shaker vibrates the sieve continuously. Through an electro-magnetic on-off valve, the carrier gas subsequently transports the abrasive particles to the machining chamber. Abrasive particles with a high velocity of 200 m/s are ejected from the nozzle onto a workpiece that is passing beneath the jet to complete the machining process.

1.2.3. Electron Beam Machining (EBM)

Electron Beam Machining (EBM) is a non-contact machining process that uses a high-velocity beam of electrons to cut and shape materials precisely. It stands at the forefront of precision manufacturing technologies, offering a remarkable capability to shape and cut materials with extraordinary accuracy and precision and minimal thermal impact. This non-contact, non-thermal machining process has found applications in aerospace, medical device manufacturing, microelectronics, and other fields where extreme precision is paramount.

1.2.4. Laser Beam Machining (LBM)

The machining technique known as laser beam machining (LBM) employs the heat energy of a laser beam to remove material from a surface without making contact. LBM is a precise and powerful tool that can be used to cut, drill, engrave, and more. It's often used in the automotive and electronic industries.

1.2.5. Ultrasonic Machining (USM)

Ultrasonic machining is a subtractive manufacturing process that removes material from a part's surface by vibrating a tool at a high frequency and low amplitude on the material surface when there are tiny abrasive particles present. The tool moves at amplitudes of 0.05 to 0.125 mm (0.002 to 0.005 in.) either vertically or orthogonally to the part's surface. The part and the tip of the tool are coated with a slurry made from fine abrasive grains and water. The abrasive material's grain sizes typically fall between 100 and 1000, with smoother surface finishes being produced by smaller grains (higher grain number). The micro-cracking mechanics of ultrasonic vibration machining make it suitable for both high-hardness and brittle materials. An electroacoustic transducer and a sonotrode, which are connected by cable to an electronic control unit, are the two main parts of an ultrasonically vibrating machine. Now striking the work piece hundreds of times per second, the abrasive grains in the slurry function as a free cutting tool. An alternating current oscillating at a high frequency, typically in the ultrasonic range of 18 to 40 kHz, is produced by an electronic oscillator in the control unit. A mechanical vibration is produced from the oscillating current by the transducer. Both piezoelectric and magnetostrictive transducers have been employed in ultrasonic machining.

1.2.6. Wire Electrical Discharge Machining (WEDM)

One of the EDM process's variations is wire electrical discharge machining, or wire WEDM. The cutting tool in the Wire EDM process is a wire. In order to create complex geometries on

advanced materials, wire is now utilized. Better dimensional accuracy, an extremely fine surface quality, and components with complex shapes are all produced using it. Very tiny corner radii can be achieved with a wire diameter as small as 0.05 to 0.30 mm. Unlike the conventional methods outlined by Ulutan et al. and Majumder et al., the Wire EDM process eliminates contact between the workpiece material and the cutting tool, improving machinability.

A submerged tank of dielectric fluid is typically used for the advanced machining technique known as wire EDM. The machining tool electrode, which is an electrically conducting wire. This results in a smooth surface that doesn't require Aix-en-Provence. The method is thermoelectrical, and the tool electrode is a wire. A vertical wire under tension is attached to wire supply wheels, and the wire's guides regulate its movement numerically to give the workpiece the desired shape. The wire travels downward vertically and has a very small diameter.

A computer numerical control machine governs the entire process, and the table travels horizontally. Because of the voltage differential, sparks are created as the wire moves through the work piece. In order to aid remove the eroded particles, dielectric fluid is applied through jet at the machining zone through nozzles on both sides of the workpiece. Figure 1.1 depicts the Wire EDM process in action.

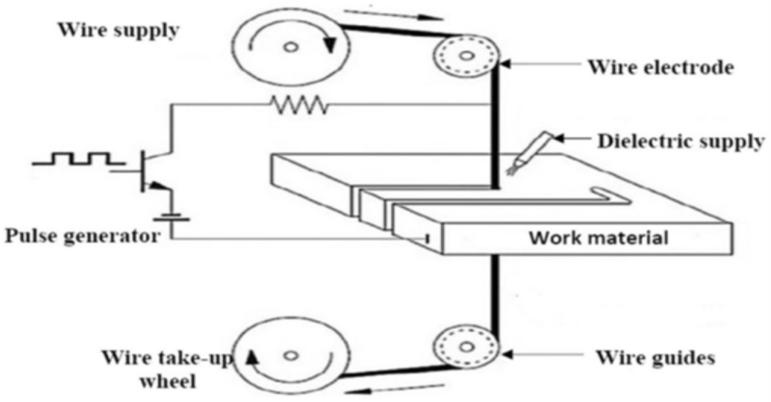

Fig.1.1 Schematic diagram of Wire EDM process

A wire EDM process has a number of different process parameters. For the wire EDM process to be more productive, certain factors must be managed during machining.

1.2.7. Electrical Discharge Machining (EDM)

EDM is a thermal method that removes material by means of a sequence of electrical discharges between an electrode and a workpiece immersed in a dielectric fluid. A localised plasma channel is ionised by each discharge, and the temperature there can rise to 10,000C, which causes the metal of both facing materials to fuse and ebulliated. A bubble is produced, with a pressure that can reach hundreds of bars. Small solid particles are created when some of the melted metal is released from the workpiece as a result of an extremely quick heat exchange with the surrounding dielectric fluid. A portion of the molten material remains and hardens, leaving distinctive traces along the crater's border.

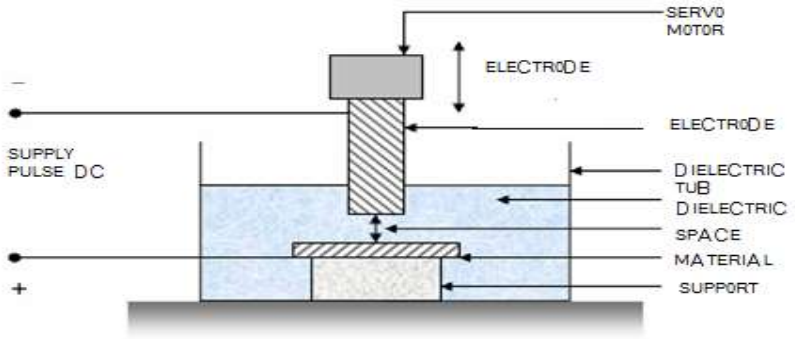

Fig.1.2. Electro-Discharge Machining schematics

The process's performance is highly dependent on the discharge energy; raising it results in larger craters and a greater feed speed, which in turn causes a rougher surface. When a relatively tiny distance between electrodes is necessary for the discharges to occur due to the lesser energy required, finishing activities face significant challenges. In the event of a very poor fluid renewal, where debris builds up in some areas, the extremely tiny matching gap can result in arcing and limit the debris evacuation. Very complex jobs may experience the same issues: poor debris evacuation may result from big frontal surface area cutting or deep hole drilling.

The workpiece's metallurgical properties are significantly impacted by the thermal way the process is combined with, with the high temperature discharges causing the surface structure changes. according to numerous research papers on the topic. Three layers are visible in the entire impacted area when carbon machining is used: The white layer, whose solidification was accelerated and which has a carbon enrichment, is highly asymmetrical and dotted with

microcracks as a result of the contraction-extension phenomenon that occurs during the metal's harsh solidification.

The temperature of the tempered layer, where the metal has not melted but has been sufficiently heated to surpass the austenitic transition temperature in a brief period of time before dropping suddenly, is what causes temper. The reheated layer serves as a transition between the metal base and the tempered layer.

The entire affected zone exhibits depth-dependent hardness changes, thermal residual stresses, and specifically microcracks, which are to blame for the reduced fatigue life; the maximum allowable stress is frequently 60% lower than following a normal operation. Because EDM does not require direct contact between the tool and the workpiece, it is a viable option for materials that are prone to deformation.

1.3. Applications of EDM in Industry

EDM can be used to machine any material (tough, hard, brittle, exotic, etc.) provided it is electrically conductive. Thus, the industrial application of EDM is enormous.

It is currently widely utilized in the die casting, mold-making, automotive, and aerospace industries. It is used for making through cavities, and miniature holes. EDM is also used in the manufacturing of components for plastic injection moulding machine. EDM can also be used for making moulding dies, casting dies, forging dies, stamping dies, coining and forming dies, etc. Dies for extrusion, wire drawing, which require through holes can also be manufactured by EDM. It is better for producing fragile features (micro-sized slots), perforations, and orifices as small as 50 um. The machining time has decreased to 50% or less in the production of intricately formed dies. Compared to dies manufactured using traditional techniques, dies that are EDM machined have a longer lifespan and are free of burrs. It enables the use of long-lasting die materials, such as exotic materials and carbide-hardened steel. The matte finish produced by EDM dies reduces the amount of time needed for final polishing.

Today EDM is widely used in the manufacturing of engine components, such as compressor blades made from titanium alloys and nickel-based super-alloys. One of the most common applications of EDM is the removal of broken taps, drills, studs, reamers, pins, etc.

EDM operations are widely used in die sinking, scanning/milling with a simple electrode and wire cutting, etc.

1.4. Literature Survey of the Past Research Works

EDM has a number of issues, some of which were covered in the preceding chapter. Many manufacturing engineers and academics are working to find solutions to these issues so that EDM technologies can be effectively applied in contemporary manufacturing sectors. However, the mechanism of material removal and the impact of different EDM process parameters remain unknown. Thus, more research is required to increase the precision and compactness of EDM in order to fully utilize its potential in the manufacturing sector. A review of previous studies conducted by various engineers and researchers has been recorded as follows:

Sabur *et al.* [1] found that machining non-conductive ceramic materials was challenging and that most unusual techniques were inapplicable because of their high brittleness. The purpose of this study was to examine the material removal mechanism and the impact of input power on the material removal rate (MRR) through experiments. Nonconductive ceramic ZrO2 was processed utilising the electro discharge machining (EDM) technique, a noncontact machining method, with an auxiliary electrode. The pyrolytic carbon layer that was created on the ceramic surface by the carbonic dielectric's cracked carbon was essential to this method's continuous EDM. The workpiece material, tool electrode material, dielectric substance, polarity, discharge time, and input power all affected the stability and production of pyrolytic carbon.

Lee T.C. and Lau W.S. [2] examined the mechanics underlying the EDM machining of conductive composite ceramic. It was also correlated the different properties with this removal process. Initially, a significantly greater amount of energy was needed to overcome the high electrical resistance and melt and evaporate the material with a high melting temperature. Second, due to their low thermal conductivity, these materials primarily failed under heat stress. Finally, the high electrical resistance of the material limited the pulse frequency. Further research revealed that other mechanisms, such as thermal spalling, were involved in the material removal process in ceramics in addition to the melting and evaporation that occurred in the case of conductive materials.

Second, due to their low thermal conductivity, these materials primarily failed under heat stress. Finally, the high electrical resistance of the material limited the pulse frequency. Further research revealed that other mechanisms, such as thermal spalling, were involved in the

material removal process in ceramics in addition to the melting and evaporation that occurred in the case of conductive materials.

Mohri *et al.* [3] found that the assisting electrode method makes it simple to machine insulating ceramics. The innovative EDM machining technique for insulating ceramics was the subject of the paper. As an auxiliary electrode, a metal plate or metal mesh was placed on the ceramic insulator's surface in this technique. It is quite easy to mill the ceramics using a copper electrode or a brass wire electrode in in sinking EDM and WEDM respectively using kerosene as the working fluid. On the ceramics' surface, electrically conductive compounds including fractured carbon from working oil were produced. It kept the work piece's surface electrically conductive throughout the milling process. Examples of products that were machined using this technique were shown. The process of machining insulating ceramics was examined using the idea behind the EDM surface modification technique, which was created recently.

Schubert *et al.* [4] studied the various applications in industry of ceramic materials, which is attributed because of their excellent mechanical and physical properties. It was stated that there was a demand for alternative machining process of ceramics. Micro electrical discharge machining, or micro-EDM, is a thermal abrasion method that depends on electrical discharges between the tool and the workpiece. The advantages of micro-EDM were the focus of ceramic machining. The non-contact nature of the technology, its independence from material hardness and brittleness, its little impact on materials, and its achievable microstructure were among these advantages. Therefore, the present state of ceramic micro-EDM research was examined in this paper. The techniques used to machine and insulate ceramics were also described, in addition to the EDM process principle. Furthermore, several examples were shown to explore the possibilities of micro-EDM in connection with ceramic machining.

Abbas *et al.* [5] examined current developments in dry EDM machining, EDM with powder additives, EDM in water, electrical discharge machining by ultrasonic vibration, and modelling approaches for predicting EDM performance.

Research trends in EDM were reviewed, including modelling techniques for forecasting EDM performances, dry EDM machining, EDM with powder additives, EDM in water, and ultrasonic vibration. Methods progress during the past 25 years has been covered in each topic. Charts were used to show the development progress in each section. For a safe and comfortable working environment, EDM in water was established; EDM with powder additives

concentrated more on employing dielectric oil to increase SQ, MRR, and tool wear. The ultrasonic vibration method was suitable for dry and micromachining, and EDM modelling was applied to forecast the output parameters, resulting in the creation of precise and accurate EDM performance. The goals of every technique that was introduced and used in the EDM process were the same, e.g. to improve working conditions, to develop new techniques for cutting materials, to improve output quality, and to increase machining performance.

Hanaoka *et al.* [6] performed die sinking EDM on three ZrO_2- Y_2O_3 ceramics containing varying amounts of Al_2O_3. To examine how varying amounts of additives affected the machining characteristics of ZrO_2-Y_2O_3 insulating ceramics, three varieties of insulating ZrO_2 ceramics were sintered and machined by sinking EDM.
Estimates were made of the electrode's wear ratio, surface roughness, and material removal rate. The setup discharge current, the amount of Al_2O_3 additive, and the optimal electrode polarity were investigated as experimental parameters. Using SEM observation, the electrically conductive layer adhesion condition was noted.

Petrofes and Gadalla [7] examined how reducing recast layer hardness and increasing material removal rate (MRR) are important considerations when employing micro-electro discharge machining (micro-EDM) to machine non-conductive ceramic. This study's two primary components were the examination of MRR and hardness of recast layer and process development. Process development identifies the proper use of the tool electrode rotational speed, polarity, feed rate, gap-voltage, flushing, and assisting electrode (AE).
Copper adhesive as the AE, positive work-piece polarity, a feed rate of 3 μm/s, and a work-piece immersed in a dielectric fluid with one-way circulation showed the best machinability of ZrO_2. MRR and recast layer hardness were estimated using empirical methods. At a rotational speed of 370 rpm and a gap voltage of 80 volts, the ideal values for highest MRR and minimal recast layer hardness were discovered.

Mohri *et al.* [8] found in research that thermal abrasion procedure known as micro-electrical discharge machining (micro-EDM) is due to electrical discharges between a tool and a workpiece, The benefits of micro-EDM for ceramic machining are becoming increasingly apparent. These benefits include the noncontact technology method, the ability to achieve microstructures, the independence of material brittleness and hardness, and the little influence on the material. In this work, the current status of research on ceramic micro-EDM was

described. In addition to the EDM process theory, the methods used for ceramic machining and ceramic insulation were explained. To further illustrate the potential of the micro-EDM technique for ceramic machining, a number of machining examples were provided.

Kalajahi *et al.* [9] observed the shape and size of the heated zone (Gaussian heat distribution), temperature-dependent material properties, energy distribution factor, plasma flushing efficiency and phase change are some of the crucial factors that were taken into consideration when developing a thermal modelling and finite element simulation of electrical discharge machining (EDM) in order to predict thermal behaviour and material removal mechanism in the EDM process. Using the ANSYS finite element code, the temperature distribution on the cathode was computed, and the impact of the EDM settings on the heat distribution along the work piece's depth and radius was determined. In order to determine the theoretical material removal rate (MRR) from the cathode, temperature profiles were employed. For AISI H13 tool steel, the amount of energy that entered the cathode could be precisely determined by comparing theoretically derived MRRs with the experimental findings. This study also examined the impact of EDM parameters on MRR through the use of response surface approach and experimental design. The accuracy of the quadratic polynomial regression model that was ultimately suggested for MRR was verified by residual analysis.

Mohri *et al.* [10] found that most typical machining processes are inapplicable due to the extreme brittleness of nonconductive ceramic materials, and that machining operations for building structures from these materials are challenging. The noncontact machining method known as electro discharge machining (EDM) is used to treat nonconductive ceramics with the aid of an assisting electrode. Continuous EDM in this method is largely dependent on the pyrolytic carbon layer that is created on the ceramic surface by the carbonic dielectric's fractured carbon. The work-piece material, tool electrode material, dielectric substance, polarity, discharge time, and input power all affect the stability and production of pyrolytic carbon. This study used experiments to examine the material removal mechanism and the impact of input power on the material removal rate (MRR).

Vishwakarma *et al.* [11] demonstrated the experimental findings that the majority of the material is removed by spalling in EDM of nonconductive ceramic, and that this removal rises as input increases. Al6063/ SiC composites were electrically discharge machined using FEA

modelling of material loss rate, as reported by]. Using an axisymmetric model of Al-SiC composite, material removal rate (MRR) modelling has been performed during electrical discharge machining (EDM). A single spark EDM FEA model was created in order to determine the temperature distribution. To further replicate the second discharge, the single spark model was expanded. Material removal for multi-discharge machining was computed by counting the number of pulses. The experimental findings obtained under the same process settings were compared with the analytical results in order to validate the model.

Ho and Newman [12] found out in research that electrical discharge machining (EDM) is a proven machining technique for producing hard-material or geometrically complex parts that are very challenging for traditional machining techniques to produce. The research conducted over the last ten years, from the beginning to the invention of die-sinking EDM, was reviewed in the study. It provided information on EDM research on how to monitor and regulate the sparking process, optimize process variables, improve performance metrics, and streamline electrode design and manufacturing. The development of hybrid machining methods was emphasized along with a variety of EDM applications. The paper's conclusion covered these advancements and provided an overview of the directions for further EDM research

Lauwers *et al.* [13] examined the performance of milling EDM in comparison to traditional sinking EDM in order to determine the manufacturability of B4C, SiC, and Si3N4-TiN. It was demonstrated that even when cutting ceramic materials with relatively low electrical conductivity (B4C, SiC), milling EDM works effectively because of the favourable flushing circumstances. A novel approach to the machining of intricate 3D structures in ceramic material was created since the employed milling EDM technology removed material layer by layer (2D-machining). It included one or more finishing sinking EDM stages after an EDM pre-machining milling step. The created technique was compared to a pure sinking EDM strategy and validated on an industrial application. Over fifty percent of the time was saved.

Schubert and Zeidler [14] looked at whether micro-EDM could be used to machine nonconductive ceramics. Micro-EDM drilling was used for the tests, together with ZrO_2 ceramic workpieces and tungsten carbide tool electrodes. The EDM process was initiated by creating a closed electric circuit with a beginning layer, which is commonly referred to as a "assisting electrode" in literature. Once the initial layer was machined, the process environment could be controlled to maintain a steady EDM process by combining a carbon hydride-based

dielectric with a specifically created low-frequency vibration setup to stimulate the workpiece. ZrO_2 workpieces stabilized with Y_2O_3 and MgO were employed, together with a tungsten carbide tool electrode. In order to compare the features of the discharges in metallic material with those in the starting layer, base material, and transition stages of the process, the current and voltage signals of the discharges were recorded. Monitoring of the electrode feed was also done. In relation to the discharge type, electrode wear, and process speed, the effects of the process parameters were examined.

Fukuzawa *et al.* [15] looked into the use of wire cut electrical discharge machining (EDM) and sinking in the processing of the insulating ceramics. The new technology was designated as the helping electrode method. The electrical discharge began when the electrically conductive substance was affixed to the insulating workpiece's surface during the milling process. Because the processing was done in oil, the electrically conductive result, which was made of working oil's breakdown carbon element, stuck to the workpiece when it was discharged. As the electrically conductive layer formed, discharges were continuously produced. The insulating ceramics then switch to the EDM-machinable material. They described how to machine insulating ceramics like Si_3N_4 and ZrO_2, as well as their use.

Pandey and Singh [16], in order to investigate EDM, initiated quick, recurring spark discharges between the tool and workpiece, which were spaced apart by a very small distance of around 0.01 to 0.50 mm. This process made it possible to carefully erode materials that conduct electricity. Either flooding or a dielectric fluid was used to fill this gap. Managed direct current pulsing between the tool and the work piece produced the spark discharge. The EDM method as it exists today is the outcome of numerous studies conducted throughout the years. EDM researchers used a variety of experimental concepts to investigate several approaches to increase the sparking efficiency. Every new study had the same goals, despite a variety of alternative strategies: to achieve a high metal removal rate while reducing tool wear and improving surface quality. This study examined the wide range of studies conducted in recent decades to advance EDM. The primary focus of this study was on surface quality and metal removal rate, which are the most crucial factors for choosing the best process conditions and considering economic considerations.

Chandramouli *et al.* [17] found in research that MRR, TWR, and SR are significantly impacted by current, pulse on time, and pulse off time. The MRR increased as current

increased, decreased at first as pulse on time increased, and then increased again as pulse on time increased. When pulse off time increased, MRR increased as well, although the rise was less pronounced than when pulse on time increased. As the current increased, TWR increased linearly. As pulse on time increased, the TWR decreased; conversely, as pulse off time increased, the TWR increased. When current and pulse on time increased, the SR increased; however, when pulse off time increased, the SR decreased.

Rajmohan *et al.* [18] investigated using the Taguchi technique, how electrical discharge machining factors, including pulse on time, pulse off time, voltage, and current, affected MRR in 304 stainless steels. It was discovered that in order to attain increased MRR, distinct groupings of EDM process parameters were necessary. The most important machining parameters for MRR were the current and pulse off time. Additionally, it was noted that the best cutting parameters were determined by conducting a minimum number of trials. The Taguchi method appears to be a successful process for determining the ideal cutting parameters.

Darji *et al.* [19] using the Taguchi methodology, investigated the machining properties of Hastelloy C276 with a 0.5 mm graphite rod as electrode by conducting tests and research for altering machining parameters such as polarity, peak current, electrode rotational speed, and pulse on time. Using the signal to noise ratio and ANOVA, significant machining parameters for MRR were found. The maximum material removal rate (MRR) was achieved at negative polarity, the material removal rate was lower at 50 rpm, and it increased as the electrode's rotational speed increased because of the higher centrifugal force and the ease with which the wreckage detached. Similarly, MRR increased to a higher value peak current of 2 A after being low at a low peak current of 0.3 A.

Yadav *et al.* [20] looked into how electrical discharge machining (EDM) produced strong temperature gradients at the gap, which led to significant localized thermal stresses in a tiny heat-affected zone. Microcracks, a reduction in strength and fatigue life, and even catastrophic failure could result from these thermal stresses. To estimate the temperature field and thermal strains caused by a spark's Gaussian distributed heat flux during EDM, a finite element model was created. Analysis was done on how several process variables, such as duty cycle and current, affected the distribution of temperatures and thermal stress. High temperature gradient

zones and areas of high stress exceeded the material yield strength, according to the analysis's findings.

Lauwers *et al.* [21] found out that, ceramic materials are now crucial for a range of industrial uses. Numerous varieties of these materials have been created. Ceramic materials that are particularly well-suited for electrical discharge machining (EDM) are still the subject of little research and development. The material removal methods of a few commercially available electrically conductive ceramic materials were thoroughly examined in this paper by analyzing the debris and surface/subsurface quality. Electrically conductive phases such as TiN and TiCN have been added to ceramic materials based on ZrO_2, Si_3N_4, and Al_2O_3.

Keskin *et al.* [22] found that, surface roughness was the most crucial performance metric in EDM, outperforming other performance metrics including material removal rate (MRR) and tool wear rate (TWR). In order to identify the parameters influencing surface roughness, tests were conducted in this study. Utilizing design of experiments techniques, the data collected for performance metrics has been examined. Power, pulse time, and spark time factors were used to derive a very deep equation for surface roughness.

Patel *et al.* [23] carried out the experiment by using mild steel, kerosene oil as the dielectric fluid, and copper, brass and graphite as tool electrodes. As the discharge current increased for all three electrodes, MRR increased as well. It is probable that the nonlinear MRR with pulse energy was caused by thermal energy losses by conduction to the dielectric fluid and surrounding material. Because copper's electrical and thermal conductivity increased, it responded well to high discharge current values in terms of metal removal rate. When comparing brass to other electrodes, it responded well to surface polish at all current levels. SEM (scanning electron microscopy) analysis of the EDM surface revealed that the molten mass had been expelled from the surface as sheets and ligaments as well as pieces that had become adhered to the surface because of the molten state. After being machined using various electrodes, each specimen had a unique HAZ pattern.

Singh and Kumar [24] investigated that for many years, the tool, mould, and die industries relied heavily on EDM as a production technique. The procedure is becoming more and more popular in industry because it can create geometrically complicated shapes and manufacture hard materials that are very challenging to machine using traditional methods. In addition,

despite recent technological developments, complex geometries in hard and temperature-resistant alloys and die steels cannot be produced using traditional machining techniques. EDM, a non-traditional machining technique, was created with these needs in mind. Operating principles were characterized in the current study as the use of heat energy to process parts through the discharge of sparks, vapour, and erosion processes.

Pachauri and Tandon [25] concentrated on the metals' technological constraints. The need for sophisticated ceramic materials in industry is constantly growing. Because ceramics are extremely difficult to shape with traditional sintering techniques, this need has pushed manufacturing researchers to work hard at developing procedures that can form these hard and brittle materials. This report outlines several research trends that use EDM to machine ceramic materials that provide insulation. In order to machine different ceramic materials such as ZrO_2, Al_2O_3, Si_3N_4, SiC, and their composites, the study provides a taxonomy of ceramic materials and a thorough discussion of EDM methods and their variations, including hybrid ones. Important standards have been found and introduced for the machining of insulating ceramics. Presenting the wider spectrum of work that has been done towards the machining of advanced ceramics is the main goal of this study. The experimental studies as well as the numerical simulation and finite element models developed to investigate the machining of insulating ceramics using spark discharges are included in this review. The difficulties in machining insulating materials using the EDM technique are examined, and these difficulties are compared to the process's capacity to machine composites.

Pei *et al.* [26] found that tool wear in electrical discharge machining (EDM) is an unavoidable occurrence that negatively impacts the geometrical correctness of machined features, according to research by. The electromagnetic (EM) theory was used in this study to propose a model of tool wear in EDM that takes into consideration the electric field inside the dielectric fluid. The location of the spark was suggested to be where the local electric intensity peaks and surpasses the dielectric fluid's breakdown strength. Comparing this approach to more conventional geometric property-based modelling, it was demonstrated to offer a more accurate prediction of tool wear as well as the physical insight into the actual EDM scenario. Because of these advantages, the suggested model can be used to forecast tool wear in a variety of machining operations. Simulations of ED milling and EDM die sinking were performed in order to assess this concept.

The outcomes of this electric field model were contrasted with those of tests and geometric models. The distinctions between the electric field and geometric models' mechanisms were found by examining the tool end profiles. Furthermore, the conic tool making process in the fix-length compensation with micro-milling, which the geometric model is unable to fully capture, was also simulated using this electric field model. The main characteristics of tool wear in a range of machining operations can be captured by the model described in this study.

Pham *et al.* [27] concentrated on the electrode wear issue and EDM process planning. Particular attention was given to elements and practices that affect the accuracy that can be attained, such as positioning strategies used during electrode grinding and EDM. An overview of the primary problems restricting the use of micro-EDM and impacting its performance was provided in this research. Planning the process within the anticipated tolerances could be aided by the outcomes that were reported.

All components of the process, including the type of electrode grinding, the placement, and the operation length, should be taken into account when establishing process tolerances for micro-EDM. Errors from all of these activities were added up and taken into consideration. Reliable algorithms and techniques with repeatable outcomes were employed in micro-EDM processes to maintain their competitiveness as a micro-manufacturing technology. The suggested micro-milling approach substituted straightforward length measurement for the intricate computations of other current techniques. Because of this, industry found the new approach appealing.

Murray *et al.* [28] investigated that the material of the ablated work piece quickly solidified after being ejected into the dielectric during electrical discharge machining (EDM) and was believed to not reattach to the electrode surfaces. Debris reattachment onto the tool electrode was dependent on its re-melting in the dielectric by the secondary discharge process and did not occur randomly after high aspect ratio slots were machined. This was explained by the use of SEM and EDS techniques in combination with single discharge and cross-sectional analysis. No attachment took place outside of the areas affected by the discharge; the subsequently bound material was mostly found in the center of the discharge crater. As a result, depending on the makeup of the material deposited, the electrode surfaces exposed to strong secondary sparking were susceptible to transient surface characteristics. Additionally, it was noted that the substance that was deposited on the tool electrode might provide a shield against additional secondary discharge wear, thereby extending tool life. To investigate their impact on the pace

and method of deposition or material transfer, a number of additional process parameters, such as polarity, work piece/tool materials, and dielectric type, could be changed.

Trych [29] concentrated on the behavior of carbon fibers under EDM conditions, particularly tool wear, which was a crucial characteristic for a material to be deemed an excellent tool material for electrodes. The results and experiments of several machining factors that significantly impacted the process will be presented. The analysis establishes the optimal machining parameters and provides a solution to the electrode wear question, which differed from that of standard electrodes. The newly created experimental setup was also validated using the scheduled tests. There was occasionally a discernible bending of the fiber following a short circuit.

The voltage threshold settings for short circuit detection were carefully selected. Time that could have been used for appropriate machining was lost due to the electrode's frequent back movement in several trials. The computed linear tool wear value, which accounts for the entire experiment duration, was similarly impacted by this. The back movement time was impossible to quantify or estimate. However, the carbon fiber electrode experiment setup managed to run tests according to the plan, and the linear tool wear relationship was taken into account for certain input parameter values.

D'Urso *et al*. [30] changed a number of process parameters, including peak current, voltage, and frequency. Brass and tungsten carbide were the two materials used to make the tubular electrodes. During the drilling procedure, the tool wear ratio (TWR) and in-progress material removal rate (MRR) were examined. There are certain mathematical rules that control the relationship between process parameters and performance indicators. For various electrode materials, TWR and MRR were determined as a function of hole depth. For the two electrode materials, the evolution of MRR and TWR during the various drilling processes displayed diverse behaviors. The cumulated MRR's technical window highlights a linear trend for tungsten carbide and a second-degree polynomial trend for brass.

All of the solutions under consideration saw an increase in TWR as the hole depth increased because debris evacuation became more challenging. The wear behavior was essentially linear for tungsten carbide and logarithmic for brass. A basic scheme for predicting the TWR range utilizing brass and tungsten carbide electrodes was developed within the parameters of the tests. The characteristics of the electrode material may be the cause of a notable variation in the absolute values of DOC and TR. High electrical conductivity generally led to faster drilling but less precise holes in terms of dimensions and geometry.

Hosel *et al.* [31] looked at the possibility of using an aiding electrode in conjunction with spark erosion to process insulating materials. This work established a new lacquer-based aiding electrode that may be used to initiate a continuous erosion process and is simple to apply using screen printing and doctor knife procedures. Over the erosion depth, zirconia samples were arranged and the process was described in terms of removal rate, wear rate, and wear removal ratio. Additionally, the impact of two distinct dielectrics and two electrode materials was examined, and it was shown that the dielectric and electrode material had a significant influence. Accurate channel geometries were created and described using the knowledge acquired.

Chen *et al.* [32] concentrated on developing a workable procedure and fine-tuning the parameter levels for EDM processing of electrically nonconductive ceramics. The current study set out to optimize the electro discharge machining (EDM) parameters for ZrO_2 ceramic machining. Adhesive conductive copper and aluminium foils were applied to the electrically non-conductive ceramic surface during the EDM process in order to reach the electrical conductivity threshold. Using an L18 orthogonal array and the Taguchi experimental design approach, the experimental investigation investigated the machining properties related to the EDM process, including material removal rate (MRR), electrode wear rate (EWR), and surface roughness (SR). To investigate the important machining parameters influencing the machining features, analysis of variance was performed. According to the experimental results, the adhesive conductive substance was the key parameter connected with EWR, while peak current and pulse duration had a substantial impact on MRR and SR. Additionally, the response graph of signal-to-noise ratios for each level of machining parameters was used to identify the best combination levels of machining parameters.

Chevalier and Gremillard [33] focused that the therapeutic use of ceramics for medical applications, who also offered a picture of how they might develop over the following 20 years. Additionally covered is the role of ceramics in a gradual medical approach, ranging from tissue regeneration to traditional implants. They claimed that either non-oxide ceramics or nano-structured ceramics and composites based on zirconia and alumina should be used to meet the demand for tough, strong, and stable bio inert ceramics. For bone replacement and tissue engineering, additional research indicated that porous bioactive glasses and nano-structured

calcium phosphate ceramics, perhaps in combination with an organic phase, might offer the required qualities.

Kucukturk and Cogun [34] introduced a novel electric-discharge machining (EDM) technique for non-conductive ceramic workpieces. Graphite powder was added to the dielectric fluid for machining, and a conductive layer (CL) was applied to the milling surfaces of nonconductive workpieces. Workpiece samples made of glass, ZrO_2, SiC, B_4C, and Al_2O_3 were machined using this technique. Each sample underwent testing under various machining settings, and the ideal machining parameters were identified. It was examined how the workpieces' electrical, thermal, and melting points affected the material removal rate (MRR). There has also been discussion and presentation of surface photos of workpieces acquired with an optical microscope and a scanning electron microscope (SEM) following machining.

Liu *et al.* [35] introduced a novel electrical discharge (ED) milling method for cutting insulating ceramics. They looked into how ED milling uses a water-based emulsion as the work fluid and a thin copper sheet that is fed to the tool electrode along the workpiece's surface as the helping electrode. On insulating ceramics, this method successfully machined a sizable surface area. The process's machining principle has been presented. Additionally, the impact of tool polarity, peak voltage, tool electrode rotation speed, and workpiece feed speed on process performance has been examined.

Ferraris *et al.* [36] examined the micro-EDM behaviour of electrically conductive ceramic composites based on Al_2O_3 and ZrO_2. The impact of generator settings on material removal rate (MRR), surface quality (SQ), relative tool wear (TWR), and material removal process was examined in order to identify appropriate micro-EDM technologies. A basic analysis of the generator parameters served as the foundation for the study's experimental design. With the exception of the tool wear performance, similar tendencies of variance to the machining of steel were noted within the examined process window. Finally, industrial demonstrators were constructed to validate the established EDM technologies.

Mehta *et al.* [37] examined the evolution of conductive ceramic materials and the advancement of EDM technology from its inception to the present. Important research topics such material removal optimization, electrode wear monitoring, and surface quality impact are covered in detail. The current and expanding variety of applications for these materials has also been taken

into consideration. Enhancing process efficiency, optimizing process variables, and monitoring and controlling processes are the main areas of focus. Notable attempts have been made to demonstrate how electrical and non-electrical characteristics affect response parameters for different combinations of electrode workpiece materials.

Lajis *et al.* [38] the Taguchi technique was used to cut tungsten carbide ceramic utilizing electro-discharge machining (EDM) with a graphite electrode. The experimental design, the impact of each parameter on the machining properties, and the prediction of the best option for each EDM parameter—such as peak current, voltage, pulse duration, and interval time—were all done using the Taguchi technique. It was discovered that these factors significantly affect machining characteristics including surface roughness (SR), electrode wear rate (EWR), and metal removal rate (MRR). According to the Taguchi method analysis, the pulse duration mostly influences the MRR, although the peak current generally has a substantial impact on the EWR and SR.
Experimental results have been provided to verify this approach.

Lee and Li [39] observed that, the tungsten carbide EDM's operating conditions have an impact on the machining properties. The EDM process's efficacy using tungsten carbide was assessed based on the workpiece's surface finish quality, relative wear ratio, and material removal rate. The most appropriate material for use as a tool electrode in EDM of tungsten carbide was found to be copper tungsten. In general, using the electrode as the cathode and the workpiece as the anode resulted in better machining performance. Higher material removal rates, less tool wear, and improved surface polish were all achieved with a negative polarity tool. The ideal dielectric cleansing pressure was discovered to be 50 kPa.
The ideal conditions for the relative wear ratio and surface roughness of tungsten carbide precision machining are 120V gap voltage, 24A discharge current, 12.8μs and 100μs pulse duration and interval, 50kPa dielectric flushing pressure, and copper tungsten (CuW) as the negative polarity tool electrode material. According to the study, there is an ideal situation for precisely machining tungsten carbide, albeit this condition may change depending on the material's composition, the machine's accuracy, and other outside variables.

1.5. MAJOR RESEARCH GAP

From the review of past literature, it is found that the mechanism of electro-discharge machining (EDM) process is still not fully comprehended by the researchers during machining of advanced engineering materials e.g. electrically non-conducting ceramic materials, shape memory alloys although it has potential for applications in manufacturing industries for machining these advanced materials. Therefore, the effective utilisation of EDM process for machining of ceramic materials demands extensive research in controlling the performance characteristics of machining process and also to study the influences of various process parameters and the combined influence of various physiochemical phenomena occurring at the sparking zone. As discussed, some non-conventional machining processes have great potential to manufacture a product with electrically non-conductive materials. Although ultrasonic machining (USM) is frequently used to machine electrically non-conductive materials, there are certain inherent drawbacks to this method, including tool wear, high capital costs, and the possibility of tool bending. Because of its rapid cutting speed, abrasive water jet machining (AWJM) is a dangerous process that demands a large initial investment and ongoing maintenance. Additionally, low surface quality contributes to the products' subpar quality. Although electrically non-conductive materials can be machined using the electrical diamond wheel grinding technique, there are certain drawbacks, including the need for expensive equipment, ongoing maintenance, and expert workers. During the micro-machining process in laser beam machining, a strong monochromatic light source is employed. However, the procedure is exceedingly expensive, and the goods' quality is lowered by the development of a wide, undesired heat-affected zone. The tight adherence between the tool and the work material is the reason for tool wear once more. In the phenomenon of metal cutting, the tool must be able to maintain its cutting capability even at elevated temperatures. Traditional mechanical machining techniques find it extremely challenging to create fine forms free of microcracks, which is one of the fundamental needs of machining ceramic materials.

Even so, many basic characteristics of the EDM method for milling eclectically non-conducting ceramics have previously been the subject of researches by earlier researchers. For a thorough investigation and analysis of the parametric impacts on the machining characteristics of the EDM process, many fundamental aspects still need to be addressed. This will ensure that the process criterion goals for machining operation on electrically non-conducting ceramics are maximised. A very few investigations have been documented to analyze the machining characteristics of EDM process during machining of advanced engineering materials such as

ceramics and shape memory alloy (NiTinol) by utilizing assisted methods. Also, an exhaustive experimental investigation is needed to understand the feasibility of EDMing of advance engineering materials at different environments.

1.6. OBJECTIVES OF THE PRESENT RESEARCH WORK

From the literature review it is evident that there are lot of aspects need to be investigated to control the machining parameters so that the desired machining rate could be achieved with adequate dimensional accuracy and EDM process shall be effectively utilized to machine electrically non-conductive materials such as ceramics and other advanced engineering materials e.g. shape memory alloy (NiTinol). To accomplish machining problems during machining of advanced engineering materials, the objectives of the present investigation are given as below:

(i) To study the feasibility of machining electrically non-conducting materials such as ceramic materials by electro-discharge machining (EDM) process.

(ii) To study the influences of various process parameters such as peak-current, pulse on-time and flushing pressure etc. on material removal rate (MRR), tool wear rate (TWR) and overcut (OC) during machining of ceramic i.e. Alumina (Al_2O_3) by electro-discharge machining process.

(iii) To analyse the influences of input process parameters such as polarity, peak current, pulse on-time, spark time etc. on MRR and Taper angle during drilling on shape memory alloy such as Nitinol by electro-discharge machining (EDM) process based on Taguchi method.

(iv) To develop mathematical models to correlate various process parameters to different performance characteristics e.g. MRR and overcut during drilling on shape memory alloy such as Nitinol based on response surface methodology (RSM).

(v) To analyse the influences of many process parameters such as gap voltage, peak current, pulse on-time etc. on MRR, overcut based on the developed models during drilling on Nitinol by electro-discharge machining (EDM) process.

(vi) To search out the optimal machining conditions of EDM process for maximum MRR and minimum TWR and overcut during drilling operation on Alumina using multi-criteria decision methods (MCDM).

(vii) To find out the optimal parametric combinations of EDM process for maximum MRR and minimum taper angle during drilling operation on Nitinol based on Taguchi method

as well as to search out the optimal machining conditions of EDM process for maximum MRR and minimum overcut during drilling operation on Nitinol based on the developed models by using distance optimality technique of RSM.

Further, the above-objectives have been shown graphically as below:

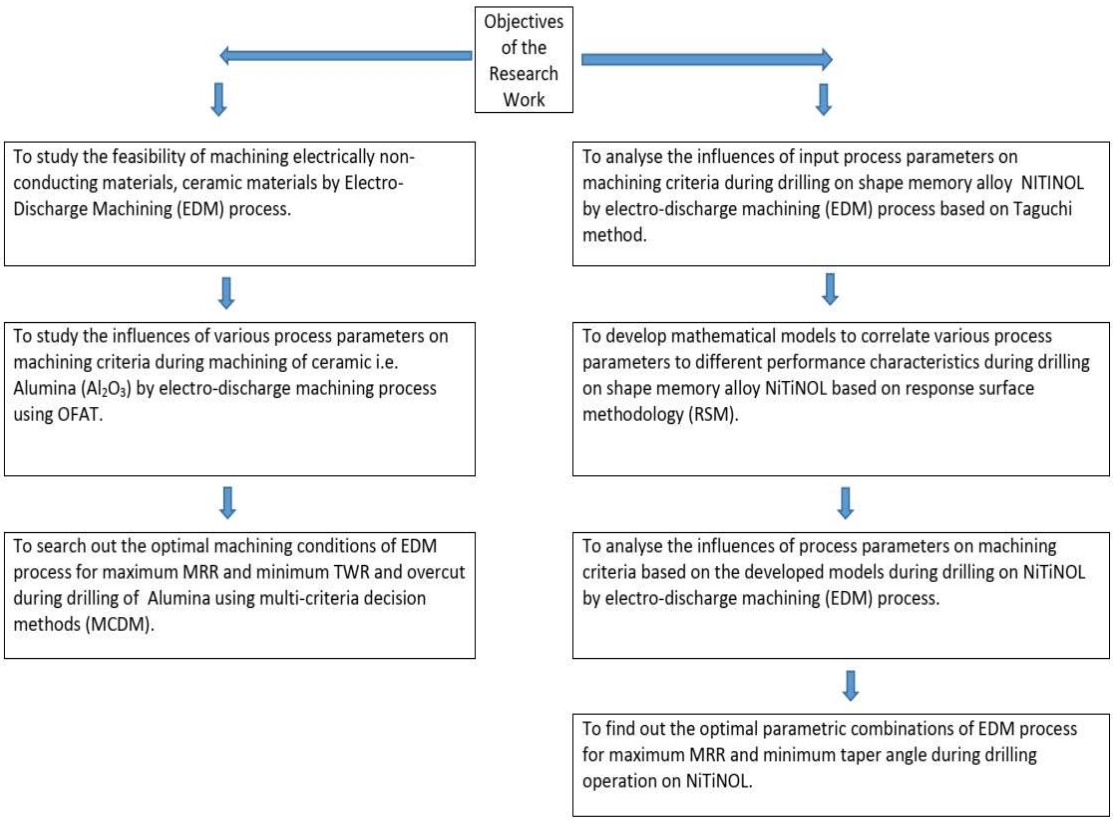

2. DETAILED CHARACTERISTICS OF EDM

Electrical Discharge Machining (EDM) is a highly effective and widely adopted non-traditional machining method, particularly suited for producing complex shapes and small apertures with high precision. This process operates on a thermoelectric principle, using electrical discharges to generate intense heat that melts and vaporizes material from the workpiece, which is submerged in a dielectric fluid. Unlike conventional machining techniques such as cutting or grinding that rely on harder tools or abrasive materials to remove softer workpiece material, EDM removes material through controlled electrical pulses and thermal energy. One of the key advantages of EDM is that its performance is not affected by the mechanical properties of the material being machined. As a result, it is especially useful for processing materials that are hard, brittle, or extremely strong materials that are typically difficult to machine using traditional methods.

2.1. Mechanism of EDM

Electrical Discharge Machining (EDM) is a thermo-electrical material removal process in which the shape of the tool electrode is precisely replicated onto the workpiece. The EDM system comprises several key subsystems, including the machine tool system, power supply unit, and control and delivery system. In operation, the machine tool holds the pre-shaped electrode and moves it toward the workpiece, generating a high-frequency series of electrical sparks. The tool and workpiece are separated by a small gap ranging from 0.01 to 0.5 mm, which is filled with a dielectric fluid. A voltage, typically between 20 and 120 volts, is applied across the tool and workpiece, creating an electric field strong enough to cause electrical breakdown in a small zone approximately 10 μm in radius. Usually, the workpiece is connected to the positive terminal and the tool to the negative terminal of the power supply. Once the electric field is established, electrons on the negatively charged tool experience electrostatic forces. If the electron binding energy (work function) is sufficiently low, electrons are emitted from the tool surface this process is known as cold emission.

These emitted electrons travel through the dielectric fluid toward the workpiece, accelerating as they move. Along the way, they collide with dielectric molecules. These collisions cause ionization of the dielectric, depending on the energy of the electrons and the properties of the dielectric fluid. This leads to the formation of more free electrons and positive ions.

As this ionization cycle continues, the density of charged particles increases, eventually forming a high-concentration plasma channel in the gap between the tool and workpiece. This plasma has very low electrical resistance. At this point, a sudden surge of electrons flows from the tool to the workpiece and ions from the workpiece to the tool an effect known as the avalanche motion of electrons. This rapid movement of charge appears as a visible spark. The electrical energy of the spark is converted into thermal energy. High-velocity electrons and ions strike the surfaces of the tool and workpiece, respectively, and their kinetic energy is transformed into intense, localized heat. This results in a sudden temperature rise exceeding 10,000°C, causing the workpiece material to melt and vaporize in a highly confined region a process known as ablation. Material removal occurs primarily through vaporization and, to a lesser extent, melting. However, not all of the molten material is expelled immediately. When the voltage is turned off, the plasma channel collapses, producing a shock wave that ejects the remaining molten material from the crater formed by the spark. This process leaves behind a small cavity on the workpiece surface, and repeated sparking eventually forms the desired shape. A schematic representation of the EDM setup is shown in Fig. 2.1.

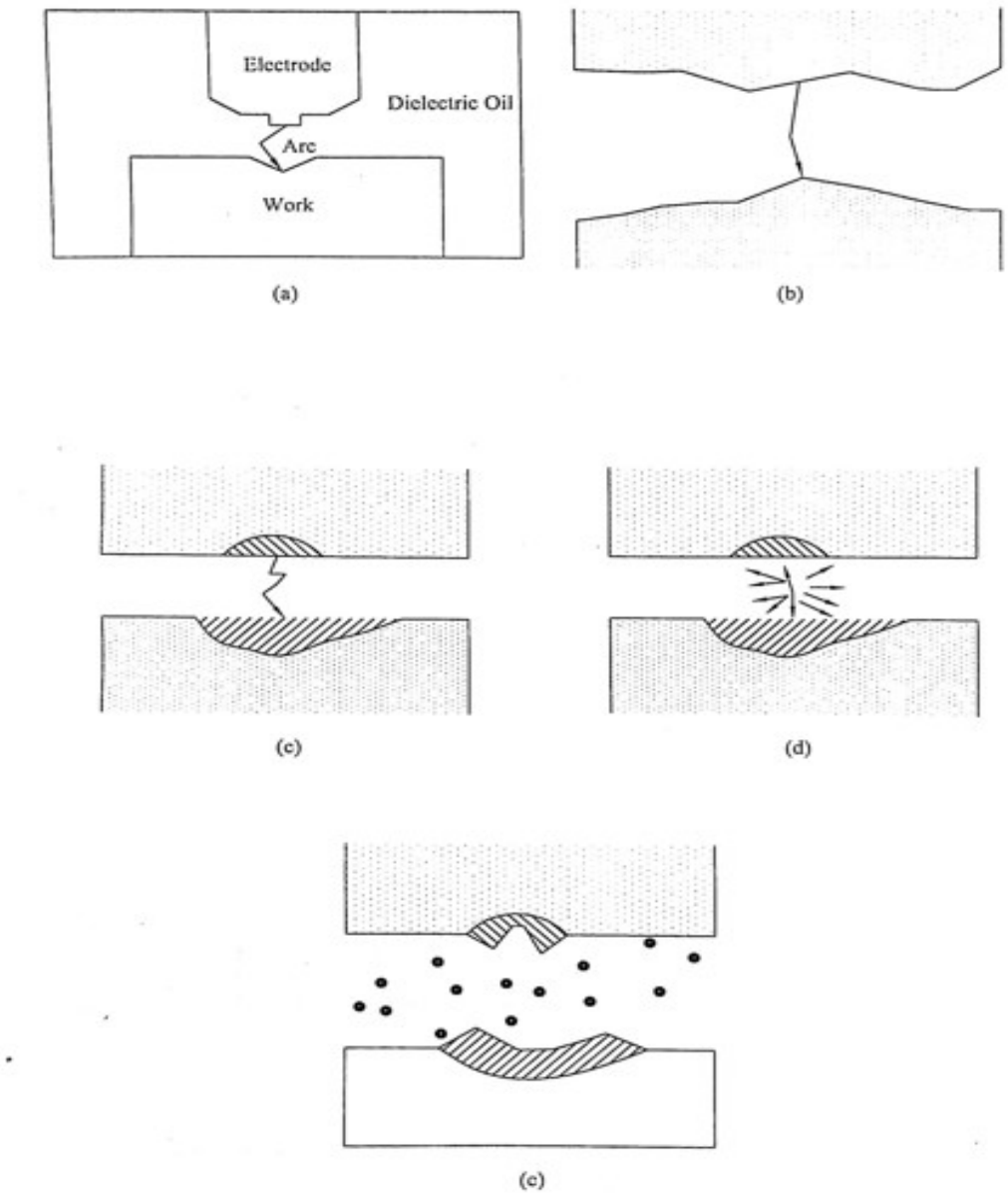

Fig.2.1 Mechanism of EDM [19]

2.1.1. Electro Discharge Machining (EDM) using Assisting Electrode Method

In this method, a conductive layer is initially applied to the surface of an insulating ceramic, allowing the machining process to start with this conductive layer. The key principle behind this technique is that machining the thin conductive layer also causes the ablation of the underlying workpiece material. Furthermore, carbon is produced as a result of the breakdown

of hydrocarbons in the dielectric oil. As the process progresses, a secondary conductive layer forms on the ceramic surface, enabling continuous EDM on the insulating ceramics. With precise control, this cycle of removing the conductive layer, ablating the underlying material, and depositing a secondary layer can be repeated consistently. The machining can continue as long as the conductive layer can be reliably regenerated. Additionally, the formation of this conductive layer during the assisting electrode method also leads to a change in the shape of the discharge pulses. A schematic diagram of the assisting electrode method is shown in Figure 2.2.

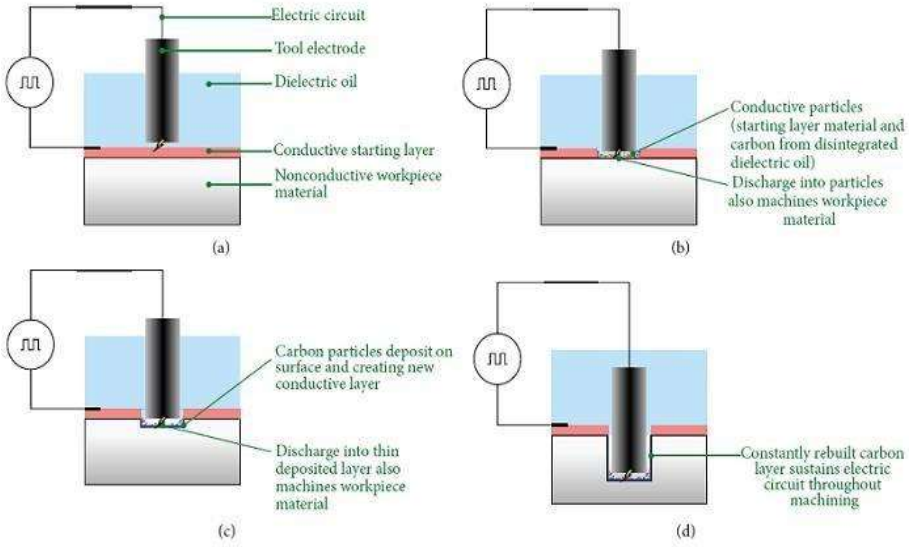

Fig.2.2. Assisting electrode scheme for machining of non-conductive ceramics

Because an intermediate conductive layer forms at the interface between the Assisting electrode and the non-conductive ceramics, instabilities in the machining operations are likely to arise, which makes material removal by electric discharges easier. One pulse or spark is responsible for the formation of the molten crater in EDM, which is thought to be hemispherical in shape and have a radius of r. The loss of material in a single spark can therefore be written as

$$\Gamma s = (1/2)(4/3\ \pi\ r3)$$

$$\Gamma s = 2/3\ \pi\ r3 \qquad (2.1)$$

Now, the energy content of a single spark (Es) is given as

$$Es = VIton \qquad (2.2)$$

Where, V is open circuit voltage (V), I is the current (A) and ton is on time (μs).

The impinging electrons and ions share the remaining spark energy, with some of it being wasted in heating the dielectric. Consequently, the energy that is accessible as heat at the workpiece (Ew) is determined by

$$Ew \alpha Es$$
$$Ew = K\, Es \qquad (2.3)$$

Logically, then, the amount of material removed in a single spark should be proportionate to the energy of the spark. Therefore,

$$\Gamma s \alpha Es \alpha Ew$$
$$\therefore \Gamma s = g\, Es \qquad (2.4)$$

The material removal rate is now defined as the ratio of cycle duration to the amount of material removed in a single spark. Thus

$$MRR = \frac{\Gamma s}{tc} = \frac{\Gamma s}{ton + toff}$$

$$MRR = g\frac{VIton}{ton+toff} = g\frac{VI}{1+\frac{ton}{toff}} \qquad (2.5)$$

The above is the mathematical model for MRR in RC circuit in EDM.(Please ref 2.3 EDM circuits & operating principles). However, for machining of ceramics by EDM the principle is same but mechanism is a little different than the conductive materials. In ceramics the melting and evaporation process is followed by thermal ablation process. There are two options that enable nonconductive ceramics to be machined. Doping the ceramics with a conductive phase is the first possibility. The conductivity can therefore be raised above $10^{-2}\Omega^{-1}cm^{-1}$, allowing for EDM machining of these ceramics. The "assisting electrode method" is the second choice. The process for this procedure starts with an electrically conductive beginning layer.

2.2. Process Parameters for performing EDM

In theory, we can say that the process parameters of EDM are those parameters which directly have effect on the output responses. With the use of dielectric fluid, electrodes in electro discharge machining use electric discharge to cut away metal by releasing pulses, improving machining accuracy. Additionally, it is said that the principles of macro and micro EDM are similar, with the process mechanism based on an electro-thermal process that uses a discharge through a dielectric to provide heat to the work piece's surface. A number of EDM process parameters are covered below.

(i) ***Discharge voltage***

In EDM, the discharge voltage, which is expressed in volts (V), is directly correlated with the spark gap and the breakdown strength of the dielectric. The open gap voltage first rises until it reaches a point where current can flow through the dielectric due to the creation of an ionisation channel. The voltage decreases and stabilises at the operating gap level as soon as the current starts. The width of the spark gap between the workpiece and the leading edge of the electrode is determined by the preset voltage. A wider gap produced by higher voltage settings improves cleansing conditions and aids in machining process stabilisation. The electric field intensity increases with the discharge voltage, which raises the material removal rate (MRR), tool wear rate (TWR), and surface roughness.

(ii) ***Peak current***

This is one of the most important EDM characteristics and refers to the power required during discharge machining, expressed in amperage (A). When every pulse occurs on schedule, the current increases until it reaches a predetermined value called the peak current. In addition to increasing the tool wear rate (TWR) and having a detrimental effect on surface finish, higher currents can improve the material removal rate (MRR).

(iii) ***Pulse-On-Time (Ton)***

An on-time and an off-time, both expressed in microseconds, make up each cycle. Both the pulse duration and the number of cycles per second are important considerations because all material removal takes place during the on-time. The amount of energy applied during the on-time directly affects the metal removal rate. This energy is controlled by the peak current and the pulse duration. A longer on-time results in a deeper and wider crater compared to one produced by a shorter on-time. However, excessive on-time can be detrimental. If the optimal

on-time for a given electrode-workpiece combination is exceeded, the material removal rate may begin to decrease. The cycle is completed when sufficient off-time is allowed before the next cycle begins.

(iv) ***Pulse-Off-Time (Toff)***

The off-time affects the machining process's stability and speed. The machining procedure proceeds more quickly the shorter the off-time. On the other hand, if the off-time is too short, the dielectric fluid will not be deionised and cannot effectively remove the by-products produced during machining. Instability in the subsequent spark may result from this. Unstable conditions lead to erratic cycling and retraction of the advancing servo, which ultimately slows down the cutting process more than longer, stable off-times would. To ensure smooth operation, the off-time must be longer than the deionization time to prevent continuous sparking at a single point.

(v) ***Polarity***

The electrode's polarity might be either positive or negative. High temperatures produced by the current flowing through the spark gap cause material to evaporate at both electrode surfaces. Since electron processes occur more quickly, the anode material (usually the workpiece) undergoes more wear. This results in minimal wear on the tool electrode, which is beneficial during finishing operations, especially with shorter on-times. It is referred to as reverse polarity when the workpiece is connected to the negative terminal and the tool to the positive terminal. In contrast, straight polarity occurs when the workpiece is positive and the tool is negative. Because it removes more material, reverse polarity is favoured in die-sinking EDM. However, straight polarity offers the advantage of reducing tool electrode wear, even though it results in a slower material removal rate.

(vi) ***Electrode Gap***

The servo mechanism is an essential component of EDM's effective operation since it maintains and modifies the working gap in accordance with the predetermined value. The most popular systems for this use are electro-mechanical ones. Key factors for optimal performance include maintaining gap stability and ensuring a fast response time from the system. Additionally, the presence of backlash in the electrode gap is highly undesirable and should be avoided to ensure consistent and accurate machining.

(vii) ***Duty cycle (τ)***

This is the ratio of on-time relative to total cycle time. This parameter is calculated by dividing pulse-on time by total cycle time. The calculation of duty cycle is given in Eq.2.6.

$$\tau = \frac{Ton}{Ton+Toff} \qquad (2.6)$$

2.3. EDM Circuits and Operating Principles

There are a number of essentially distinct electric circuits that can supply the pulsating DC over the work-tool gap. Though the operational characteristics are different, in almost all such circuits a capacitor is used for storing the gap. The suitability of a circuit depends on the machining conditions and requirements. Fig. 2.2 shows various types of EDM circuits.

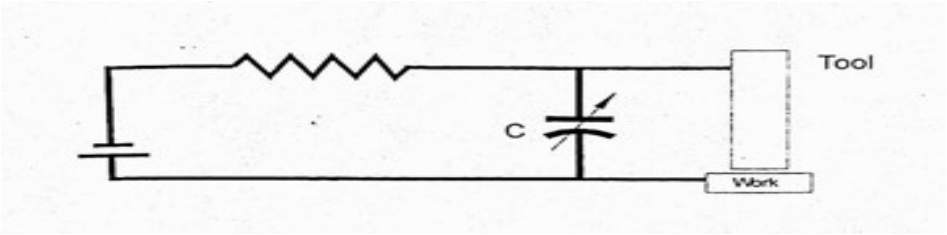

(a) Relaxation Circuit

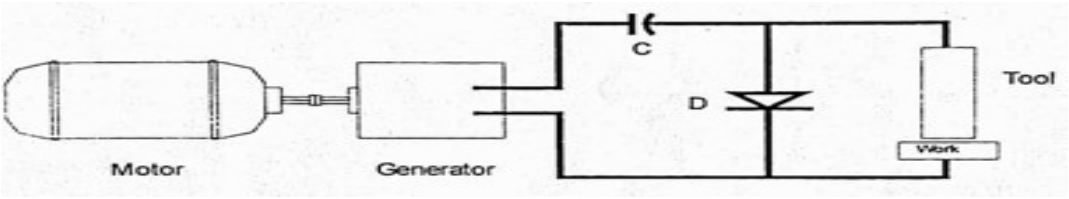

(b) Rotary Impulse Generator

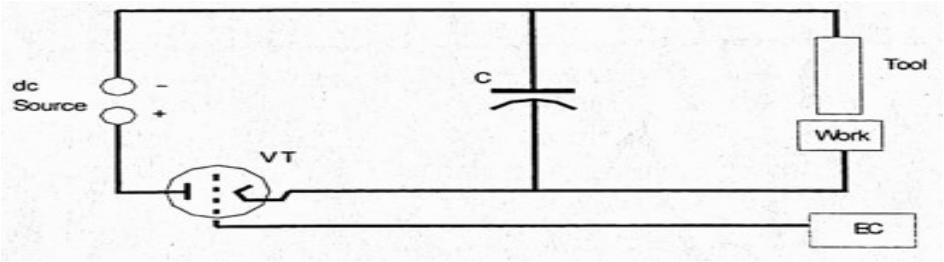

(C)Controlled Pulse Circuit

Fig.2.3 Various Types of EDM Circuits

2.3.1. Relaxation circuit

Figure 2.3(a) shows a simple resistance-capacitance relaxation circuit as is clear from this figure, the capacitor C (which can be varied) is charged through a variable resistance R by the

dc source of voltage Vo. The relationship between the voltage across the gap (which is nearly identical to the voltage across the capacitor) and time

$$V = Vo\ (1 - \exp(-t/RC)) \qquad (2.7)$$

Where t denotes the time starting at the instant Vo is applied. So, V will approach Vo asymptotically if allowed to do so. When the voltage across the tool-work gap (V) hits V_d, also referred to as the discharge voltage, a spark will occur, fully discharging the capacitor if the tool-work gap and the dielectric fluid are positioned so that a spark can occur when the voltage across the gap reaches V_d. The discharge time is much smaller (about 10%) than the charging time.

2.3.2. Rotary Impulse Generator

The relaxation circuit for spark generation, though simple, has certain disadvantage is that the MRR is not high. For increasing the removal rate, an impulse generator is used for spark generation. Figure 2.2(b) shows the schematic diagram of such a system. During the first half cycle, the capacitor is charged via the diode, and the work-tool gap receives the total voltage produced by the generator and the charged capacitor. The frequency at which sine waves are generated and which is influenced by motor speed is known as the operating frequency. Such a method does not yield a satisfactory surface polish, even though the MRR is higher.

2.3.3. Controlled Pulse Circuit

There is no mechanism in place for the automatic stopping of current flow when a short circuit develops in the two systems we have seen. This kind of automatic control is accomplished by using a vacuum tube (or transistor) as the switching device. We refer to this technology as a regulated pulse circuit. A system of this type is schematically depicted in Figure 2.2(c). The current that passes through the gap during sparking originates in the capacitor. As the current passes across the gap, the valve tube (VT) acts as an infinite resistance and is biassed to cut off. It is an electric control (EC) that controls the bias.

2.4. Analysis of the Pulses used in EDM

Performance parameters such as material removal rate (MRR), tool wear, and surface finish are influenced by the shape of the current pulses, even when the energy remains constant. Based on the conditions within the gap separating the electrodes, four distinct types of electrical pulses can be identified:

(a) Open Voltage or Open Circuit

(b) Real Sparks or Effective Discharges

(c) Arcs

(d) Short Circuits

As seen in Figure 2.3, the time development of the discharge voltage and/or current usually defines these pulses. They can have rather different effects on tool wear and material removal. Material removal and tool wear are not caused by open voltages, which happen when the electrode gap is too great. In addition to not aiding in material removal, a short circuit happens when the tool and workpiece come into direct contact. A realistic working gap occurs between these two extreme circumstances when real discharges, like as arcs and sparks, take place. The typical voltage drop across the gap during a pulse is seen in both types of pulses. It's hard to say what makes sparks different from arcs. It is generally accepted that arcs happen on the electrode surface or at the same location, and they have the potential to seriously harm the workpiece and the tool. It is believed that arcs occur when the current from the subsequent pulse preferentially flows along the same path because the plasma channel from the prior pulse has not completely deionised. This eliminates the time needed to create a new gaseous current path, which is typically necessary to start a fresh spark breakdown. It is frequently suggested that the distinct behaviour of EDM arcs sets them apart from actual sparks. It is widely acknowledged that only sparks can effectively and in the intended way contribute to material removal. The degree to which arcs contribute to material loss and tool wear is still unknown, though.

2.5. Tool Electrode

2.5.1. Electrode Material

The selection of the electrode material depends on the following factors:

(i) Material removal rate,

(ii) Wear ratio,

(iii) Conductivity,

(iv) Ease of shaping the electrode,

(v) Availability,

(vi) Cost.

Brass, copper, graphite, aluminium alloys, copper tungsten alloys, and silver-tungsten alloys are the most often utilized electrode materials.

2.5.2. Electrode Wear

During the EDM operation the tool also gets eroded due to the sparking action. The tool electrode will inevitably erode. Very low wear rates are the result of recent advancements in tool material and pulse form, as well as the choice of ideal machining conditions. As a result, it is common practice to have the tool electrode for finish machining become closer to the workpiece's desired size and shape. The material having good electrode wear characteristics are the same as those that are generally difficult to machine. One of the principal materials used for the tool is graphite which goes directly to vapour phase without melting. The volume of tool material withdrawn divided by the amount of workpiece material worn out during the same time period is known as the "wear ratio," and it is typically used to quantify tool wear. The corners and edges of the instrument have greater electrode wear than the rest. The wear ratio can range from 0.05:1 to 100:1, depending on the nature of the operation, machining circumstances, and the materials of the tool and workpiece.

2.6. Dielectric Fluid In EDM

A power supply with one lead attached to the workpiece—which is immersed in a tank filled with dielectric fluid—makes up the EDM setup. The oil reservoir, filter system, and pump are all connected to the tank. The filter system captures and eliminates dirt from the fluid, and the pump is responsible for circulating the oil and delivering pressure to clean the work area. In addition to storing extra oil, the oil reservoir serves as a receptacle for oil draining in between operations.

The dielectric fluid serves the following main purposes:

(i) To flush eroded particles from the discharge gap during machining and pass them through the filter system to remove contaminants from the oil.

(ii) To provide insulation between the electrode and workpiece, preventing electrical short circuits.

(iii) To cool the heated sections of the workpiece and electrode that are affected by the discharge.

De-ionized water and petroleum-based hydrocarbon mineral oils are the two most often used dielectric fluids. High density and viscosity are desirable for oils since they aid in concentrating the energy and discharge channel. However, these oils may struggle with effectively flushing the discharge products. Most EDM operations use kerosene as a dielectric fluid, which is usually combined with additives to avoid gas bubbles and smells. Additionally, silicon fluids and their blends with petroleum lubricants have demonstrated outstanding outcomes, particularly in machining titanium alloys, where they yield high material removal rates, reduced tool wear, and improved surface finishes. Other dielectric fluids, such as aqueous solutions of ethylene glycol, water-based emulsions, and distilled water, have been used with varying degrees of success. The characteristics of a good dielectric fluid are as follows:

(a) Flash point

The vapours in the fluid will ignite at this temperature. Although this explanation is a little oversimplified, the higher the temperature, the better for safety and clarity because the testing conditions are more complicated.

(b) Dielectric strength

(c) Viscosity

This explains the fluid's ability to recover rapidly with little OFF time and to maintain high resistivity prior to a spark discharge. High dielectric strength oils offer superior control over a broad frequency range, especially in situations with high duty cycles or inadequate cleansing conditions. This lowers the chance of arcing and improves cutting efficiency. The accuracy and surface finish that can be obtained improve with decreasing fluid viscosity. Spark gaps in tight tolerance procedures like mirror finishing can be as narrow as 0.005mm or less. With such narrow gaps, it is easier to flush them effectively using lighter, thinner oils. For good finishing, EDM oils tend to be on the thinner side. In operations that require moderate finishes, such as those used in forging dies, heavier oils can be employed. In these cases, higher viscosity is acceptable due to the larger spark gaps, and it helps reduce fluid loss from vaporization.

(d) Specific gravity

This is the "weight" of a substance, as determined by a hydrometer, and is frequently confused with viscosity. Heavy particles, such chips, settle more quickly in oils with lower specific gravities, or "lighter" oils. As a result, there is less chance of arcing or secondary discharges and gap pollution.

(e) Colour

The use of any dielectric oil will eventually cause it to darken. For the purpose of ensuring visibility of the submerged components, it is logical to start with a liquid that is as transparent as feasible. Whether the fluid is clear or "water-white" should be up to the user, since any fluid that isn't transparent when it's first made probably contains unwanted or dangerous pollutants.

(f) **Odour**

Oils with a strong smell indicate the presence of sulphur, which is undesirable in the EDM process, in addition to the obvious aesthetic reasons for selecting a fluid with no detectable fragrance.

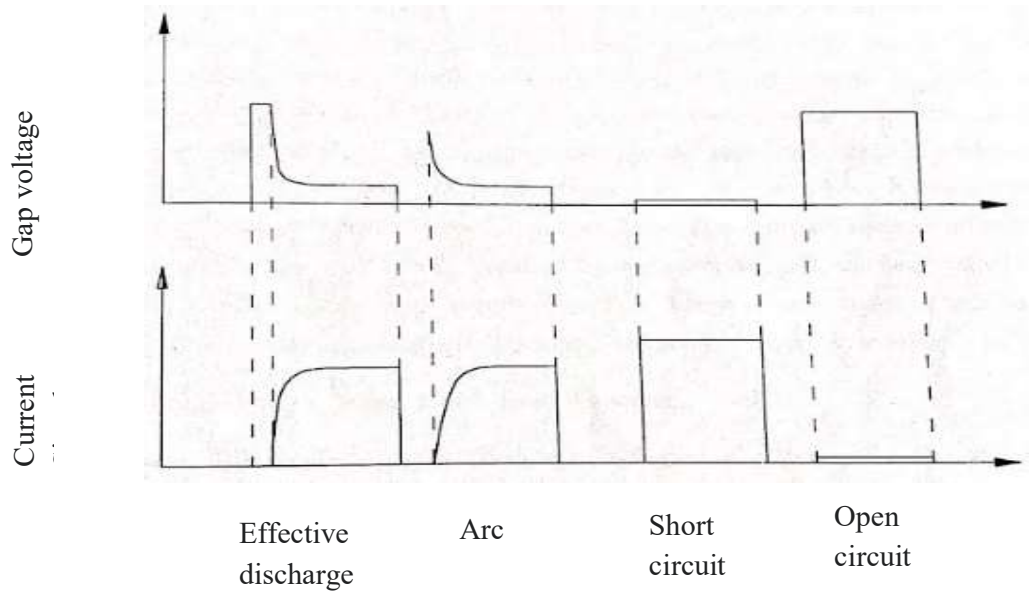

Fig. 2.4 Various Types of EDM pulses

3. EDM SETUP FOR EXPERIMENTATION

The S-35 ZNC Die-Sinking EDM setup, manufactured by Electronica Machine Tools Private Limited in Pune, along with an SRP Control Panel, was used for the experiments. Three subsystems make up the experimental setup: the dielectric supply unit, the power supply and control unit, and the main machining chamber. Fig. 3.1 displays the EDM setup from a photographic perspective.

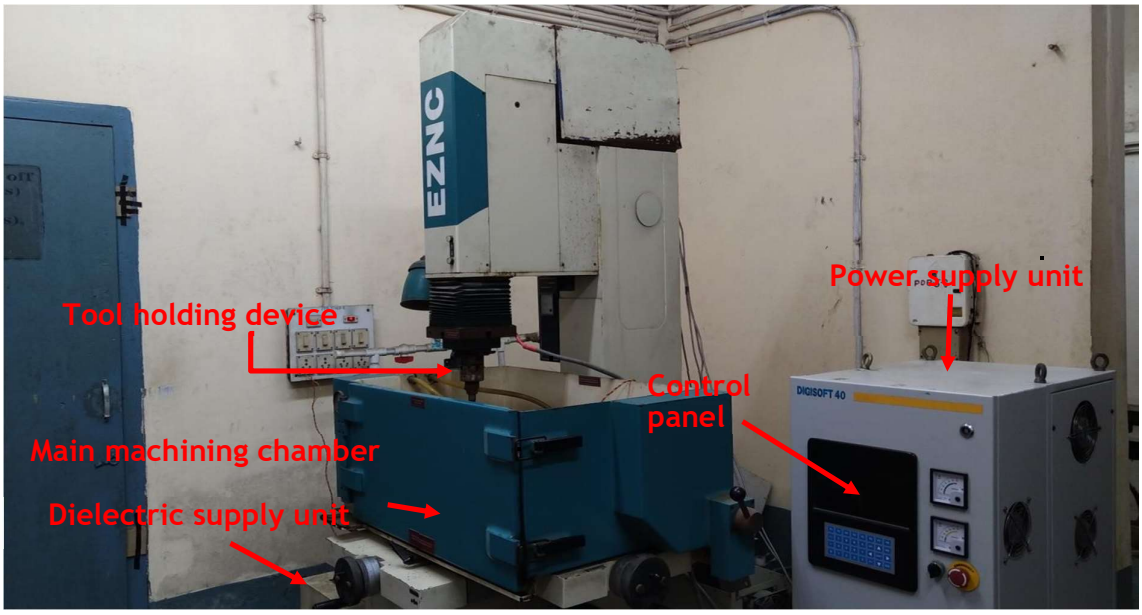

Fig. 3.1 Photographic view of S-35 ZNC Die-Sinking EDM Machine

3.1. Hardware Unit

S-35 ZNC Die-Sinking EDM has various sub-systems, e.g. main machining chamber, tool holding unit, job holding unit etc. which are described as below:

3.1.1. Main machining chamber

In the S-35 ZNC Die-Sinking EDM, the dimension of the main machining chamber is 600mm × 370 mm × 250 mm. The body is made up of cast iron. A workpiece holding vice is generally kept in the main machining chamber, which is used to hold the job and that is also made up of cast iron. Four clamping devices made up of brass, are generally used to hold the job rigidly. A pressure gauge is used to control the flushing pressure of dielectric. Generally, two types of valves are used for two different purposes in the left side of main machining chamber. One is the inlet ball valve and another is injection flushing valve. Inlet ball valve is used to control the amount of dielectric enters into the main machining chamber and injection flushing valve is used to maintain a certain level of dielectric at main machining chamber. There is also a drain handle at the left side of main machining chamber for drain out the dielectric after the machining operation. Two circular handle is used manually for precision movement of the work-table. At the inner right side of the chamber a floating valve is used to maintain the dielectric level at 50 mm above the workpiece to avoid the fire related accident. A schematic and photographic diagram of main machining chamber is shown in the Fig.3.2 and Fig 3.3 respectively

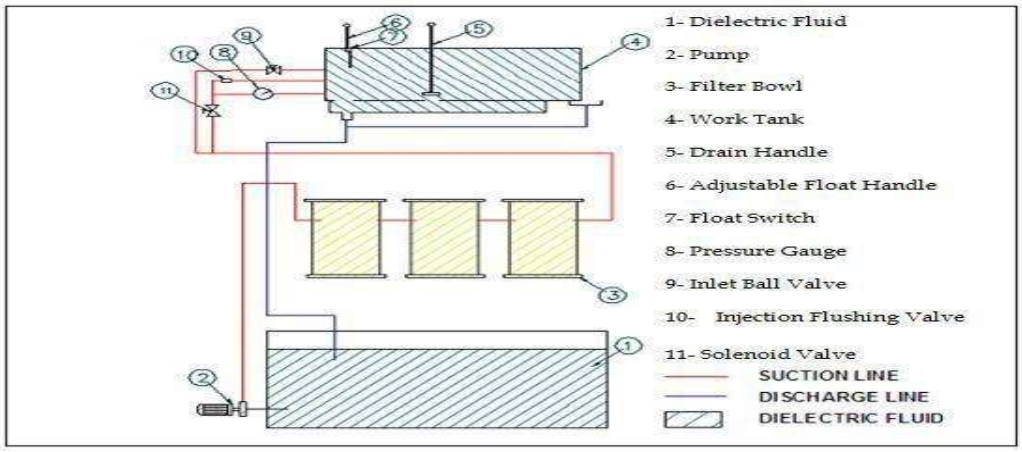

Fig.3.2. Schematic diagram of main machining chamber and dielectric supply unit

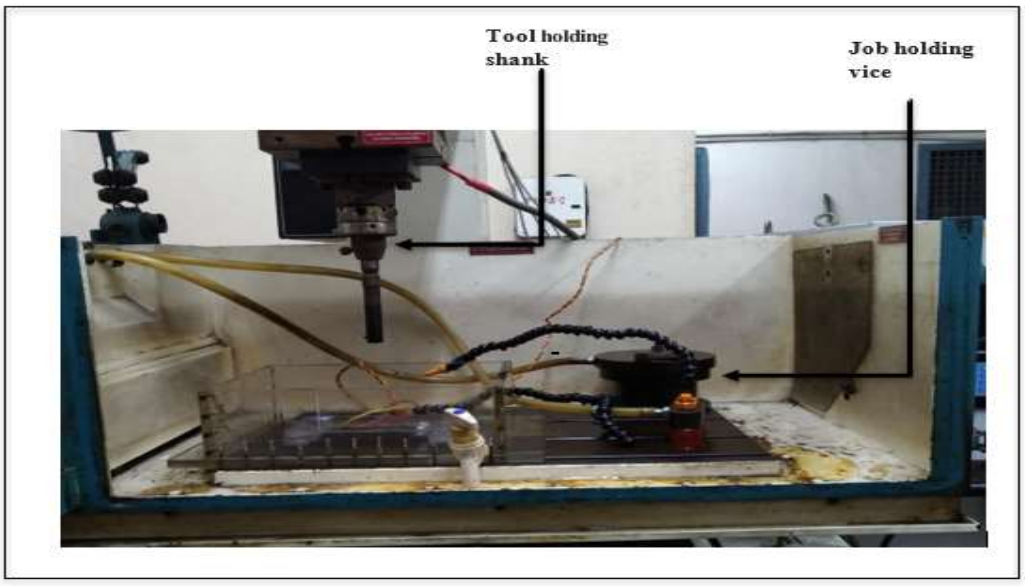

Fig.3.3. Photographic view of main machining chamber

3.1.2. Tool holding unit

In the existing EDM set up it cannot be possible to hold a tool in the shank of the EDM tool holding machine since the diameter of the tool is just 1 mm. So, there has to be an alternative provision of tool holding device in order to hold the tool in proper place. For this purpose, a three-jaw chuck tool holding device has been used for the experimentation. The tool holding device has teeth cut out on it so as to tighten and loosen the tool in it with the help of a key, by engaging and disengaging the key in the teeth of the tool holding device. The engagement and disengagement are done by keeping the teeth of the key and tool holding device at 90º with respect to each other. This tool holding device is then fitted into the shank of the EDM machine with the help of allen key, so as to perform the experimentation. The orthographic and photographic views have been shown in the Fig.3.4 and Fig.3.5 respectively.

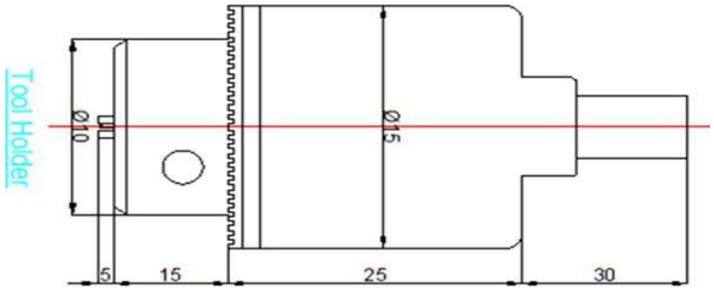

Fig.3.4. Orthographic view of the tool holder

Fig.3.5. Photographic view of tool holder

3.1.3. Job holding unit

In the existing EDM set up there is a workpiece holding vice kept in the main machining chamber on which the jobs are held. Alumina workpiece of 5 mm thickness is clamped by both the sides on this vice and machining is performed. First Alumina (Al_2O_3) workpiece thickness being 5 mm, hence could be held on the vice in the main machining chamber and the thickness of the other Alumina (Al_2O_3) workpiece being 1 mm, was also clamped on this vice. The photographic view of the job holding units of both the main machining chamber has been shown in Fig.3.6.

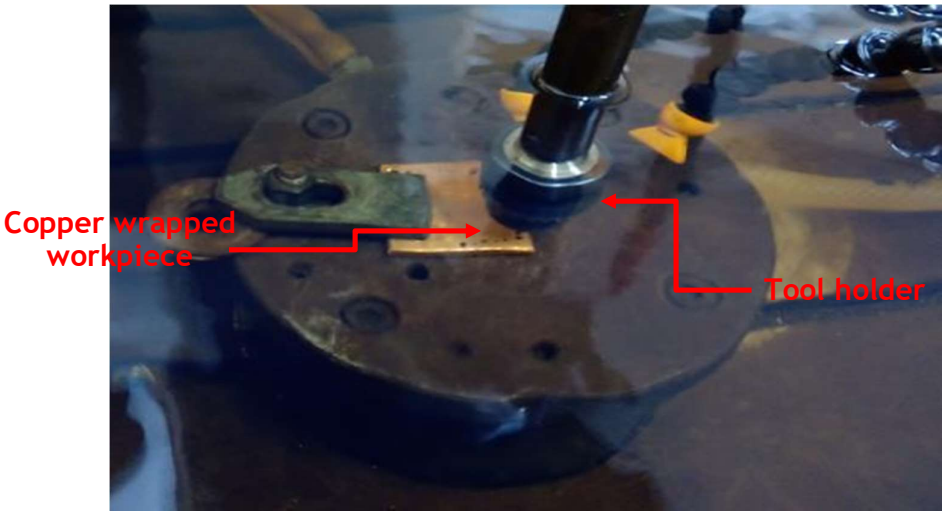

Fig.3.6. Job holding vice in main machining chamber

3.2. Power Supply Unit

S-35 ZNC Die-Sinking EDM has 415V, 3 Phases, 50 HZ supply unit. This power supply unit is of static pulse generator type. Using the latest embedded system, it can be able to produce

the feature that expanded automatic control and monitoring during the EDM process, resulting in much higher efficiency. The design features an automatic monitoring system against current surges. MOSFETs are protected against overload when properly grounded the power supply unit will not produce shocks of other electrical hazards. A stabilizer is used to supply continuous DC power supply to the control panel The main specifications of the experimental EDM set-up are shown in Table 3.1 below.

Table 3.1. The main specifications of the experimental EDM set-up

Work Tank Dimensions	600 mm × 370 mm × 250 mm	Maximum Job Weight	150 Kgs
Table Size	350 mm×200 mm	Dielectric Tank Capacity	100 Lits
X – Axis Travel	200 mm	Machine Weight	450 Kgs
Y – Axis Travel	120 mm	Gross Weight	600 Kgs
Z – Axis Tarvel	150 mm	Day Light	410 mm
Maximum Job Height	140 mm	Throat	250 mm
Maximum Electrode Weight	50 Kgs	Overall Dimensions	800 mm × 800 mm × 1800 mm

A brief technical specification of the power supply unit has been listed in the Table 3.2.

Table 3.2. Technical specifications of the power supply unit

Model Name	S-35 ZNC Die-Sinking EDM
Supply Voltage	415V± 5%, 3 Phases, 50 HZ
Open Gap Output Voltage (V)	65 ± 5%
Power Factor	0.8 (Approx.)
Connected Load (KVA)	3 KVA
Machining Current Max (Amps)	35 Amp
Current Range Selection	Programmable
Pulse On Duration	2-2000 µs
Weight	80 g (Approx.)

In the control panel there is a data display TFT LCD monitor. It has basically two modes, one is ‘DRO’ mode and another is ’EDM’ mode. In the ‘DRO’ mode we can set the workpiece position. In the ‘EDM’ mode we can set all the input parameters like peak current, gap voltage, pulse-on-time, duty ratio, sensitivity, arc sensitivity and the Z-depth etc. The interelectrode gap is set also by using this control unit. It is fully automatic control provided with a joystick and can be manually controlled as well, by clicking the sticky keys on the control panel.

3.3. Dielectric Supply Unit

The dimension of the main machining chamber is 800 mm × 800 mm ×1800 mm. The capacity of the tank is approximately 100 litres. The machine basically recommends ESSO- MENTOR - 28/ BAYOL 35 as dielectric fluids though, equivalents may also be used. Dielectric is supplied through the nozzles to the inter-electrode gap for the removal of debris. Dielectric is circulated by the pump through the filters such as a fresh dielectric always remains in the main machining chamber. Three filters’ bowls with 10 μm of mesh size is used to filter the dielectric every time of its recirculation. A pressure gauge is used to control the flushing pressure.

3.4. Servo Controlled Unit

Signals from the power supply's gap voltage sensor system are used to command the servosystem, which regulates the electrode or workpiece's infeed to exactly match the rate of material removal. The servosystem will respond by reversing direction until the dielectric fluid clears the gap, the infeed starts up again, and the cutting process continues if the gap voltage sensor system detects that a piece of electrically conductive material has filled the space between the electrode and workpiece. The selection of dielectric flushing technique has direct effect on the function of the servosystem. If the flushing system is inefficient in removing the process by-products from the cutting gap, the servosystem may have to spend most of the time reversing to clear the cutting gap. This results in extremely long cycles. However, the servosystem will spend nearly no time retracting if the flushing process is successfully eliminating the by-products, leading to substantially faster cycles. Other servosystem-related auxiliary operations that are most frequently employed during drilling include electrode refeed, touch-off sensing, and breakthrough sensing.

3.5. Tool Electrode for performing EDM of Ceramic Materials

The selection of tool material is an important factor, because the performance of EDM depends on the combination of workpiece and tool materials. Copper, brass, tungsten, and tungsten composite such tungsten carbide or tungsten copper are the most recent known and effective tool electrode materials for EDM. Copper's great electrical and thermal conductivity makes it an appealing material. Of all non-precious metals, copper has the highest conductivity, which is 65% more than that of aluminium. Copper is the preferred material for tool electrodes because of its high ductility, medium strength, ease of connecting, and strong resistance to corrosion. Copper also has corrosion resistance properties and has good machinability. Moreover, it is easy to obtain, very consistent in quality and low in cost as compared to other electrodes.

Brass is also a well-known material used as a tool electrode in EDM because of its high electric and thermal conductivity, easily available, consistent in quality and low cost. But due to low melting point, this tool material wears rapidly in the high machining temperature. Also, the fabrication and low metal removal rate make this tool materials low acceptance in EDM.

Tungsten is a very hard, dense, and strong metal. It is highly resistant to the thermally destructive impacts of the EDM process, with a melting point close to 3400ºC. One of tungsten's drawbacks is its extremely expensive cost. Its great hardness makes it challenging to machine as well. Tungsten is used with ductile substances like copper to increase its appeal for specific uses. Tungsten copper, the resultant substance, is more conductive than regular copper, much more wear resistant, and easier to process. Copper tungsten is utilized as the tool electrode material, particularly in the fields of surface finishing and micro-structuring.

Tungsten carbide (WC) is a chemical compound containing equal amount of tungsten and carbon atoms. It is approximately twice as stiff as steel, with young's modulus of approximately 540-700 GPa. Tungsten carbide has very high strength for a material so hard and rigid. Compressive strength is higher than virtually all melted and cast or forged metals and alloys. Moreover, thermal as well as electrical conductivity of tungsten carbide is also desirable to be used as tool electrode.

3.6. Dielectric Fluids for performing EDM

In the EDM process, the dielectric fluid serves a number of purposes. In order to attain a high current density in the plasma channel, it separates the tool electrode from the workpiece

electrode. Additionally, it applies a counterpressure to the expanding plasma channel and cools the heated electrode surfaces. After the discharge process, flushing with dielectric fluid eliminates the particles and stops the formation of particle linkages that could cause short circuits or damage to the electrode surfaces, which would interrupt the operation. The dielectric fluid also acts as a coolant for the secondary purpose. There are two main types of dielectric fluids one is deionized water and other is dielectric fluids. The differences are depicted in the Table 3.3.

Table 3.3. Difference between Hydrocarbon Dielectric Fluid and Deionized Water

Type of dielectric fluid	Hydrocarbon dielectric fluids	Deionized water
Electrical conductivity	<0.1 W/m-K	1 W/m-K
Technological behaviours	High material removal rate, small tool wear, big influence on peripheral zone	High material removal rate, High surface quality, high wear
Properties	No corrosion of work piece, no deionization necessary, special disposal, low flash point	Not flammable, no hazardous vapors, no special disposal, corrosion
Environmental impact	Hazardous vapors	Nonhazardous vapors
Applications	Die sinking	Die sinking & wire electrical discharge machining.

3.7. Performance Criteria for EDM operations

In EDM, performance criteria can be affected by the various factors such as pulse energy i.e. a function of capacitance, voltage, current, dielectric flushing, aspect ratio, debris distribution, dielectric, gap voltage etc. When EDM is employed to generate feature, part or mold, it is necessary to consider these factors for optimal performance criteria. The major EDM performance characteristics are material removal rate (MRR), tool wear rate (TWR), discharge gap, surface roughness and recast layer. Wear ratio (WR), over cut (OC), taperness, roundness

etc., are also performance characteristics of the EDM process. Major performance criteria of EDM process are described as follows:

(i) ***Material removal rate (MRR)***

Material removal rate is the amount of removed material from the workpiece material divided by time taken for machining. Generally, MRR mainly depends on the discharge pulse energy (a function of capacitance and voltage). The larger pulse energy results in higher MRR. The increase in voltage and capacitance also increase MRR. MRR also depends on the movement of the tool. MRR can also be increased by increasing the tool moving speed and rotation of the tool in EDM. When drilling a deep hole, the ejection of debris from the machining area becomes difficult. The debris concentration causes the abnormal discharge. One solution to this problem is the application of planetary movement to the electrode or application of vibration to the workpiece. It reduces the occurrence of abnormal discharge and thus improves the MRR. The type of dielectric also influences the MRR. The carbon decomposed from the hydro-carbon oil contaminates the dielectric, resulting in an increase of abnormal discharge occurrence. The de-ionized water does not present such a problem. Therefore, the machining time of the deep hole drilling using de-ionized water is much shorter than the hydro-carbon oil.

(ii) ***Tool wear rate (TWR)***

Tool wear rate is the amount of eroded material from the tool material divided by time taken for machining. TWR increases with an increase of pulse energy (voltage and capacitance). Drilling a deep hole or a blind hole, the ejection of debris from the machining area becomes difficult and the debris concentration causes the abnormal discharge. Planetary movement to the electrode provides an extra space for an effective removal of debris and gaseous bubbles. It was found that in EDM, the electrode area affects the tool wear ratio and it can be improved by the increase of electrode working area.

(iii) ***Discharge gap***

The discharge gap is calculated by dividing the difference between the width of slot and the diameter of the electrode by two. It increases with an increase of pulse energy, i.e. voltage and capacitance.

(iv) ***Surface roughness***

Three unique layers comprise the electrical discharge machined surface: the unaffected parent material, the heat affected zone (HAZ), and the white/recast layer. Following the cessation of discharge and subsequent phase transformation, the molten metal's solidification behaviour is tolerated by the EDMed surface. The high temperature gradient has been shown to induce cracks and high tensile residual strains on the EDMed surface. Furthermore, the migration of carbon from the oil dielectrics to the workpiece surface, which forms iron carbides in the white layer or HAZ, explains the EDMed surface's comparatively high micro hardness. Only through SEM micrographs, one can measure the thickness of these layers. The surface roughness also increases with an increase of pulse energy.

(v) ***Recast layer***

As EDM is a thermal process, it generates a heat affected zone consisting of a recast layer and cracks. The expansion of the plasma channel during sparking can be used to determine the degree of thermal damage to the electrode and the thickness of the recast layer that forms on the workpiece surface. The white layer has a significant impact on the workpiece's surface characteristics because it is the topmost layer exposed to the environment. ECM or laser procedures can be used to remove the recast layer, or it can be decreased by adjusting the tool path or layer depth. It is very difficult to measure this recast layer thickness because there is no such instrument which can directly measure this recast layer.

(vi) ***Heat affected zone (HAZ)***

Beneath the recast layer, a HAZ is formed due to rapid heating and quenching cycles during EDM. This layer is approximately 25 μm thick. The heating-cooling cycle and diffused material during machining are the responsible reasons for the presence of this zone. Thermal residual stresses, grain boundary weaknesses and grain boundary cracks are some of the characteristics of this zone. Below HAZ there is a conversion zone characterized by a change in the grain structure from the original structure.

From the above discussions it is clear that EDM performance is influenced by several factors such as, process parameters, properties of workpiece, tool materials and dielectrics etc. By changing any of the above parameters or characteristics changes the response of the electro discharge machining process.

4. INVESTIGATION ON CERAMIC MATERIAL

Although, conventional EDM process have significantly improved the performance criteria such as material removal rate (MRR), tool wear rate (TWR) etc., but still low efficiency and poor surface quality for low or non-conductive and difficult to cut materials such as ceramics are the key problems restricting its development. Therefore, it is the most challenging issue to improve the machining efficiency and surface quality of ceramic materials by performing EDM. For this purpose, some techniques such as doping ceramic materials and assisting electrode method have been incorporated in EDM to increase the machining rate, accuracy and surface finish of ceramics.

4.1. Planning for Experimentation

4.1.1. Selection of Assisting Electrode Material

To investigate the influences of various process parameters, which have been mentioned in above paragraph on different performance criteria while performing EDM process on ceramics, tool diameter of 1mm and workpiece of Alumina (40mm × 40mm × 5mm) have been chosen for experimentation. A copper adhesive tape has been selected to be used as an assisted electrode. Many trial experiments have been carried out to find the range of peak current (Ip), pulse on-time (Ton) and flushing pressure. The other process parameters like duty ratio, gap voltage, work-time, lift-time, inter-electrode gap and machining depth have been kept constant during all the experiments. A tungsten carbide drill bit (WC) tool has been selected as the tool due to its high melting point, hardness, impact strength, high electrical conductivity and brittleness. The drill bit has been provided with flutes for proper passage of the chips and also proper flow of the dielectric. Alumina (Al_2O_3) of 5 mm thickness has been selected as the workpiece material since these ceramics have low conductivity, high melting point and poor machinability. Copper adhesive tape of thickness 0.025mm has been used as an assisting electrode because of its excellent electrical conductivity and being an adhesive tape it was easily applicable on the workpiece surface.

4.1.2. Experimental Conditions

During trial experimentation with above mentioned tool of diameter 2 mm, it was observed that the sparking occurs at the range of 0.5-40 A of current and 0.5 µs-3 s of pulse on time but above 4 A of peak current and 10µs of pulse on time the hole size and tool wear rate was found

more in case of Alumina (Al_2O_3). At the range of 1-4 A of current and 3-10 µs of pulse on time, hole size was found to be more prominent. For this reason, it was decided to conduct the experiments at four different peak currents, four different pulses on time levels and four different flushing pressures i.e. at 1A, 2A, 3A, 4A and 3µs, 5µs, 7.5µs, 10µs and 0kg/cm2, 5 kg/cm2, 10 kg/cm2, 15 kg/cm2 respectively.

Tool was connected to positive as well as negative terminal of power supply and these were referred to as reverse polarity and direct polarity of the tool respectively. EDM oil and deionized water were considered as the dielectric medium for the trial experimentation.

Copper used as the assisted electrode provides the starting conducting layer to machine the ceramic surface forming the intrinsic conducting layer. This further breaks down the hydro carbons of EDM oil resulting from the high temperature at the machined area which further helps in the machining. So EDM oil is more suitable as compared to deionized water for machining ceramics using EDM. After performing several trial experiments 6 layers of copper tape i.e. 0.150 mm was applied on both the ceramic workpieces to perform the experimentation. The next step of experiment plan is to find out the feasibility of machining of both the Alumina (Al_2O_3) workpiece with EDM oil and deionized water as dielectric and to search out the significant effects of EDM parameters and its effective working range on the workpieces. To fulfill this the experiments will be performed varying one process at a time on both the workpieces separately. The machined surface has been analyzed using XRD and optical photograph.

4.1.3. Selection of Workpiece and Tool Electrode Material

The selection of the material of job sample and tool electrode in EDM is an important task because the machining performance totally depends on the combination of job and tool electrode. The common ceramic material like Alumina (Al_2O_3) due to its hardness in the sintered state make it difficult to machine with conventional cutting techniques. One approach for a solution is the use of EDM. Due to the removal of material by thermal ablation, it is independent of the mechanical properties. Therefore, considering the existing non- traditional machining processes EDM is considered as one of the best processes to machine ceramics because of its simple and cost-effective nature. The strength of the tool should be high due to the various pressures acting on the tool and tool tip. A tungsten carbide (WC) tool exhibits more strength and hardness that pure tungsten, moreover it has high melting point as well which is one of the characteristics a tool should possess. It should also allow proper passage of the

chips removal during machining and also allow smooth flow of dielectric for good machining efficiency. So, a tungsten carbide (WC) drill bit tool has been chosen as the tool material.

4.1.3.1. Properties of workpiece and tool material

The choice of job and tool combination depends on the numerous properties of workpiece and tool materials. The physical, thermal, electrical and mechanical properties of the Alumina (Al_2O_3) and tungsten carbide (WC) are shown in Table 4.1.

Table 4.1. Properties of job sample and tool electrode material

Properties	Alumina (Al_2O_3)	Tungsten carbide (WC)
Density (g/cm3)	≥ 3.85	15.63
Melting Point (ºC)	2072	2870
Boiling point (ºC)	2977	6000
Thermal conductivity (W/m/k) at 25ºC	33	110
Electrical resistivity (Ω.cm)	1×10^{14}	2.5×10^{-7}
Modulus of Elasticity (GPa)	300-390	≥ 600
Poisson's ratio	0.22	0.31
Hardness (kg/mm2)	1440	2400
Coefficient of thermal expansion (/ºC)	6.5 to 7.5×10^{-6}	5.5-6 $\times 10^{-6}$

4.1.3.2. Applications of Workpiece Material

Aluminium oxide, which is produced synthetically, is the common name for alumina. It is a chemical compound made up of aluminium and oxygen. It is a colourless, crystalline material that occurs naturally in sapphire and ruby, among other forms. Alumina is significantly more flexible than other technical ceramics and has exceptional strength and wear resistance, in contrast to conventional ceramics that are often hard and brittle. Their primary application is in the manufacturing of aluminium metal. Thermometry sensors, ballistic armour, grinding media, furnace liner tubes, high voltage insulators, electronic substrates, thread and wire guides

and laboratory instrument tubes are just a few of the many applications for alumina. Aluminium oxide is a component in several glass formulations. Purification, or the elimination of water from gas streams, is its application. High-performance applications make use of them. As an abrasive, they are widely utilized. Aluminium oxide crystals are used in a variety of sandpapers.

4.1.4. Experimental Procedure and Performance Characteristics

After setting the aims of the investigation, the conditions have been made to analyze the effects of different process parameters on the various characteristics of EDM while machining non-conductive ceramic material Al_2O_3 using assisted electrode method using copper adhesive tape as an assisting electrode. The fixed machining parameters adopted for investigations are listed below in Table 4.2.

Table 4.2. Constant machining parameters for machining Alumina using EDM

Work condition	Description
Dielectric	EDM oil
Duty factor (%)	10
Machining depth	1.2 mm
Work time (spark time)	2 sec
Lift time	0.5 sec
Gap voltage	50 V

The experiments have been conducted at above mentioned conditions shown in Table according to the following procedures. Procedural steps for the fulfillment of the present research works are enlisted below:

(i) Firstly, the machining chamber is cleaned properly with pure distilled water.
(ii) Before machining, the weight of each workpiece and tool is measured by METTELER TOLLEDO weighing machine (LC of 1×10-2 mg).
(iii) The diameter of each tool is recorded with the help of LEICA microscope at magnification of 10X (LC of 1×10-3 μm).
(iv) The workpiece surface is cleaned using acetone and copper tape is mechanically applied as assisting electrode avoiding any air gap.
(v) The workpiece is clamped just below the tool tip and kept just 2 mm above the upper level of dielectric, cleaned carefully with acetone.

(vi) Main power is switched on and the inter-electrode gap (5 μm) is automatically maintained by the ATPS switch of control panel.

(vii) The current tool position is set at 0-0-0 level at 'DRO' mode and followed by set the various process parameters are set at the 'EDM' mode in the control panel.

(viii) The machining operation was performed according to the experimental plan and the reading of machining time is recorded by a digital stop watch.

(ix) After the machining operation, the main power is switched off and the workpiece was removed, dried and cleaned carefully with acetone. The weight of the job was measured with METTELER TOLLEDO weighing machine (LC of 1×10^{-2}mg). The entrance and exit diameters of machined micro-holes were measured at magnification of 20X in LEICA microscope (LC of 1×10^{-3} μm).

(x) Composition of tool and the workpiece material after machining is measured by X-ray diffraction technique with the help of RIGUTA-ULTIMA (at 40 kV, 30 mA).

(xi) Finally, the optical photographs of the machined surfaces of Alumina have been taken under LEICA optical measuring microscope.

Experimental investigations and the studies of many research works have been revealed that the most influencing process parameters in EDM are peak current, polarity, pulse on- time and flushing pressure of dielectric fluid. In the present research work attempt has been made to investigate the effects of different process parameters on EDM performance characteristics such as material removal rate (MRR), tool wear rate (TWR) and overcut (OC) on the ceramic materials by using assisted electrode method. During the machining, peak current (Ip), on time (Ton) and flushing pressure have been considered as process parameters for each set of experimentation. Furthermore, the range of the process parameters have been optimized by three different MCDM techniques and is followed by validation by performing experiments.

4.1.5. Different Multiple Criteria Decision Making (MCDM) Methods

The process of choosing the best option from a range of viable options while taking into account several competing criteria is known as multiple criteria decision making, or MCDM. To be more specific, criteria are seen to be "strictly" conflicting if raising one leads to lowering the other. There are always two competing criteria and at least two options in an MCDM process. A few helpful resources for resolving MCDM issues are:

(i) Simple Additive Weighting method (SAW)

(ii) Multi Objective Optimization Ratio Analysis (MOORA)

(iii) Technique for Order Preference by Similarity to Ideal Solution (TOPSIS)

(iv) Analytical Network Method (ANP)

(v) Analytical Hierarchy Method (AHP) etc.

MCDM are divided two broad categories: Multiple Objective Decision Making (MODM) and Multiple Attribute Decision Making (MADM). Differences between them are listed below which helps to choose which technique can be used in the present analysis. Table 4.3 shows the comparison between both the techniques.

Table 4.3. Differences between MADM and MODM technique

Subject	**MADM**	**MODM**
Criteria	Different attribute	Objective function
Objective	Implicit	Explicit
Attribute	Explicit	Implicit
Constraint	Inherent	Mathematical form
Alternatives	Finite number	Infinite number
Usage	Selection or Evaluation	Design

4.1.6. Multi Attribute Decision Making

Multi Attribute Decision Making problems are considered in this situation, where several objectives or attributes or the criteria are conflicting and explicit in nature. During decision making through MADM always there is a restriction. MADM constraints are very much inherent and there is no explicit mathematical form. Thus, the process involves the selection of the alternatives, which are predefined and finite in number. So, the decision space considers the finite number of points. In MADM, the criteria are commensurable in nature because they are measured in different units. MADM process considers normalization technique as the units of different criteria are in different scale. MADM also has its application where the criteria are conflicting in nature. From the above discussion it can be concluded that the problem in the present research work should be solved by MADM technique [47, 48, 49]. In this research work, three techniques e.g. Simple Additive Weighting method (SAW), Technique for Order Preference by Similarity to Ideal Solution (TOPSIS), Multi Objective Optimization Ratio Analysis (MOORA) have been considered to optimize the process parameters during EDM of ceramic. The steps involved for the above-mentioned techniques are discussed hereunder:

(i) Simple Additive Weighting (SAW)

Step 1: Decision matrix formation A table called a Decision Matrix, which consists of a

collection of columns and rows, can be used to compile the criteria results of several decision options. Decision possibilities are represented by the matrix rows, while criteria are represented by the matrix columns. A criterion result, or the measured or anticipated performance of a choice alternative on a criterion, is represented by a value located at the intersection of row and column in the matrix. A key component of the MCDA/MCDM is the decision matrix, which houses the information needed to compare the various options.

$$X = \begin{array}{c} \\ A_1 \\ \vdots \\ A_i \\ \vdots \\ A_m \end{array} \begin{array}{c} \begin{array}{cccccc} C_1 & & C_J & & C_n \end{array} \\ \begin{bmatrix} x_{11} & \cdots & x_{1j} & \cdots & x_{1n} \\ \vdots & \cdots & \vdots & \cdots & \vdots \\ x_{i1} & \cdots & x_{ij} & \cdots & x_{in} \\ \vdots & \cdots & \vdots & \cdots & \vdots \\ x_{m1} & \cdots & x_{mj} & \cdots & x_{mn} \end{bmatrix} \end{array}$$

x_{ij} is the performance rating of alternative ***i*** with respect to criterion ***j***,

A_j is i^{th} alternative, C_j is the j^{th} criterion

Step 2: Formation of Weight Matrix

Different importance weights to various criteria may be awarded by the decision makers. These importance weights form the weight as follows.

$W = [W_1 \ldots\ldots\ldots\ldots\ldots W_J \text{----------} W_n]$ (Eq.10)

Step 3: Normalization of performance rating

The performance ratings of the columns under criterion have different dimensions and units. The following formulae are used to normalise these performance ratings and transform them into dimensionless units for comparison.

$\dot{X}_{ij} = X_{ij} / (\max X_{ij})$ for benefit criteria j (Eq.11)

$\dot{X}_{ij} = (\min X_{ij}) / X_{ij}$ for non-benefit criteria j (Eq.12)

Normalized decision matrix

$$X = \begin{array}{c} \\ A_1 \\ \vdots \\ A_i \\ \vdots \\ A_m \end{array} \begin{array}{c} \begin{array}{cccc} C_1 & & C_J & & C_n \end{array} \\ \begin{bmatrix} x_{11} & \cdots & x_{1j} & \cdots & x_{1n} \\ \vdots & \cdots & \vdots & \cdots & \vdots \\ x_{i1} & \cdots & x_{ij} & \cdots & x_{in} \\ \vdots & \cdots & \vdots & \cdots & \vdots \\ x_{m1} & \cdots & x_{mj} & \cdots & x_{mn} \end{bmatrix} \end{array}_{mxn}$$

Step 4: Composite scores (CS_i). Computation of composite scores (CS_i) for the alternatives i

$$CSi = \sum_{j=1}^{n} (\hat{W}j * \dot{X}o) \qquad \text{(Eq.13)}$$

Step 5: Ranking and selection of best alternative: Ranking of products in descending order of composite scores.

(ii) Technique for Order Preference by Similarity to Ideal Solution (TOPSIS)

One evaluation technique frequently employed to address MCDM issues is TOPSIS. In practice, it can be used for a variety of purposes, including comparing the performance of different companies, analysing financial ratios within a particular industry, and investing in sophisticated manufacturing processes. It does have certain limitations, though. Thus far, efforts to enhance the original TOPSIS technique have mostly focused on increasing the weight in order to make the R value more sensitive. Additionally, there have been advancements in the R value formula, such as the "Miqiezhi" technique. A better and more straightforward approach is needed to comprehend the intrinsic connection between the R value and alternative evaluation because evaluation difficulties are so complex. The distance between the alternatives and the reference points in the D+ D−-plane is calculated, and the R value is constructed to assess the quality of the alternatives. This study describes a novel, modified TOPSIS (M-TOPSIS) method.

Step 1: All the original criteria receive tendency treatment. We usually transform the non-beneficial criteria into benefit criteria, which is shown in detail as follows;

(i) The reciprocal ratio method ($X_{ij} = 1/X_{ij}$), refers to the absolute criteria;

(ii) The difference method ($X = 1 - X_{ij}$), refers to the relative criteria.

After tendency treatment, construct a matrix

$X' = [X']_{nxm}$, i = 1, 2, 3……m Eq.14

Construction of weighted matrix depends upon the weight value assigned to the different criteria. The summation of the all weight must be equal to one. In TOPSIS method the assigned weighted values are 0.3340, 0.3330 and 0.3330. These weighted values have been assigned using entropy method.

Step 2: Calculate the normalized decision matrix A. The normalized value a_{ij} is calculated as

$$A = [a_{ij}]_{n\times m}, a_{ij} = \frac{x'_{ij}}{\sqrt{\sum_{i=1}^{n}(x'_{ij})^2}} \quad i = 1,2,3 \ \ldots\ldots\ldots\ldots n \ \& j=1, 2, 3 \ \ldots\ldots\ldots\ldots m$$

Step 3: Determine the positive ideal and negative ideal solution from the matrix A.

$$A^+ = (a_{i1}{}^+, a_{i2}{}^+, \ldots\ldots\ldots\ldots\ldots\ldots a_{im}{}^+, a_{ij}{}^+) = \max(a_{ij}), \quad j = 1,2,\ldots\ldots\ldots\ldots m$$

$$A^- = (a_{i1}{}^{-+}, a_{i2}{}^-, \ldots\ldots\ldots\ldots\ldots\ldots a_{im}{}^-, a_{ij}{}^-) = \min(a_{ij}), \quad j = 1,2,\ldots\ldots\ldots\ldots m$$

Step 4: Calculate the separation measures, using the n-dimensional Euclidean distance. The separation of each alternative from the positive ideal solution is given as:

$$D_i^+ = \sqrt{\sum_{j=1}^{m} W_j(a_{ij}{}^+ - a_{ij})^2} \qquad \text{(Eq.15)}$$

Similarly, the separation from the negative ideal solution is given as

$$D_i^- = \sqrt{\sum_{j=1}^{m} W_j(a_{ij}{}^- - a_{ij})^2} \qquad \text{(Eq.16)}$$

Step5. For each alternative, calculate the closeness index R_i as:

$$R_i = \frac{D_i^-}{D_i^- + D_i^+} \qquad \text{(Eq.17)}$$

Step 6: Rank attributes in increasing order according to the closeness index value.

The attributes having highest value of closeness index is most preferable and the other attributes are taken in the decreasing order of their closeness index value.

Table 5.3 is the decision matrix in this problem and above sequential operations are performed on the basis of decision matrix to obtain the closeness index value for each and every alternative. Then the

Closeness index values are arranged in chronological order to get the best available alternative. The maximum closeness index value indicates the best alternative and lowest closeness index indicates the worst.

(iii) Multi Objective Optimization Ratio Analysis (MOORA)

Brauers introduced the MOORA approach, a multi-objective optimisation strategy that may be used to effectively tackle a variety of MCDM problems. The following is a discussion of the MOORA method's algorithms:

A matrix of answers (performance measures) from several possibilities on various criteria (objectives or qualities) is the first step in the MOORA approach. Below is the matrix.

$$X = \begin{array}{c} \\ A_1 \\ \vdots \\ A_i \\ \vdots \\ A_m \end{array} \begin{array}{c} \begin{array}{ccccc} C_1 & \cdots & C_j & \cdots & C_n \end{array} \\ \begin{bmatrix} x_{11} & \cdots & x_{1j} & \cdots & x_{1n} \\ \vdots & \cdots & \vdots & \cdots & \vdots \\ x_{i1} & \cdots & x_{ij} & \cdots & x_{in} \\ \vdots & \cdots & \vdots & \cdots & \vdots \\ x_{m1} & \cdots & x_{mj} & \cdots & x_{mn} \end{bmatrix} \end{array}$$

Where, x_{ij} is the performance rating (response) to the ith alternative (A_i) under jth Criterion (C_j) m is the number of alternatives and n is the number of criteria.

$$x_{ij}^{*} = \frac{x_{ij}}{\sqrt{\sum_{i=1}^{m} (x_{ij}^{2})}} \qquad \text{(Eq.18)}$$

x_{ij}^{*} is normalized value of response i with respect to attribute j. The maximum score for each feature has also been employed as the denominator of the ratio system in the current study, and an attempt has been made to demonstrate that this ratio system is likewise appropriate for identifying the best answer. The second-best ratio system for the MOORA normalisation process is the one below.

$$x_{ij}^{*} = \frac{x_{ij}}{\max_{i}(x_{ij})} \qquad \text{(Eq.19)}$$

Finding the highest score for each feature is the first step in calculating the normalized answer using the aforementioned Eq. 18. Next, using Eq. 19, all of the scores under a particular attribute benefit or not are reduced by the relevant maximum score, where x * is a dimensionless number in the range [0,1] that represents alternative I's normalized score on attribute j. On occasion, though, the interval might be [-1; 1]. For instance, the interval becomes [-1;1] when the productivity growth of certain factories, industries, sectors, regions, or nations is negative rather than positive.

These normalized performances are deducted in the case of minimisation and added in the case of maximisation for multi-objective optimisation. The optimisation issue then turns into:

$$y_i^* = \sum_{j=1}^{g} x_{ij}^* - \sum_{j=g+1}^{n} x_{ij}^* \qquad \text{(Eq.20)}$$

Where *g* is the number of benefit criteria to be maximized and *(n-g)* is the number of n-benefit criteria to be minimized. y_i^* is final score of i^{th} alternatives with respect to all the attributes. In the above case it is assumed that all the attributes are of same importance.

$$y_i^* = \sum_{j=1}^{g} w_j * x_{ij}^* - \sum_{j=g+1}^{n} w_j * x_{ij}^* \qquad \text{(Eq.21)}$$

Where, w_j^* is the weight of j^{th} attribute (criterion), which can be evaluated using any well-known approach either AHP or Entropy method. The value of y_i^* may be positive, negative or zero. These y_i^* values are arranged in descending order. The best alternative is one which is associated with highest y_i^* value and the worst alternative is one which is associated with the lowest y_i^* value.

4.2. EXPERIMENTAL RESULTS AND DISCUSSIONS

In the current research effort, experiments have been conducted following changes in process parameters, such as peak current (Ip), on time (Tonne), and flushing pressure, and their impacts on the responses, such as material removal rate (MRR), tool wear rate (TWR), and overcut (OC). Numerous measurements have yielded a variety of data, including the amount of weight reduction in the workpiece and tool, the machining time, and the blind hole entrance hole

diameters for the Alumina (Al_2O_3) workpiece, respectively. Ten trials in all have been conducted, and the performance characteristics have been analysed using the data collected.

4.2.1. Analysis based on Experimental Results

4.2.1.1. Effect of Coating Layer Thickness

Coating layer thickness has a very significant effect on the machining of ceramic workpiece. In the present research work, trial experiments have been performed on the alumina workpieces by varying the coating layer thickness. Firstly, eight wraps of coating (i.e. 0.2 mm) on the alumina workpiece have been done for performing the trial experiments. It has been observed that with the increment of coating layer thickness more conductive thickness comes in contact with the spark, thus more heat is dissipated during EDM machining and once the copper layer has been machined, the tool reaches ceramic surface. So, it has been observed that with the increment of coating layer thickness more internal thermal stresses have been generated in the ceramic material which has led to increase in thermal cracks on the ceramic workpiece.

After this it has also been observed that with the reduction in the coating layer thickness, thermal cracks on the ceramic workpiece have been reduced due to decrease in the thermal stresses. After several trial experiments with different coating layer thicknesses, it has been observed that the optimum conditions have been achieved with wrapping of the six layers of copper foil i.e. 0.15 mm. This has led to arrive at a conclusion that an optimum value of assisting electrode layer thickness leads to more stable machining in case of ceramic materials. Thus, it is needed to select an optimum thickness of the assisting electrode in order to perform machining on ceramics. Thus, in thus research work 0.15 mm of coating layer thickness has been chosen as the optimum coating layer thickness for the further research work.

4.2.1.2. Effect of Dielectric Fluid

Dielectric fluids play a very crucial role in case of EDM machining on ceramics. In the present research work, several trial experiments have been performed with two types dielectric i.e. deionized water and EDM oil. In the former case, it has been observed that EDM machining on ceramics is not suitable due to the non-formation of carbon layer on the machined surface which is very much essential for carrying out the further machining. It has been observed that it can machine to the depth which is exactly the thickness of the assisting electrode. As the non-conducting surface of ceramic comes in contact with the tool the machining ceases. But in the case of EDM oil, due to the formation of carbon layer on the machined surface machining is

possible up to the desired depth. In EDM oil there is dissociation of hydro-carbon taking place at the machining site and carbon gets deposited on the non-conducting workpiece. This carbon forms a pyrolytic carbon layer which assists further machining of ceramics. This carbon deposition is not possible in case of deionized water because of absence of hydro-carbon. Thus, it can be concluded that hydro-carbon based EDM oil is the only option for machining of alumina. Hence, in this experimentation EDM oil has been selected as the dielectric fluid and performed further experiments.

4.2.1.3. Effect of Tool Materials

Trial experimentation has been performed with two types of electrodes i.e. copper electrode with OD as 4 mm and ID as 3 mm and a solid tungsten carbide tool with diameter of 2 mm. In the first case, internal flushing of dielectric fluid has been incorporated and in the latter case vertical flushing has been used. The former case has not given the desire result because of the two things. Firstly, because of internal flushing carbon deposition is not taking place on the machined surface due to high pressure of flushing which ceases machining after certain depth. Secondly, the more tool diameter results in the heat energy getting unevenly dissipated in the alumina workpiece resulting in more HAZ. But in the latter case i.e. tungsten carbide the desired output has been obtained because of the desirable tool diameter with solid tool and vertical flushing. Because in case of solid tool more heat energy gets focused on the machining area which results in the better machining with reduced HAZ. Hence, from this experimentation it can be concluded that tungsten carbide (WC) is the most suitable tool material for machining of alumina. Thus, in the present research work tungsten carbide tool has been used for further machining.

4.2.1.4. Effect of Tool Shape

The machining is also affected by the tool's form. Copper and tungsten carbide electrodes have been used in the current research trial investigation. The former is a hollow tool electrode with a cylindrical shape, and the latter is a drill bit with built-in flutes around the edge. Because of its small diameter and the flutes on its outside periphery, the tungsten carbide drill bit tool has been shown to produce better machining during trial operations.

These flutes' presence facilitates the easy removal of machined by-products and aids in the dielectric's smooth flow into the machining zone, both of which are highly desirable in ceramic machining. There is no chance of machined by-products becoming stuck in the cutting region

because they are quickly eliminated through these flutes, resulting in smooth machining. Therefore, it may be said that the ideal tool electrode for EDM alumina machining is a tungsten carbide drill bit. As a result, the tungsten carbide drill bit has been selected as the tool electrode for the additional research.

4.2.1.5. Effect of Workpiece Thickness

It has been noted that in non-conducting ceramics, workpiece thickness is crucial when cutting alumina with EDM. Alumina (Al_2O_3) workpieces with two distinct thicknesses—5 mm and 1 mm—were selected for the experimental experiment. A 5 mm thick workpiece has blind holes machined into it, whereas a 1 mm thick workpiece has through holes cut into it. A 1 mm thick workpiece has been found to be unable to tolerate the thermal stresses produced during EDM operation, leading to the formation of cracks on the workpiece's exit side.

Similar to EDM, thermal ablation is used to remove material, which results in a variety of three-dimensional surface and subsurface flaws. Thus, as Fig. 4.1 illustrates, thermal cracks spread readily in workpieces that are 1 mm thick. Alumina workpieces with a thickness of 5 mm, on the other hand, are resistant to the aforementioned surface and subsurface flaws, meaning that the machined surface shows no signs of heat cracking. As a result, a 5 mm thick alumina workpiece has been chosen for additional testing.

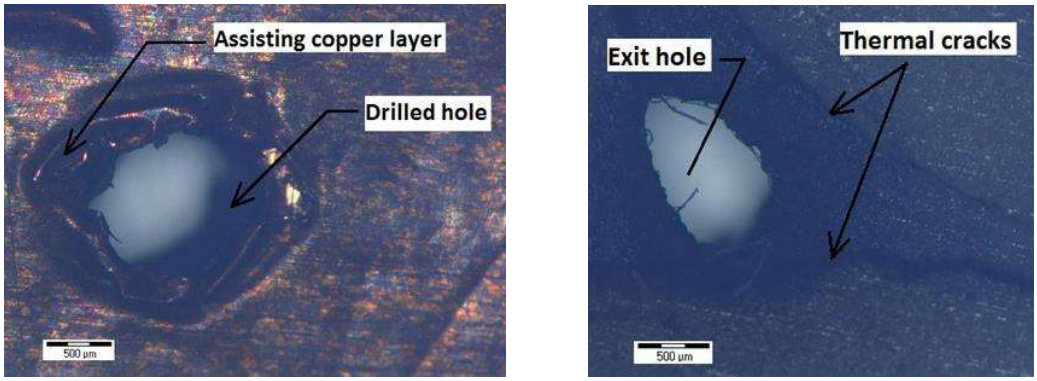

(a) Hole at the entry side of workpiece (b) Hole at the exit side of workpiece

Fig. 4.1. Thermal cracks propagated in the Alumina of 1 mm thickness

4.2.1.6. Effect of different process parameters on Machining Performances

In the present research work the main aim is to study the influence of major process parameters e.g. peak current (Ip), on time (Ton) and flushing pressure on the machining responses e.g. the material removal rate (MRR) and minimize the tool wear rate (TWR) and overcut (OC). Therefore, a suitable range of these process parameters i.e. peak current (Ip) (1A, 2A, 3A, 4A),

on time (Ton) (3µs, 5µs, 7.5µs, 10µs) and flushing pressure (0kg/cm2, 5 kg/cm2, 10 kg/cm2, 15 kg/cm2) have been selected and the graphs have been plotted accordingly.

4.2.1.6.1. Effects of different process parameters on material removal rate (MRR)

(i) ***Peak current (Ip)***

One of the most important factors in EDM material machining is peak current. However, conductive materials and non-conductive ceramics are machined using different principles. When it comes to conductive materials, the material removal rate rises as peak current (Ip) rises because larger peak currents result in more energy at the machining site, which raises the material removal rate and, ultimately, MRR. However, as our experiment showed, in the case of non-conductive ceramics, increasing peak current results in a decrease in the rate of material removal. The trend between Ip and MRR is displayed in the graph in Figure 4.2.

There is a decrease in MRR beyond peak current (Ip) of 1 A because increasing peak current leads to more carbon deposition in the workpiece and on the tool, which produces a very sharp spark while machining and reducing the removal of material from ceramic.

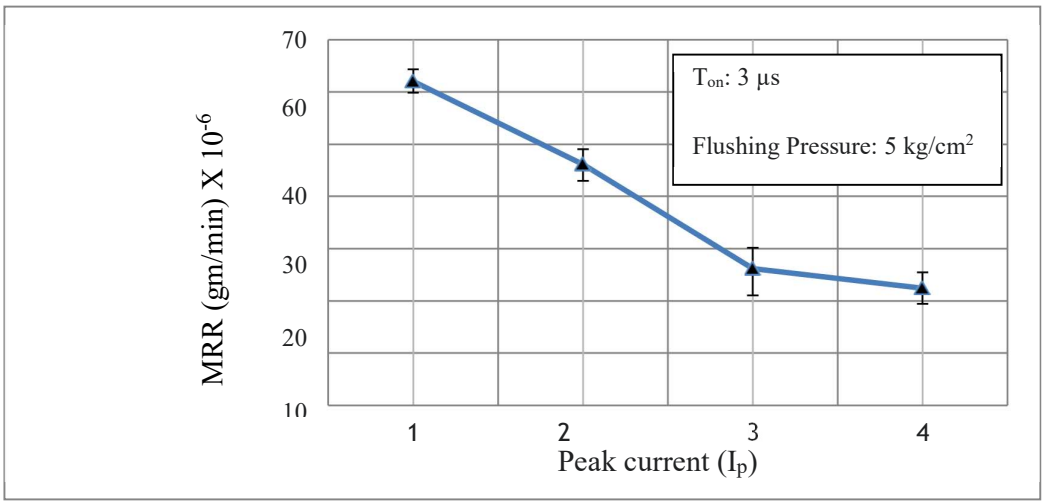

Fig. 4.2. Variation of MRR (gm/min) due to variation in Peak current (A)

To investigate the carbon deposition on the Alumina (Al_2O_3) workpiece XRD analysis has been done of both the machined and unmachined surfaces as shown in Fig.4.4. The machined surface shows the deposition of pyrolytic carbon layer on the machined surface of alumina whereas as shown the Fig.4.3 the unmachined surface is free from carbon.

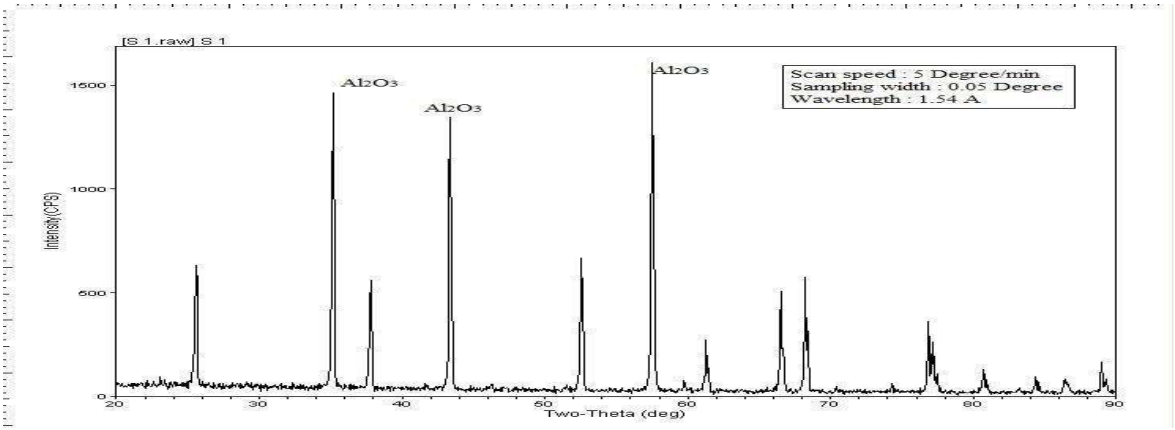

Fig. 4.3. XRD analysis of the unmachined Al_2O_3 workpiece

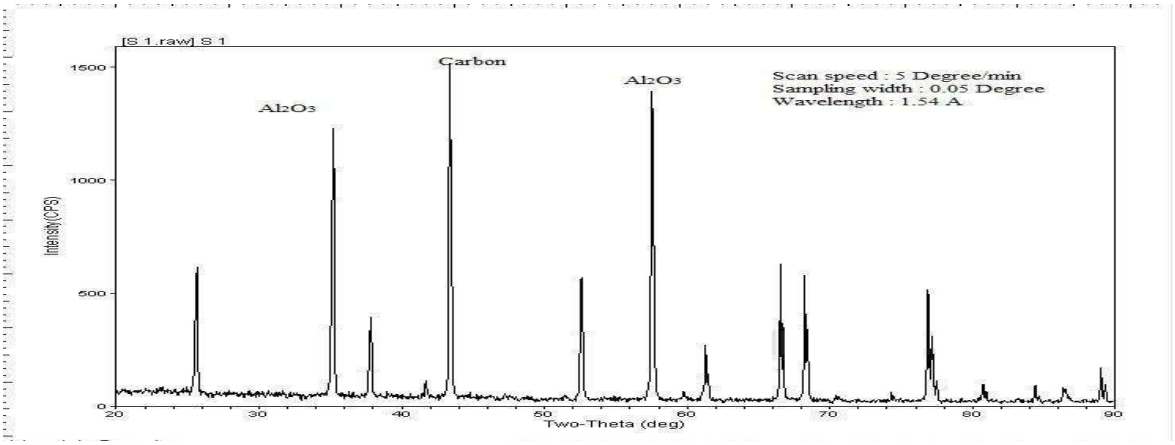

Fig. 4.4. XRD analysis of the machined surface of Al_2O_3 workpiece

(ii) ***On time (Ton)***

One of the most crucial factors in figuring out the material removal rate (MRR) is on time (Ton). In conductive materials, increasing on time often results in increased material removal due to the increased thermal energy on the machining surface. However, in ceramics, specifically alumina, MRR currently exhibits a decreasing tendency as on time (Ton) increases. The trend is displayed on the graph in Fig. 4.5. The MRR decreases as on-time increases because, in the case of ceramics, on-time increases result in increased carbon deposition on the workpiece, which makes it more difficult for the tool electrode to remove material. Hence, decreasing the material removal rate.

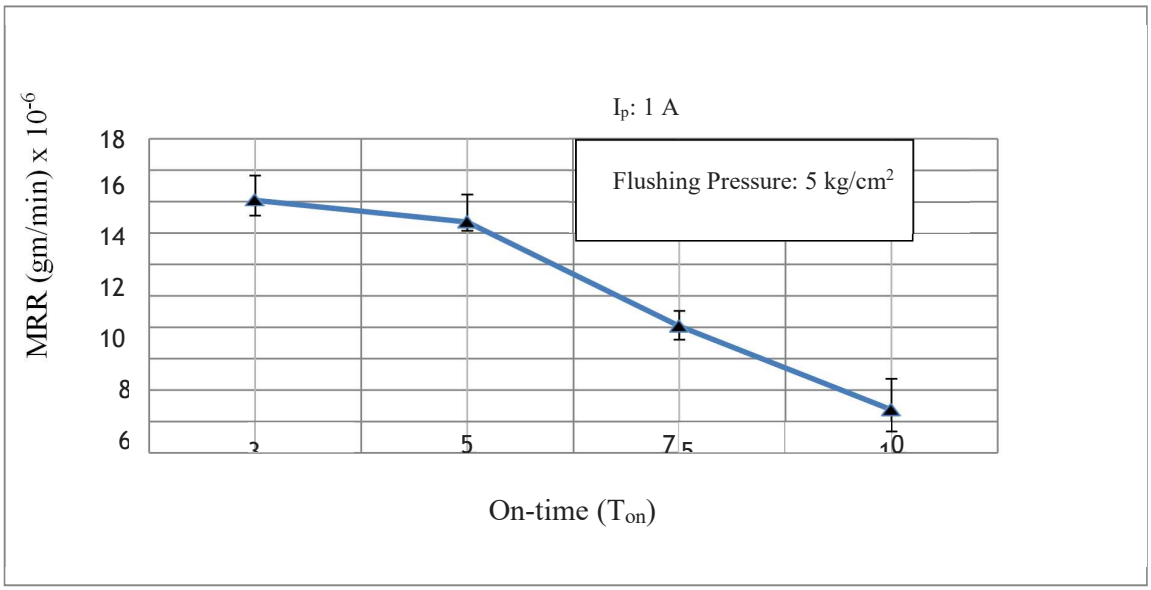

Fig.4.5. Variation of MRR (gm/min) vs On-time (µ-sec)

4.2.1.6.2. Effects of different process parameters on tool wear rate (TWR)

(i) ***Peak current (Ip)***

Peak current (Ip) has a major impact on the rate of tool wear. Since more energy is focused on the machining surface in EDM, more heat is produced, which leads to tool wear. Generally speaking, raising the peak current also increases the tool wear rate. However, when it comes to ceramics (in this example, Al_2O_3), raising the peak current causes more carbon to be deposited on the tool tip surface, preventing wear and eventually extending the tool's wear life (Fig. 4.6).

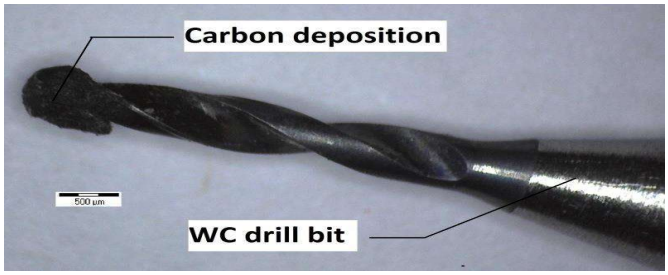

Fig.4.6. Deposition of carbon on the tool tip surface

Thus, deposition of the carbon on the tool is helpful in increasing tool life and reducing tool wear. Hence increasing peak current decreases tool wear in case of non-conducting ceramics. In Fig.4.7 the graph shows the trend.

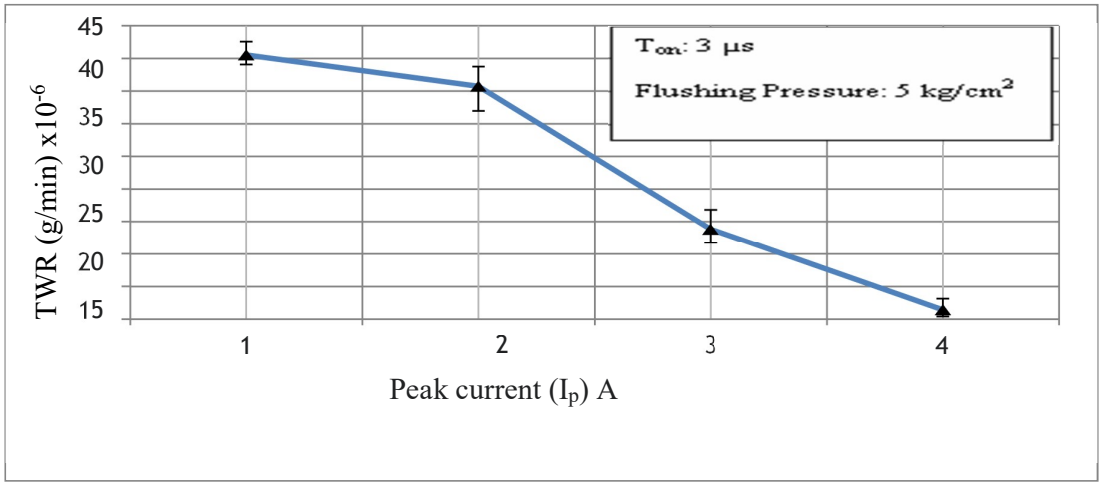

Fig.4.7 Variation of TWR (gm/min) on Peak current (A)

Further it is seen that since carbon deposition is taking place on the tool by increasing peak current, therefore a XRD report has been plotted in Fig.4.8 to show the presence of carbon on tool electrode, which prevents tool wear.

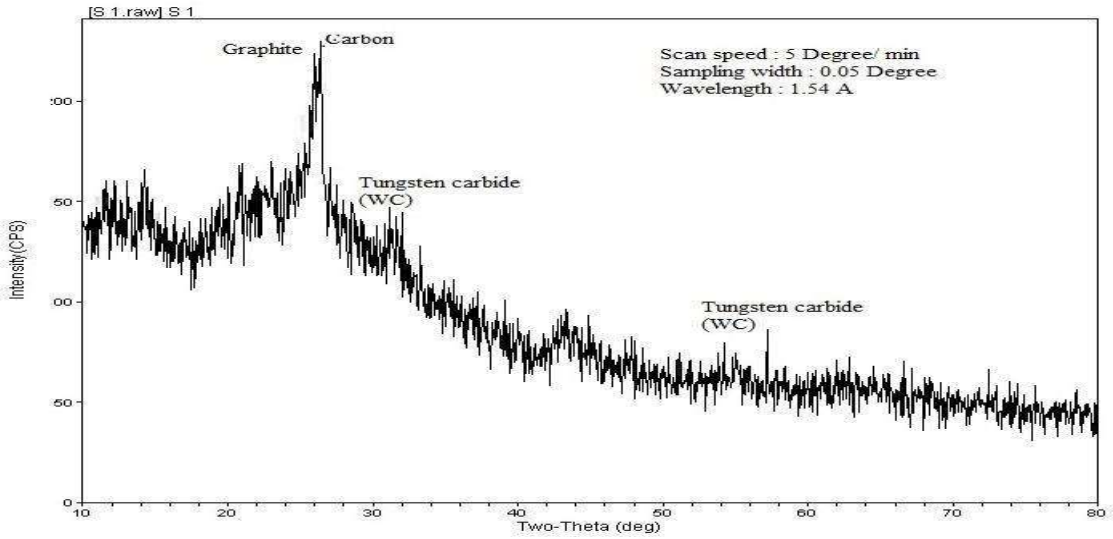

Fig.4.8 XRD analysis of the tungsten carbide tool after machining

(ii) ***On time (Ton)***

Increasing on time leads to increase in tool wear rate in normal EDM process because increasing on time results in increase of energy on the machined area eventually increasing temperature which is unfavorable for the tool electrode material thus, resulting in the increase in tool wear rate. But in case on non- conducting materials Al_2O_3 (in our case) the behavior is entirely reverse. Increasing the on time leads to increase in the heat thus resulting in more

dissociation of hydro-carbon dielectric, thus forming carbon on the tool electrode material. The carbon deposited on the tool surface increases the tool life and thus reduces the tool wear rate. In Fig.4.9 graph shows the trend of on time vs tool wear rate.

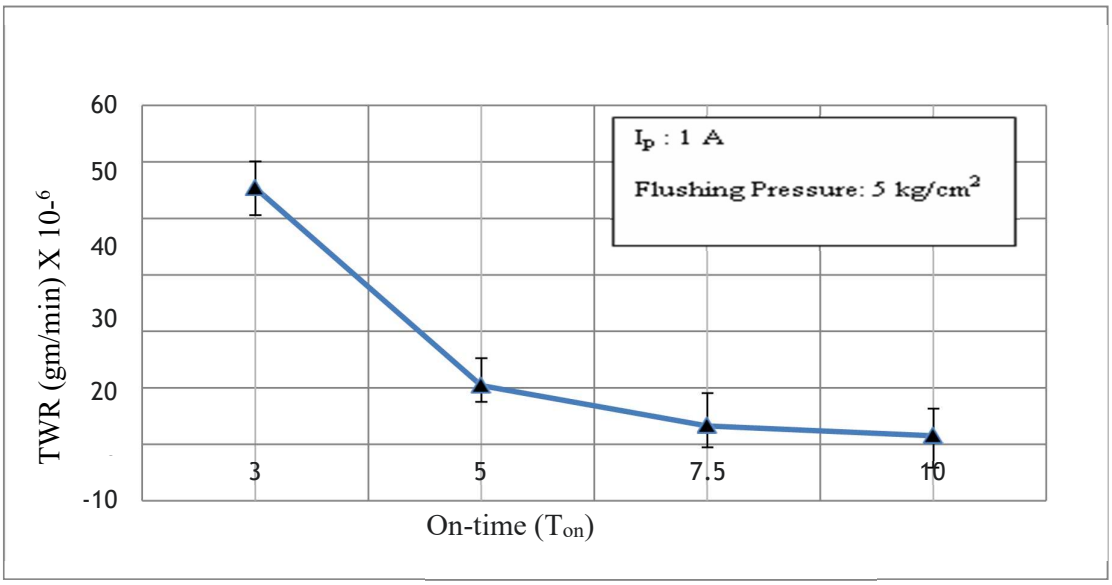

Fig.4.9 Variation of TWR (gm/min) vs On time (µ-s)

4.2.1.6.3. Effects of different process parameters on overcut (OC)

4 ***Peak current (Ip)***

Increasing peak current results in the more heat dissipation on the machining surface, resulting more heat getting distributed. This leads to an increase in the HAZ of the machined area and increased overcut. Hence overcut (OC) shows an increasing trend with the peak current. In Fig.4.10 graph shows the trend

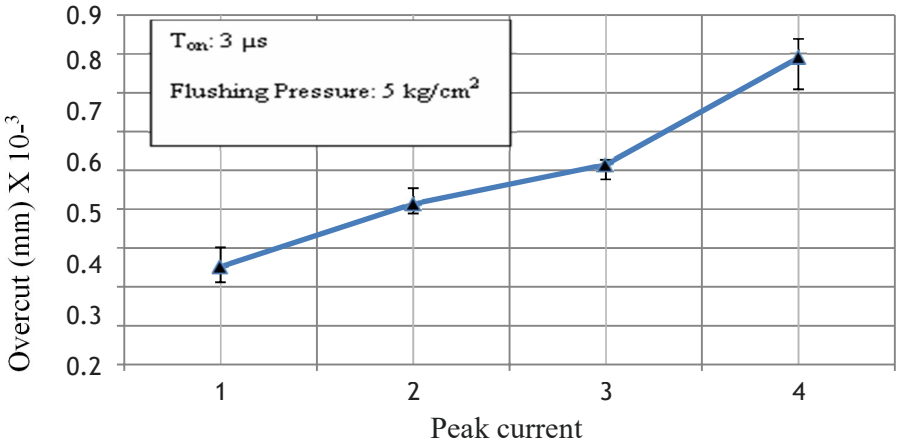

Fig. 4.10 Variation of Overcut (OC) (mm x10^{-3}) vs Peak current (Amp)

5 ***On time (Ton)***

Increasing on time results in the more heat concentration thus increasing the HAZ of the machined area. Hence overcut (OC) shows an increasing trend with the peak current. So basically, on time has the same effect on the over cut (OC) as that of the peak current. In Fig.4.11 graph shows the trend

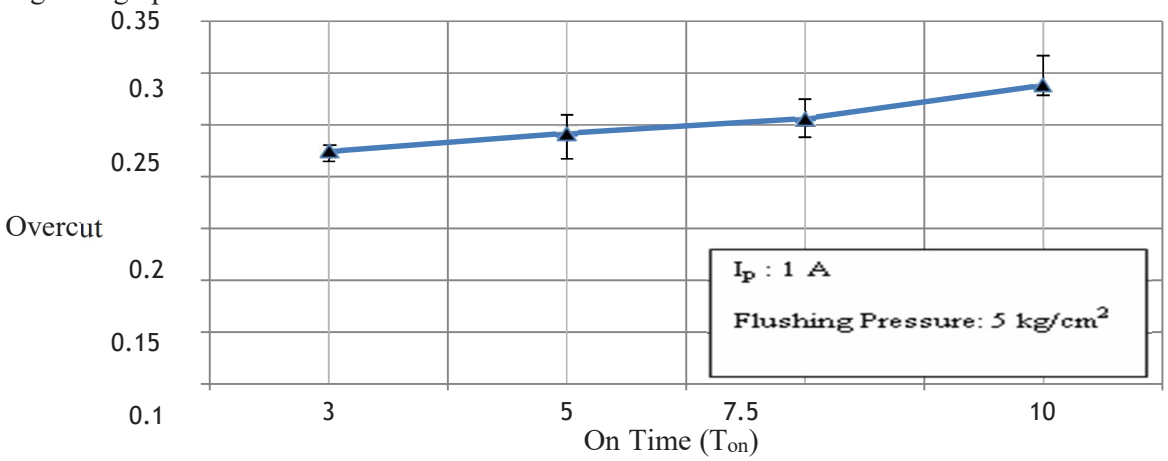

Fig.4.11 Variation of Overcut (OC) vs On-time

4.3 Determination of Suitable Parametric Combination Based On Different Multi-Criteria Decision Making (MCDM) Methods

In different MCDM methods, the final result obtained on the basis of some calculated mathematical value of each and every alternative. In this study, the whole interest is subjected to best three available alternatives from every MCDM analysis. Then the common best parametric combination has been obtained from every technique selected. That particular parameter setting has been further used to perform machining on Alumina (Al_2O_3) workpiece for validation of the result obtained.

Decision matrix has been formed on the basis of the parametric combinations based on which the experimentation has been done as depicted in Table 4.3. In this section most influencing parametric combination has to be searched out based on the steps followed in SAW, TOPSIS and MOORA method which have been mentioned in the earlier chapter.

(i) TOPSIS method

In TOPSIS method normalized decision matrix has been obtained based on the Eq.16 as listed in below Table 4.3

Table 4.3. Normalized decision matrix obtained

Experiment no.	MRR	TWR	Overcut(OC)
1	0.4888	0.0361	0.9020
2	0.3638	0.0410	0.5485
3	0.2064	0.1060	0.4410
4	0.1768	1.0000	0.2875
5	0.9300	0.0325	0.3381
6	0.1261	0.0729	0.8676
7	0.1103	0.0760	1.0000
8	1.0000	0.1410	0.9394
9	0.5099	0.4478	0.8866
10	0.0591	0.9756	0.7881

In TOPSIS method, determination of positive ideal solution has been done by taking the maximum values of each column from the normalized decision matrix i.e. 1, 1 and 1. Similarly, the negative ideal solution has been calculated by taking the minimum values of each column from the normalized decision matrix i.e.0.0591, 0.0325 and 0.2875. Finally, the ranking of the parametric combinations has been done based on the closeness index which is calculated with the help of separation measures i.e. Di^+ and Di^-. The values of Di^+ and Di^- have been calculated with the help of Eq.15 and Eq.16 as depicted in Table 4.4.

Table 4.4. Values of Separation measure

Experiment no	(Di^+)	(Di^-)	R_i	Rank
1	0.6323	0.4329	0.4064	
2	0.7137	0.2317	0.2451	
3	0.7619	0.1300	0.1457	
4	0.6288	0.5624	0.4722	
5	0.6776	0.5041	0.4266	
6	0.7397	0.3378	0.3135	
7	0.7407	0.4130	0.3580	
8	0.4969	0.6642	**0.5720**	**1st**
9	0.4313	0.4948	**0.5343**	**2nd**
10	0.5575	0.6161	**0.5250**	**3rd**

From the Table 4.4 and Fig. 4.12 it can be observed that the experiment number 8, 9 and 10 having separation measures of 0.5720, 0.5343 and 0.5250 respectively. So as per the result is concerned experimental parameter setting number 8 i.e. 1 A peak current, 5µs on time and 5 kg/cm2 flushing pressure is the best parametric combination as it comes by minimizing the non-beneficial criteria and maximizing the beneficial criteria.

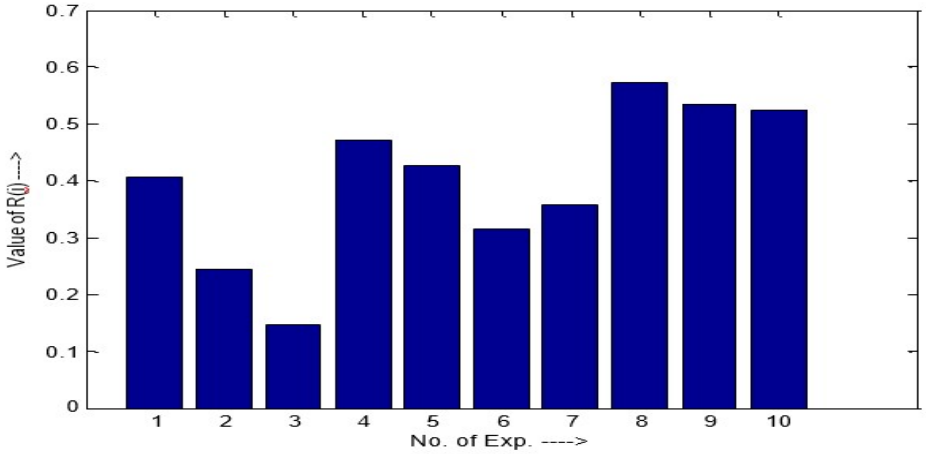

Fig.4.12 Graph showing the best parametric condition using TOPSIS method

(i) ***MOORA*** **method**

In *MOORA* method normalized decision matrix has been obtained on the basis of Eq.20 as listed in the following Table 4.5

Table 4.5. Normalized decision matrix obtained

Experiment no	**MRR**	**TWR**	**Overcut(OC)**
1	0.3031	0.5217	0.1825
2	0.2255	0.4600	0.3002
3	0.1280	0.1779	0.3734
4	0.1096	0.0188	0.5727
5	0.5766	0.5796	0.4870
6	0.0782	0.2586	0.1898
7	0.0684	0.2480	0.1647
8	0.6200	0.1337	0.1753
9	0.3162	0.0421	
10	0.0366	0.0193	0.2089

The weighted normalized decision matrix in MOORA method is obtained by the Eq.21 as

listed in the Table 4.6

Table 4.6. Weighted normalized decision matrix obtained

Experiment no	MRR	TWR	Overcut
1	0.1012	0.1737	0.0608
2	0.0753	0.1532	0.1000
3	0.0427	0.0592	0.1243
4	0.0366	0.0063	0.1907
5	0.1926	0.1930	0.1622
6	0.0261	0.0861	0.0632
7	0.0228	0.0826	0.0548
8	0.2071	0.0445	0.0584
9	0.1056	0.0140	0.0618
10	0.0122	0.0064	0.0696

In *MOORA* method, the weighted multi objective optimization is done by calculating the value of 'a' which is the sum of all weighted normalized values for all beneficial column i.e. 0.8224 and the value of 'b' i.e. the sum of all weighted normalized values for all non-beneficial column i.e. 0.2345, 0.2531, 0.1836, 0.1970, 0.3552, 0.1493, 0.1374, 0.1029, 0.0759 and 0.0760.

Finally, the ranking of the parametric combinations has been done based on the basis of final score value i.e. a – b which is calculated with the help of the Eq.23 and the values of a - b obtained are 0.5878, 0.5692, 0.6388, 0.6254, 0.4672, 0.6730, 0.6849, 0.7195, 0.7465 and 0.7463.

From Fig.4.13 below it can be observed that the experimental parameter setting number 9, 10 and 8 respectively having final score 0.7465, 0.7463 and 0.7195 respectively. So as per the result is concerned experimental parameter setting number 9 i.e. 1 A peak current, 7.5 µs on time and 5 kg/cm2 flushing pressure is the best parametric combination as it minimizes the non-beneficial criteria and maximizes the beneficial criteria.

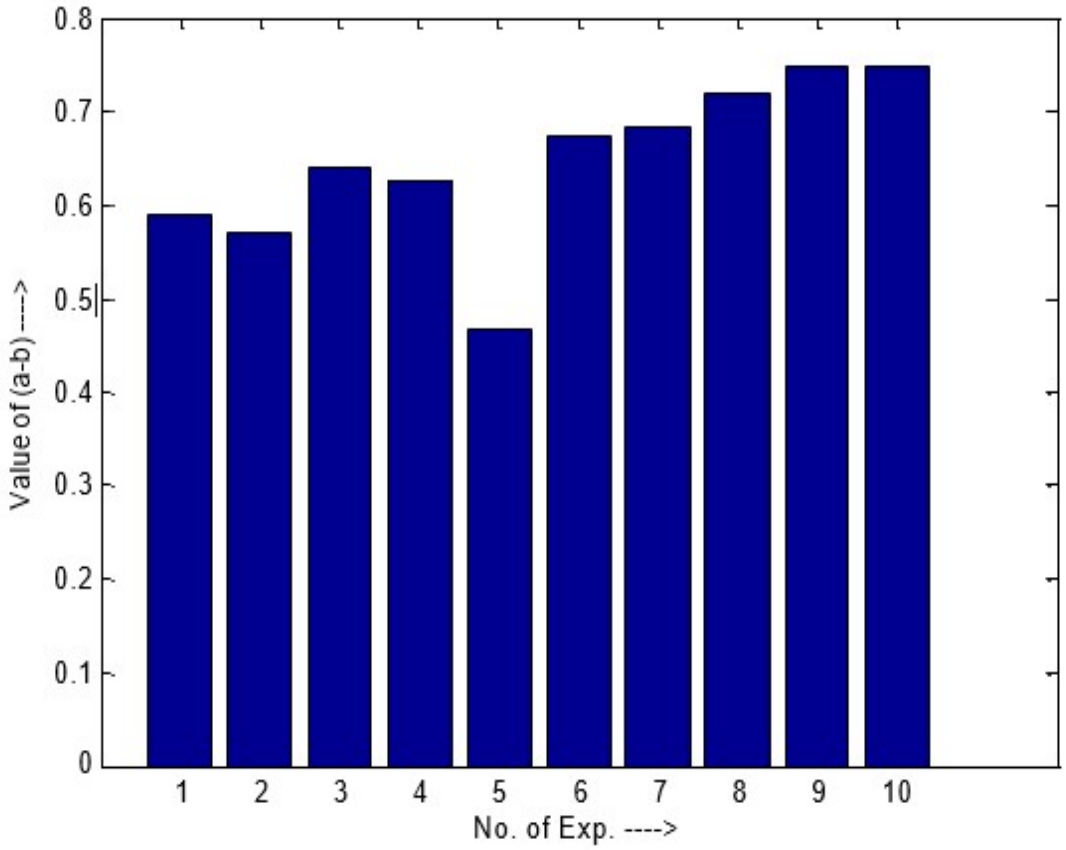

Fig.4.13 Graph showing the best parametric conditions using MOORA method

(ii) SAW method

The normalized and weighted normalized decision matrix is calculated based on the Eq.11 as listed in Table 4.7 and Table 4.8 respectively.

Table 4.7. Normalized decision matrix obtained

Experiment no.	MRR	TWR	Overcut(OC)
1	0.4888	0.0361	0.9020
2	0.3638	0.0410	0.5485
3	0.2064	0.1060	0.4410
4	0.1768	1.0000	0.2875
5	0.9300	0.0325	0.3381
6	0.1261	0.0729	0.8676

7	0.1103	0.0760	1.0000
8	1.0000	0.1410	0.9394
9	0.5099	0.4478	0.8866
10	0.0591	0.9756	0.7881

Table 4.8 Weighted normalized decision matrix obtained

Experiment no	MRR	TWR	Overcut (OC)
1	0.1633	0.0120	0.3004
2	0.1215	0.0136	0.1826
3	0.0689	0.0353	0.1469
4	0.0591	0.3330	0.0957
5	0.3106	0.0108	0.1126
6	0.0421	0.0243	0.2889
7	0.0369	0.0253	0.3330
8	0.3340	0.0470	0.3128
9	0.1703	0.1491	0.2953
10	0.0197	0.3249	0.2624

In SAW method the value of composite score 's' is calculated by sum of all weighted normalized rows and is given by Eq.14 as listed in the Table 4.9.

Table 4.9. Composite score 's' by sum of all weighted normalized rows

Rank								1st	2nd	3rd
s	0.4757	0.3178	0.2511	0.4878	0.434	0.3553	0.3952	0.6958	0.6147	0.6071

SAW method gives result on the basis of composite score 's'. From the above Table 4.9, it can be observed that the experimental parameter setting number 8, 9 and 10 having composite score value 0.6958, 0.6147 and 0.6071 respectively. Therefore, as per the result is concerned experimental parameter setting number 8 i.e. 1 A peak current, 5µs on time and 5 kg/cm2 flushing pressure is the best parametric combination as it minimizes the non-beneficial criteria and maximizes the beneficial criteria as shown in the Fig.4.14.

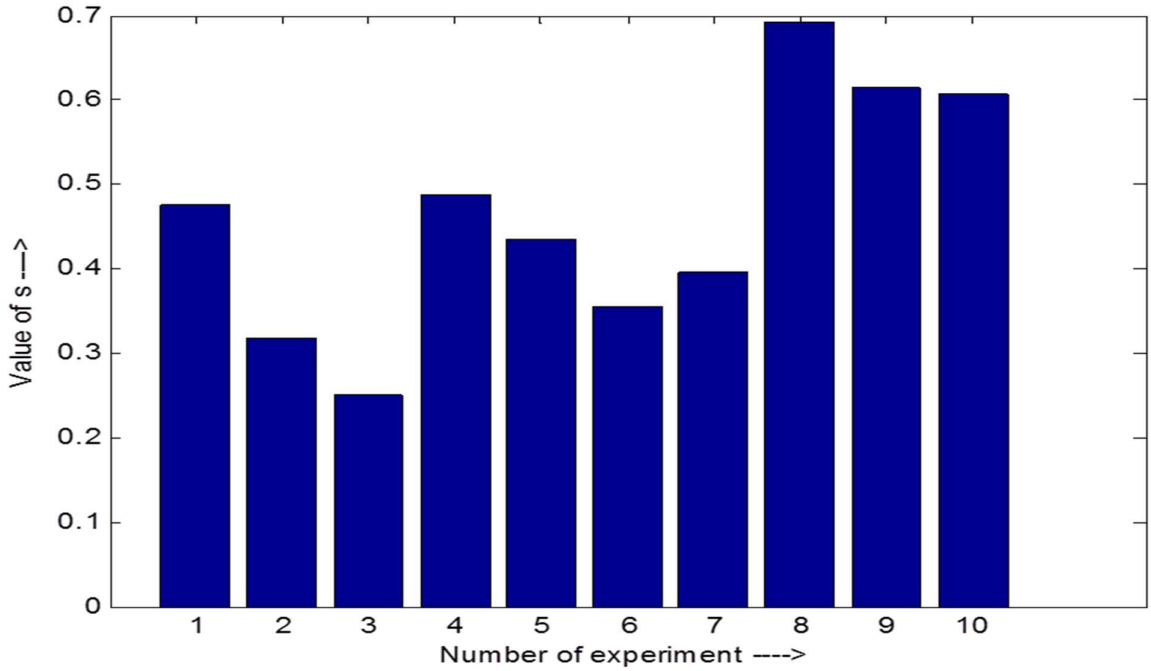

Fig. 4.14 Graph showing the best parametric condition using *SAW* method

From the above three MCDM techniques it can be concluded that the TOPSIS and SAW method exhibits the same ranking i.e. row no. 8, 9 and 10, but MOORA gives the ranking 9, 10 and 8. But, it can also be seen from the Fig.6.17 that in MOORA method the value of (a-b) of experiment no 8, 9 and 10 are very close. Therefore, the best parametric combination considering all the three optimization techniques has been selected as experiment no. 8 i.e. peak current 1A, on time 5µs and flushing pressure 5kg/cm^2 which will give the best responses i.e. maximizing material removal rate (MRR) and minimizing tool wear rate (TWR) and overcut (OC).

Therefore, considering all the above results in this chapter it can be established that the best parametric combination obtained on the basis of experiments performed by varying one process parameter at a time is the experiment no.1 i.e. peak current (I_p) 1 A, on time (T_{on}) 3µs and flushing pressure 5kg/cm^2, whereas, the best parametric combination obtained based on the optimization technique is the experiment no 8 i.e. peak current (I_p) 1 A, on time (T_{on}) 5µs and flushing pressure 5kg/cm^2 . The machined alumina surfaces considering both the parametric conditions have been shown in the Fig. 4.15 using LEICA microscope.

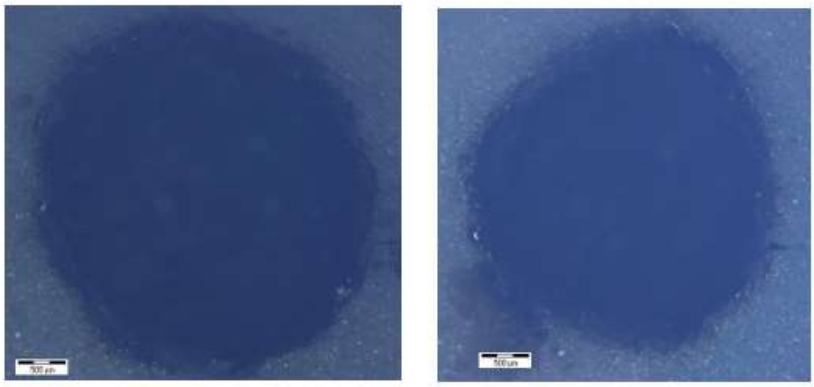

(a) (b)

(a) Machined hole at (1 A, 3 μs, 5kg/cm^2)

(b) Machined hole at (1 A, 5 μs, 5kg/cm^2)

Fig.4.15. Machined surfaces after removing the copper layer

From the above Fig.4.15 it has been very clearly observed that the quality and the accuracy of the drilled hole e.g. circularity, overcut etc. are better by using parametric combination obtained from the optimization technique as compared to the hole drilled using the experimental parametric combination. Therefore, it can be concluded that the parametric combination i.e. peak current (Ip) 1 A, on time (Ton) 5 μs and flushing pressure 5 kg/cm^2 is the best parametric combination in order to maximize MRR and minimize TWR and overcut (OC).

4.4 OUTCOMES OF THE PRESENT INVESTIGATION

(i) EDM has great potential for cutting as well as drilling of electrically conducting and non-conducting materials e.g. ceramics assisting electrode method".

(ii) It can be concluded that, as far as material of the assisting electrode is concerned, copper is best suited for EDM drilling of Al_2O_3.

(iii) In comparison to deionizer water, EDM oil is best suited for machining of Al_2O_3 due to it's ability to dissociate into hydro-carbons. This results in formation of pyrolytic carbon layer that is solely responsible for carrying out the further machining.

(iv) In comparison to cylindrical tool, drill bit is appropriate for machining of Al_2O_3 because of better flushing as well as removal of the machined byproducts through the flute of the drill bit.

(v) Peak current (Ip), on time (Ton) and flushing pressure are the most influencing parameters on the performance characteristics e.g. material removal rate (MRR), tool wear rate (TWR) and overcut (OC).

(vi) The most optimal range of peak current, on time and flushing pressure are 1 to 4 A, 3 to10 μs and 0 to 15 kg/cm^2 respectively during EDM drilling of Al_2O_3. From the experimentation, this has been observed that increasing peak current (Ip) decreases MRR and TWR but increases overcut (OC), similarly increasing on time (Ton) decreases MRR and TWR but increases overcut (OC). In case of flushing pressure all the three responses i.e. MRR, TWR and overcut (OC) decreases with increase in flushing pressure value.

(vii) From the experimentation by varying one process parameter at a time it has been observed that peak current (I_p) of 1 A, on-time (T_{on}) of 3 μs and 5 kg/cm^2 of flushing pressure is the best parametric combination.

5. EXPERIMENTAL INVESTIGATION ON SHAPE MEMORY ALLOY MATERIAL, NiTiNOL

5.1. PLANNING FOR EXPERIMENTATION

To conduct the experiments during drilling operation an EDM set-up has been utilized. A copper tool of diameter 2 mm was chosen for experimentation and connected to the negative terminal of power supply. A pulsed D.C. power was supplied between the workpiece and tool and it delivers the voltage ranging from 0 to 100 V.

The experimental scheme has been designed in such a way that experiments can be carried out for parametric analysis on EDM performances during machining of shape memory alloy. In the present set of experimental study, EDMing operation was performed on work sample NiTiNOL. The straight and reverse polarity approach selected to carry out the optimization of variable control parameters of machining operation of NiTiNOL.These properties make NiTiNOL an exceptional material for a wide range of applications, particularly in the medical field, aerospace, robotics. Its unique combination of shape memory, super-plasticity and biocompatibility distinguishes it from other materials. The material NiTiNOL utilized for the experimentation consists of chemically 49.1% Ni and 50.9% Ti. The physical properties of NiTiNOL have been listed in the Table 5.1.

Table5.1: Physical and mechanical Properties of NiTinol

Melting Temperature	1240 - 1310 °C
Resistivity (high temp. state)	82 μΩ-cm
Resistivity (low temp. state)	76 μΩ-cm
Thermal Conductivity	0.1W/cm/°C
Heat Capacity	0.077 cal/gm-°C
Latent Heat	5.78 cal/gm
Tensile Strength	Austenite: 195-690 MPa Martensite: 70 -140 MPa
Young's Modulus	Austenite: 83 GPa Martensite: 28-41GPa
Density	6.45 gm/cm^3

The selection of process parameters in EDM process is crucial for achieving desired outcomes and optimizing the machining performance. A series of trial experiments are conducted to arrive at an understanding to observe all the variables, responses, and their relationship for the drilling operation. It was found that the most influencing process parameters in EDM were peak current, pulse on time and sparking time. The present research work attempts to make investigation on EDM characteristics such as material removal rate (MRR), taper angle during machining of NiTiNOL. During machining peak current, pulse on time and sparking time will be considered as the process parameters during experimentation.

Selecting a copper electrode for EDM machining on NiTiNOL involves considering various factors to optimize the machining performance. Copper is a popular choice due to its advantageous properties such as electrical conductivity, thermal conductivity, wear resistance etc. the photographic view of the tool is shown in the Fig. 5.1 below. Selecting the right dielectric fluid is crucial for optimizing the EDM machining process of NiTiNOL. EDM oil is commonly used as a dielectric fluid due to its beneficial properties such as electrical insulation and cooling effect. To assess the effect of each machining parameter on the process and correlate between different process parameters and machining performance characteristics the Taguchi approach and Response Surface Methodology (RSM) were used.

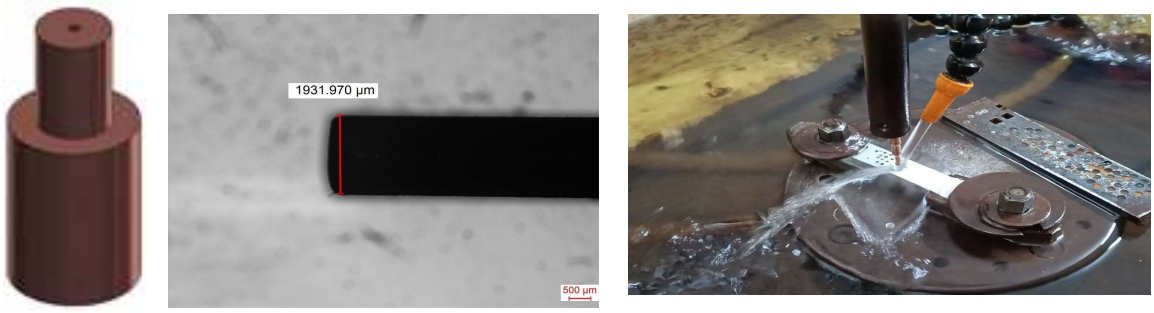

Fig. 5.1 Photographic and microscopic images of tool-electrode

5.2.INVESTIGATION BASED ON TAGUCHI METHOD

Taguchi method provides the designer a systematic and well-organized approach for conducting experimentation in order to determine optimum setting of process parameters in regard of performance and cost. It was developed by Genichi Taguchi in the 1950s and has been widely applied in various fields, including manufacturing, engineering, and quality control. The method

emphasises pushing quality back to the design stage seeking to design a product/process, which is insensitive to quality problems. This method can reduce research and development costs simultaneously by studying a large number of parameters. Orthogonal arrays are used in the Taguchi method to reduce experimental error and examine a lot of variables in a few experiments. Given the number of control elements, their levels, and the intention to examine particular relationships, an orthogonal array can be built for a given robust design project. OAs are designed to provide a balanced design by ensuring that all levels of other factors occur an equal number of times for every level of any one element. In this present study the levels of process parameters have been shown in Table 5.2. With one process parameter at two levels and three process parameters at three levels, total DOF is 8= [1+1x (2-1) +3x (3-1)] and it a mixed level combination. The interaction between the parameters is not taken into account in this study. The closest array is the L18 Orthogonal array, which includes four columns—two at two levels and three at three levels of the relevant factors—but it is determined from the DOF value that at least eight trials must be carried out to assess the effects of each machining parameter. Consequently, the selected array The Taguchi technique gives the designer a methodical and structured way to experiment to find the best process parameter settings in terms of cost and performance. Genichi Taguchi created it in the 1950s, and it has since been widely used in a variety of industries, such as engineering, manufacturing, and quality assurance. The approach places a strong emphasis on bringing quality back to the design phase in an effort to create a process or product that is insensitive to issues with quality. This approach, which examines many factors, can lower research and development expenses at the same time.

Orthogonal arrays are used in the Taguchi method to reduce experimental error and examine a lot of variables in a few experiments. Given the number of control elements, their levels, and the intention to examine particular relationships, an orthogonal array can be built for a given robust design project. OAs are designed to provide a balanced design by ensuring that all levels of other factors occur an equal number of times for every level of any one element.

In this present study the levels of process parameters have been shown in Table 5.2. With one process parameter at two levels and three process parameters at three levels, total DOF is 8= [1+1x (2-1) +3x (3-1)] and it a mixed level combination. In this study, the interaction among the parameters is not considered.

Therefore, the chosen array Taguchi method provides the designer a systematic and well-organized approach for conducting experimentation in order to determine optimum setting of process parameters in regard of performance and cost. It was developed by Genichi Taguchi in

the 1950s and has been widely applied in various fields, including manufacturing, engineering, and quality control. The approach places a strong emphasis on bringing quality back to the design phase in an effort to create a process or product that is insensitive to issues with quality. This approach, which examines many factors, can lower research and development expenses at the same time. Orthogonal arrays are used in the Taguchi method to reduce experimental error and examine a lot of variables in a few experiments. Given the number of control elements, their levels, and the intention to examine particular relationships, an orthogonal array can be built for a given robust design project. OAs are designed to provide a balanced design by ensuring that all levels of other factors occur an equal number of times for every level of any one element.

In this present study the levels of process parameters have been shown in Table 5.2. With one process parameter at two levels and three process parameters at three levels, total DOF is 8= [1+1x (2-1) +3x (3-1)] and it a mixed level combination. In this study, the interaction among the parameters is not considered. From the value of DOF, it is concluded that at least eight experiments have to be conducted to estimate the effects of each machining parameter but nearest array is L_{18} Orthogonal array, which has four columns, one at two levels and three at three levels of the corresponding factors. Therefore, the chosen array was L_{18} (1^2 x 3^4) array that has 18 rows with 17 DOFs. On the basis of input factors and their levels eighteen experiments have been conducted. The standard methods of constructing orthogonal arrays L_{18} are given bellow. The matrix form of these arrays is shown in Table 5.3, where 1, 2, 3, 4 in the table represents the level of each parameter.

Table 5.2. Process parameters and their levels

Parameters	Symbols	Levels		
		1	2	3
Polarity		+	-	
Peak current (A)	I_p	6	9	12
Pulse On-time (μs)	T_{ON}	10	20	30
Spark time (μs)	T_w	2	4	6

Here, '+ve' indicates Straight polarity when workpiece is connected with positive terminal of power supply and tool is connected with negative terminal and '-ve' indicates reverse polarity when workpiece is connected with negative terminal of power supply and tool is connected with positive terminal.

Table 5.3. Combinations of control parameters based on L_{18} Orthogonal array

Expt. No.	Col. No. & Factor assignment				Actual values of process parameters			
	1	2	3	4	Polarity	Peak current (A)	Pulse On-time (μs)	Spark time (μs)
1.	*1*	*1*	*1*	*1*	+	6	10	2
2.	*1*	*1*	*2*	*2*	+	6	20	4
3.	*1*	*1*	*3*	*3*	+	6	30	6
4.	*1*	*2*	*1*	*1*	+	9	10	2
5.	*1*	*2*	*2*	*2*	+	9	20	4
6.	*1*	*2*	*3*	*3*	+	9	30	6
7.	*1*	*3*	*1*	*2*	+	12	10	4
8.	*1*	*3*	*2*	*3*	+	12	20	6
9.	*1*	*3*	*3*	*1*	+	12	30	2
10.	*2*	*1*	*1*	*3*	-	6	10	6
11.	*2*	*1*	*2*	*1*	-	6	20	2
12.	*2*	*1*	*3*	*2*	-	6	30	4
13.	*2*	*2*	*1*	*2*	-	9	10	4
14.	*2*	*2*	*2*	*3*	-	9	20	6
15.	*2*	*2*	*3*	*1*	-	9	30	2
16.	*2*	*3*	*1*	*3*	-	12	10	6
17.	*2*	*3*	*2*	*1*	-	12	20	2
18.	*2*	*3*	*3*	*2*	-	12	30	4

The Taguchi technique analyses the data using a statistical performance metric known as the signal-to-noise (S/N) ratio. Both the mean and the variability are taken into consideration by the S/N ratio. The criterion for optimising the quality characteristic determines the S/N ratio equation. Maximising the S/N ratio, a mathematically transformed form of the quality/performance characteristic, reduces quality loss and statistically increases the additivity of control factor impacts.

From each experimental result S/N value can be calculated as follows:

For the 'larger-the-better' type problem

$$\eta = -10 log_{10}\left[\frac{1}{n}\sum_{i=1}^{n}\frac{1}{y_i^2}\right] \quad \text{(Eq.5.1)}$$

For 'smaller-the-better' type problem

$$\eta = -10 log_{10}\left[\frac{1}{n}\sum_{i=1}^{n} y_i^2\right] \quad \text{(Eq.5.2)}$$

For 'nominal-the-best' type problem

$$\eta = 10\log_{10}\left[\frac{\mu^2}{\sigma^2}\right] \quad \text{(Eq.5.3)}$$

Where, η = the S/N ratio calculated from observed values in dB,

y_i = the experimental observed value of the ith experiment

n = the number of repetitions.

$$\mu = \frac{1}{n}\sum_{i=1}^{n} y_i \text{ and } \sigma^2 = \frac{1}{n-1}\sum_{i=1}^{n}\left(y_i - \mu\right)^2$$

The Grand mean value of η_m is calculated as

$$\eta_m = \frac{1}{n}\sum_{i=1}^{N}\eta_i \quad \text{(Eq.5.4)}$$

The effect of a factor level is defined as the deviation it causes from the Grand mean. The average S/N ratio at any one level suppose A_1 for experiments 1, 2 and 3, which is denoted by η_{A1} is given by

$$\eta_{A1} = \frac{1}{3}\left[\eta_1 + \eta_2 + \eta_3\right] \quad \text{(Eq.5.5)}$$

Therefore, (ηA1 – ηm) gives the influence of that parameter at level A1. It is possible to determine the average numerical value η_{Ai} for every level of the factors by taking the numerical values of η. The S/N ratio curve is a graphic representation of these averages. The performance is influenced to varying degrees by several elements. The average η for each factor level could be used to assess the relative magnitude of the factor effects. The decomposition of the variance, sometimes referred to as analysis of variance (ANOVA), can provide a better sense of the relative impact of the various elements. It is employed to look into which machining settings had a major impact on the measured values.

In this investigation, ANOVA and the F-test were applied to analyse the experimentally obtained data to justify their significant effect on different machining characteristics. The related meaning and equations are given in the Table 5.4 as below.

Table 5.4. Analysis of Variance (ANOVA)

Sources	Sum of squares	DOF
Factor A	$SS_{AA} = 2[(\eta_{A1} - \eta_m)^2 + (\eta_{A2} - \eta_m)^2]$	(q-1)
Factor B	$S_{BB} = 3\left[\left(\eta_{B1} - \eta_m\right)^2 + \left(\eta_{B2} - \eta_m\right)^2 + \left(\eta_{B3} - \eta_m\right)^2 \right]$	(q-1)
Factor C	$S_{CC} = 3\left[\left(\eta_{C1} - \eta_m\right)^2 + \left(\eta_{C2} - \eta_m\right)^2 + \left(\eta_{C3} - \eta_m\right)^2 \right]$	(q-1)
Factor D	$S_{DD} = 3\left[\left(\eta_{D1} - \eta_m\right)^2 + \left(\eta_{D2} - \eta_m\right)^2 + \left(\eta_{D3} - \eta_m\right)^2 \right]$	(q-1)
Error	$S_{EE} = S_{TT} - \left(S_{AA} + S_{BB} + S_{CC} + S_{DD}\right)$	(N-1)-$\left(\sum (q-1)\right)$
Total	$S_{TT} = \sum_{i=1}^{N} \left(\eta_i - \eta_m\right)^2$	N-1

Where, q = no. of levels of each parameter

η_i = the mean value of each experiment (i = 1,. . .,N)

η_{Ai} = the sum of ith level of parameter A (i = 1,2 or i = 1,2,3)

N= Total no. of experiments

The mean sum of square each factor has been calculated by dividing sum of square of each parameter/ factor by its degree of freedom and then F-value of each parameter/ factor has been calculated as a ratio of Mean sum of square of each parameter/ factor to the Mean sum of square of Error. F_α, n_1, n_2 is as quoted from the "Tables for Statisticians" where (1-α) is the percentage of confidence level. If the computed F-values exceed the standard $F\alpha, n_1, n_2$, the input parameters' contribution is considered significant at the (1-α) confidence level. The anticipated optimal setting does not have to match one of the matrix experiment's rows when designing parameters using the Taguchi method. To check that the ideal circumstances recommended by the matrix experiments for the anticipated improvement are met, an experimental confirmation test is conducted at the predicted optimum levels for the control parameters under study. The recommended ideal circumstances will be implemented if the anticipated and observed benefits line up. Finding improved quality attributes or S/N ratios, varying control factors and levels, or researching a few particular interactions among the control elements are some examples of the corrective measures.

The last stage is to forecast and confirm the enhancement of the EDM process's quality attributes following the choice of the best parametric condition for the machining parameters. The following formula is used to get the S/N ratio's anticipated ideal value:

$$\eta_{opt} = \eta_m + \sum_{i=1}^{p} (\bar{\eta}_i - \eta_m) \quad \text{(Eq.5.6)}$$

Where, η_m= the grand mean of S/N ratio,

$\bar{\eta}_i$ = the mean S/N ratio at the optimal level and

p = the number of main design parameter that affects the quality characteristics.

5.2.1 EXPERIMENTAL PROCEDURE

After selection of the tool, dielectric, the ranges of peak current, pulse on-time and spark time, experiments have been carried out in S-35 ZNC EDM. The procedural steps for performing experiments are described as follows:

(i) The job has been set in position in job holding device and clamped rigidly by tightening the nut.

(ii) The levels of different process parameters e.g. polarity, pulse on-time, spark time, voltage have been set according to Taguchi Method.

(iii) The machining has been performed until through-hole is achieved and time has been recorded by a stop-watch.

(iv) The experimentations have been performed three times at each parametric combination and the average value of machining criteria has been utilized for statistical analyses.

(v) An optical Olympus measuring microscope (LC 0.5 μm) was used to measure the diameter of the machined micro-hole. The material removal rate was measured using a Metler Toledo weighing machine (LC 1x10-5 g) and computed using the weight difference method. Using the following Eqs. 5.7 and 5.8, as well as the following Fig. 5.2, the MRR and taper angle of holes have been determined.

$$MRR = \Pi [((D_{en} + D_{ex})^2 L/16)] \quad \text{(Eq.5.7)}$$

$$\text{Taper angle} = \tan^{-1} [(D_{en} - D_{ex})/2 L] \quad \text{(Eq.5.8)}$$

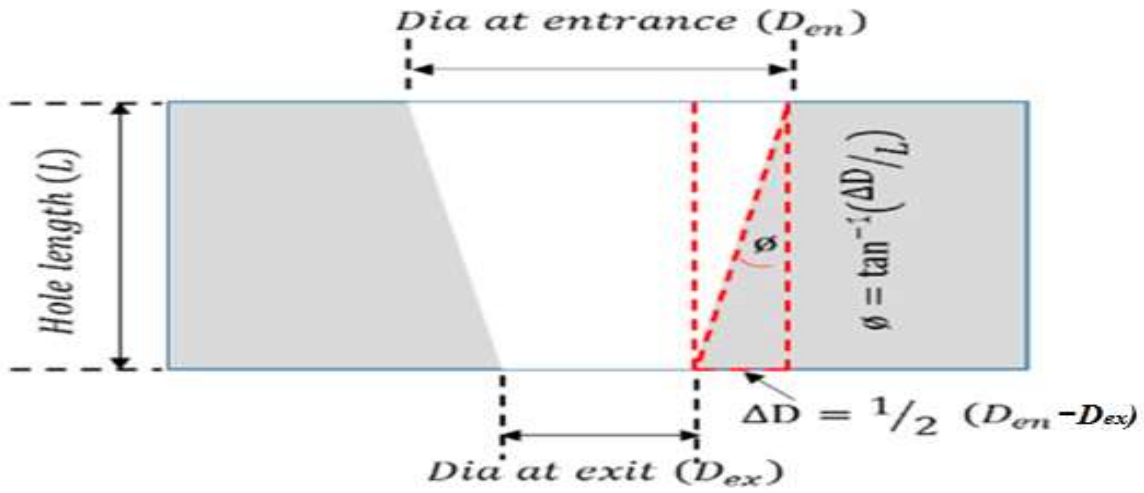

Fig. 5.2 Cross-section of a hole

5.2.2 Results and Discussion

On the basis of experiments which have been performed after setting all the parameters at different combinations, various data were obtained from various measurements such as thickness of workpiece, entry diameter, exit diameter and tool diameter. A total of 18 experiments have been carried out. The results and the discussion section aim to analyse and interpret the data collected during the experiments and provide a comprehensive discussion of the outcomes. It allows for a deeper understanding of the effects of various parameters and their impact on the machining performance.

5.2.2.1 Experimental Results

The main objective of this experiment is to get maximum value of MRR with the "Larger is better" quality type problem for maximizing the MRR. In this experiment Eq.6.1 was utilized to get signal to noise (S/N ratio) for "larger the better" type responses respectively. The average values of experimental results and corresponding S/N ratios of various performance characteristics have been listed in Table 5.5. The photographic view of workpiece NiTinol has been depicted the following Fig. 5.3.

Table 5.5: Experimental Results Based on Taguchi Method and corresponding S/N Ratios for MRR

Expt. No.	Machining Time (s)	MRR (mm^3/s)	S/N Ratio (dB)
1	164.49	0.0042322	-47.46867634

2	92.97	0.0106231	-39.47497461
3	142.96	0.0070242	-43.06806263
4	224.99	0.0036711	-48.7040757
5	79.47	0.0236991	-32.50536293
6	58.49	0.032551	-29.7487133
7	199.09	0.0099302	-40.06084009
8	86.02	0.0228584	-32.81908344
9	53.26	0.0359294	-28.8910007
10	85.4	0.0032674	-49.71595391
11	94.7	0.0047626	-46.44311785
12	163.34	0.0032074	-49.8769375
13	94.81	0.0037625	-48.49046983
14	74.82	0.0043095	-47.3114623
15	164.34	0.0023822	-52.46043559
16	97.86	0.0047116	-46.53663174
17	173.96	0.0025917	-51.72830543
18	136.04	0.0042322	-47.46867634

The other objective of this experiment is to get the minimum value of taper angle with the "smaller is better" quality type problem for minimizing the taper angle. In this experiment Eq. 6.2 was utilized to get signal to noise (S/N ratio) for "smaller the better" type response. The average values of experimental results and corresponding S/N ratios of various performance characteristics have been listed in Table 5.6.

Table 5.6: Experimental Results Based on Taguchi Method and corresponding S/N Ratios for Taper angle

Expt. No.	Entry Diameter (μm)	Exit Diameter (μm)	Taper Angle (rad)	S/N Ratio (dB)
1	1615.307	1085.942	1.145141	0.27105
2	1759.926	1473.819	0.872813	-0.27207
3	1762.865	1498.552	0.833571	-0.36407
4	1695.065	1255.14	1.071378	0.13789

5	2067.619	2399.659	0.944929	-0.11329
6	2079.741	2411.869	0.945055	-0.11324
7	2141.439	2436.572	0.888063	-0.23742
8	2128.851	2436.448	0.90822	-0.19253
9	2104.241	2399.658	0.888533	-0.23637
10	1310.517	310.952	1.335153	0.57809
11	1615.257	470.688	1.364105	0.62099
12	1679.698	593.738	1.35329	0.60508
13	1353.614	533.952	1.285955	0.50300
14	1399.812	347.747	1.346512	0.59503
15	1522.892	412.273	1.357973	0.61199
16	1628.029	483.335	1.364127	0.62103
17	1621.269	461.448	1.366748	0.62487
18	1692.115	788.403	1.311217	0.54191

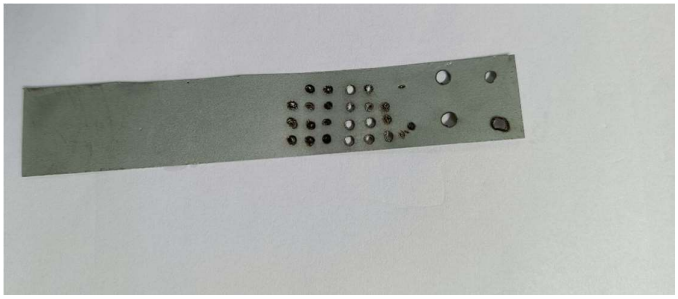

Fig 5.3 Workpiece (NiTinol) after Machining

5.2.2.2 Analysis on the effects of process parameters for different performance Characteristics

The Taguchi philosophy of orthogonal arrays effectively ascertains the effects of different parameters in robust design. Signal to noise (S/N) ratio measurements have been used as the basis for the analysis of the experimental outcomes.

5.2.2.2.1 Analysis on the effects of process parameters for MRR

The S/N ratio of graphs as shown in the Fig. 5.4 represents the variation of average S/N ratio at different level of machining parameters. According to the "Larger is better" principle the maximum value of S/N ratio refers to the Maximum MRR. In straight polarity MRR is found more compared to reverse polarity. The microscopic views of hole at different polarities are

shown in the Fig. 5.5. Peak current increases the material removal rate because it produces more intense sparks that erode the material faster. However, it also worsens surface roughness due to deeper and more irregular craters, increases electrode wear, and can cause more thermal damage to the workpiece, potentially leading to micro-cracks or a heat-affected zone. Longer pulse on time also increases the material removal rate as more energy is input per pulse, leading to more material being eroded. However, it can also increase surface roughness due to larger craters on the workpiece surface, enlarge the heat-affected zone, and result in a thicker recast layer that may need additional processing to remove. Sparking time refers to the actual duration of the spark occurrence, related to the duty cycle of the EDM process. Higher sparking time means more frequent discharges, which increases the material removal rate. However, it can degrade surface integrity due to more consistent thermal cycling, potentially causing more thermal stresses and defects. It also accelerates electrode wear and can sometimes lead to unstable machining conditions like arcing or short-circuiting, which can damage both the workpiece and the electrode.

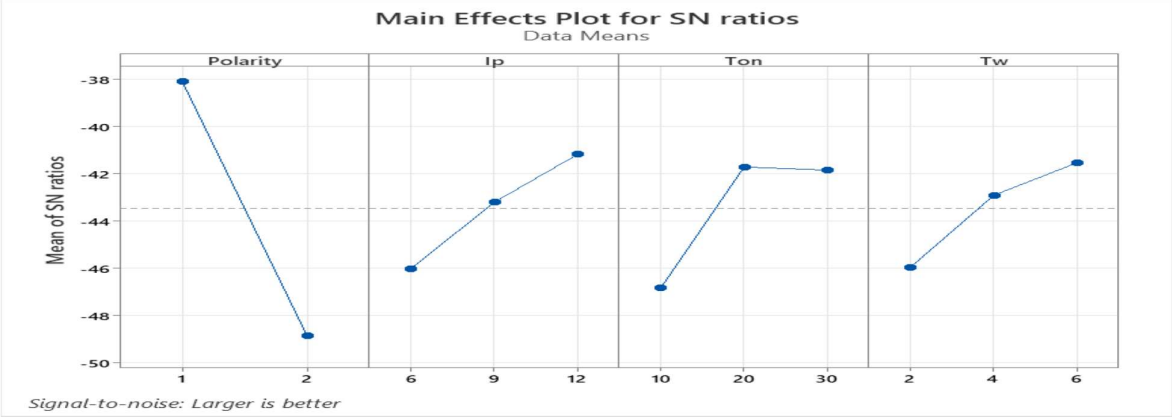

Fig 5.4 Effects of process parameters on MRR

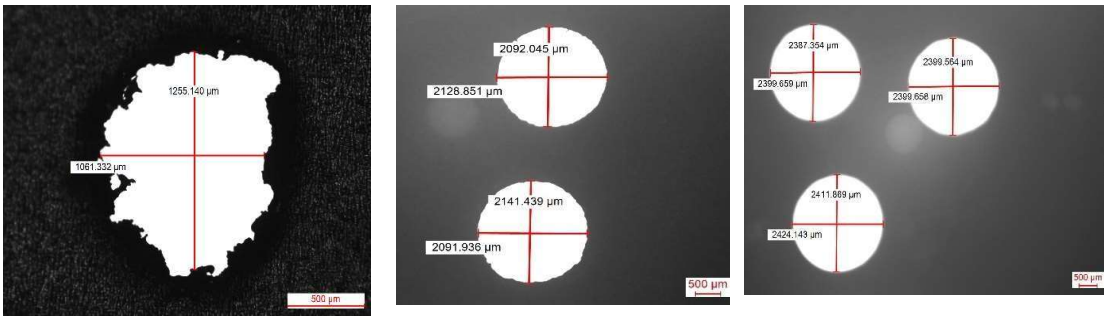

(a) Straight Polarity

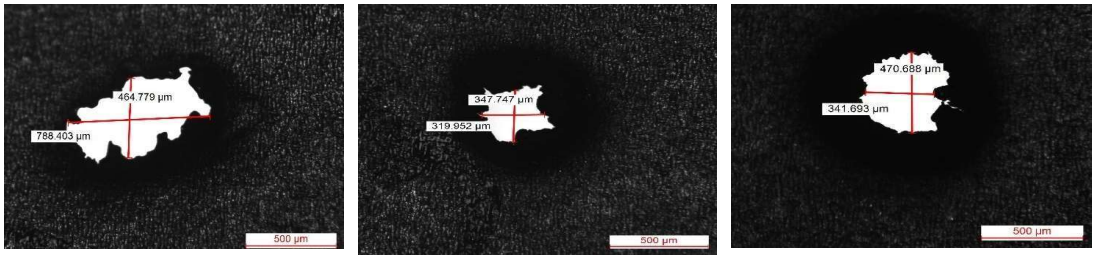

(b) Reverse Polarity

Fig 5.5 Microscopic views of NiTinol after machining at 12A/20µs/6s

5.2.2.2.2 Effect of Different Process Parameters on Taper angle

The effects of different process parameters on Taper angle have been analyzed based on S/N ratios and exhibited in the Fig. 5.6. The S/N ratio of graphs as shown in the figure represents the variation of average S/N ratio at different level of machining parameters. According to the "smaller is better" principle the maximum value of S/N ratio refers to the minimum Taper Angle. In straight polarity MRR is found more compared to reverse polarity. Peak current increases taper angle increase. The possible reason is that the sparking intensity increases with increase of peak current. Longer pulse on time also increases the material removal rate as more energy is input per pulse, which increases the material removal rate as well as taper angle. Larger sparking time means more frequent discharges. But at 6s of sparking time there may be a chance deposition of molten metal on machining zone due to improper flushing.

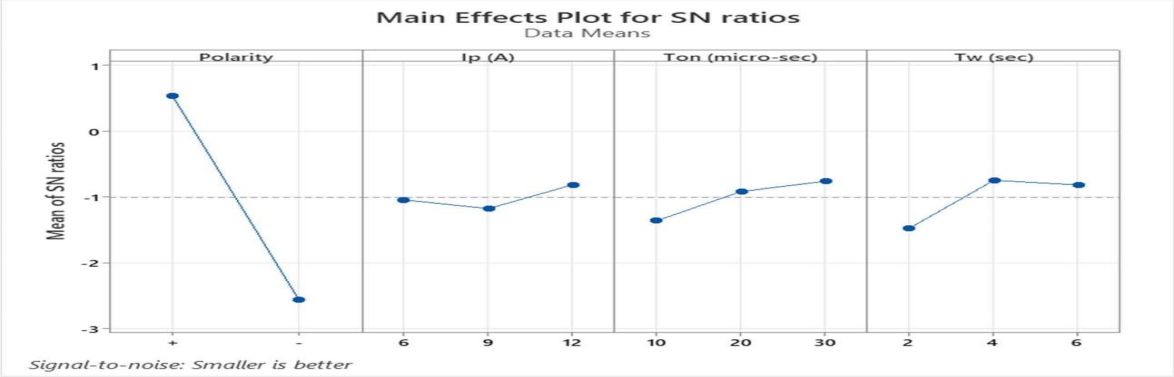

Fig 5.6 Effects of process parameters on Taper Angle

5.2.2.3 Analysis of Variance (ANOVA) test for MRR and Taper angle

The Analysis of Variance (ANOVA) was conducted to assess the contributions of various parameters to Material Removal Rate (MRR). The results are summarized in the Table 5.7. Polarity exhibits a significant influence on MRR, with a percentage contribution of 81.67%. This indicates that polarity has a substantial impact on material removal efficiency. Ip demonstrates a moderate effect on MRR, contributing 5.53% to the variance observed. Although its contribution is relatively lower compared to Polarity, it still plays a discernible role in determining MRR. Ton shows a noteworthy influence on MRR, contributing 8.01% to the overall variance. This suggests that adjusting the on-time duration can significantly affect material removal efficiency. Tw contributes 4.79% to the variance in MRR. While its influence is not as pronounced as other parameters, it still contributes to the variability observed in material removal. According to ANOVA test polarity and pulse on-time are significantly most influential process parameters.

Table 5.7 Analysis of Variance (ANOVA) test for MRR

Source	DOF	Seq SS	Adj MS	F-ratio	Percentage Contribution
Polarity	1	521.18	521.18	20.81	81.67
Ip	2	70.58	35.29	1.41	5.53
Ton	2	102.03	51.02	2.04	8.01
Tw	2	61.28	30.64	1.22	4.79
Error	10	250.53	25.05		
Total	17	1005.61			

The Analysis of Variance (ANOVA) was carried out to assess the contributions of various parameters to taper angle. Polarity exhibits a significant influence on Taper angle, with a

percentage contribution of 96.12%. This indicates that polarity has a substantial impact on material removal efficiency. Ip demonstrates a very low effect on Taper angle contributing 0.45% to the variance observed. Although its contribution is relatively lower compared to Polarity, it still plays a distinct role in determining taper angle. Ton shows a noteworthy influence on Taper angle, contributing 1.29% to the overall variance. Tw contributes 2.14% to the variance in MRR. While its influence is not as pronounced as other parameters, it still contributes to the variability observed in material removal. The results are summarized in the Table 5.8.

Table 5.8 Analysis of Variance (ANOVA) test for Taper angle

Source	DOF	Seq SS	Adj MS	F-ratio	Percentage Contribution
Polarity	1	43.231	43.231	139.99	96.12
Ip	2	0.4027	0.20135	0.65	0.45
Ton	2	1.1589	0.5795	1.88	1.29
Tw	2	1.9245	0.9622	3.12	2.14
Error	10	3.0876	0.3088		
Total	17	49.7867			

5.2.2.4 Determination of optimal parametric combination

The effects of different process parameters on Nitinol machining performance have been analysed and discuss based on the S/N ratio curves previously. At the same time there is a requirement of determining the optimal parametric condition, which can reduce the time as well as cost of machining. From the analyses of the S/N ratio curves the best combinations for the machining for different optimal requirements have been obtained and shown in the Table 5.9.

Table 5.9. Optimal parametric combination for maximum MRR and minimum Taper angle

parameters	Levels of process parameters	
	For maximum MRR	For minimum Taper angle
Polarity	Straight	Straight
Peak current (Ip)	12 A	12 A
Pulse On-time (Ton)	20 μs	30 μs
Spark Time (Tw)	6 s	4 s

Fig. 5.7 shows a hole obtained at straight polarity (+),with peak current (Ip) of 12 A, pulse on time (Ton) of 30 μs, and sparking time (Tw) of 4 second.

(a) Entry of hole **(b) Exit of hole**

Fig. 5.7 Microscopic views of hole with Straight polarity at 12A/30μs/4s

5.2.3 OUTCOMES OF THE INVESTIGATION

(i) In straight polarity MRR is found more compared to reverse polarity. Peak current increases the material removal rate because it produces more intense sparks that erode the material faster. MRR increase with pulse on-time and sparking time.

(ii) In straight polarity MRR is found more compared to reverse polarity. Peak current increases taper angle increase. Peak current increases taper angle increase. Sparking also increase taper angle.

(iii) According to ANOVA test polarity and pulse on-time are significantly most influential process parameters.

(iv) Maximum MRR and minimum taper angle are found at 12A/20μs/6s and 12A/30μs/4s respectively.

These experimental studies have been done for some particular levels of parameters without considering interactive effects. As well as, it is not sufficient to know the effect of parameters at any intermediate levels of various process parameters. Therefore, it is further needed to establish empirical relationships between significant parameters and machining criteria, which can help to analyse the interactive effect of various process parameters and find out the optimal settings at any intermediate levels of various process parameters during drilling operation on NiTinol utilising` EDM process.

5.3 INVESTIGATION BASED ON RESPONSE SURFACE METHODOLOGY (RSM)

From the previous investigation on NiTinol based on Taguchi method, it is clear that different machining criteria *e.g.* material removal rate and diametral overcut are influenced by process parameters such as polarity, peak current and pulse on-time during an EDM operation on NiTinol. But that are not adequate to analyse and also to demonstrate the co-relationship

between the effect of above process parameters and different machining criteria in the machining applications without considering interactive effects at the any level of parameters. Establishing the mathematical connection between the process parameters and the requirements for achieving ideal machining conditions is also critically important. Analysing how process variables affect the rate of material removal and diametral overcut during hole drilling operations on NiTinol is also essential. With these considerations in mind, it has been planned to develop the mathematical relationships between predominant EDM process parameters and different machining criteria such as material removal rate (MRR), radial overcut (OC) using Response surface Methodology (RSM).

Response Surface Methodology (RSM) is a set of statistical and mathematical methods that are helpful for modelling and analysing problems where the goal is to optimise a response of interest that is influenced by multiple variables.

RSM was used to create the mathematical relationship between the response, Yu, and the different machining parameter components while keeping in mind the current study aims. Parametric impacts on the different response criteria are determined using the general second order polynomial response surface mathematical model, which is shown below.

$$Y_u = B_0 + B_1X_1 + B_2X_2 + B_3X_3 + B_{11}X_1^2 + B_{22}X_2^2 + B_{33}X_3^2 + B_{12}X_1X_2 + B_{13}X_1X_3 + B_{23}X_2X_3 + \varepsilon \quad (5.9)$$

Where, Y_u = the corresponding response e.g. Material Removal Rate (MRR), Radial Overcut (OC) of the EDM process.

X_1= Ip = Peak current (A).

X_2= T_{on} = On-Time (μs).

X_{iu} = Coded values of the i^{th} machining parameters for u^{th} experiment.

n = numbers of machining parameters.

B_i, B_{ii}, B_{ij}, = second order regression coefficients.

The second, third and fourth term under the summation sign of the polynomial equation (Eq. 5.9) attributes to linear effects, whereas the fifth, sixth and seventh term of the above equation corresponds to the higher order effects, eighth, ninth and tenth terms includes the interactive effects of the process parameters. In this response surface methodology, each X-variable can take different coded values by coding each X-scale in a manner such that the upper level of 'X' is taken as +1.682 and lower level as -1.682 for designing the experiment and the observations in an optimized way.

The relationship between the coded and theoretical scale for different X- variables can be expressed as follows:

$$X_i = \frac{\text{(Chosen parametric values - Central rank value of the parameters)}}{\text{Incremental parametric value}} \quad (5.10)$$

The original values of the process parameters at various levels in this set of investigation are shown in the Table 5.10. In the present set of analysis, the Peak current Ip (X_1), the Pulse on duration T_{on} (X_2) and Gap Voltage SV, (X_3) are taken as controlling variables and their effects on MRR and Overcut are examined through a series of experiments. Although polarity has great impact on machining criteria machining of NiTinol it is no considered for development of mathematical relationship since it has only level, no intermediate levels. Instead the servo voltage is considered since it has predominant effect influence on machining criteria, which has been observed during machining of Alumina by EDM process.

From the Eq.5.10, the controlling parameters can be expressed as follows:

$$X_1 = \frac{\text{(Peak current -8)}}{1.19}$$

$$X_2 = \frac{\text{(Pulse on duration – 20)}}{11.89}$$

$$X_3 = \frac{\text{(Gap Voltage – 50)}}{11.89}$$

Where, X_1, X_2 and X_3 are coded values of I_p, T_{on} and SV respectively.

A well-designed experimental plan can substantially reduce the number of experiments. For determining the equation of the surface, several experimental designs have been developed with an attempt to formulate the mathematical relations using the smallest number of experiments possible. But the most preferred closes of surface design are the orthogonal first order design and the central composite second order rotatable design. The experimental plan for studying the relationship between the controlling parameters i.e. Peak current, Pulse-on duration and Gap voltage (SV) in EDM is based on the second order rotatable central composite design (CCD), which has been exhibited in the Fig. 5.8. Also, the components of central composite second order rotatable design are listed in Table 5.8.

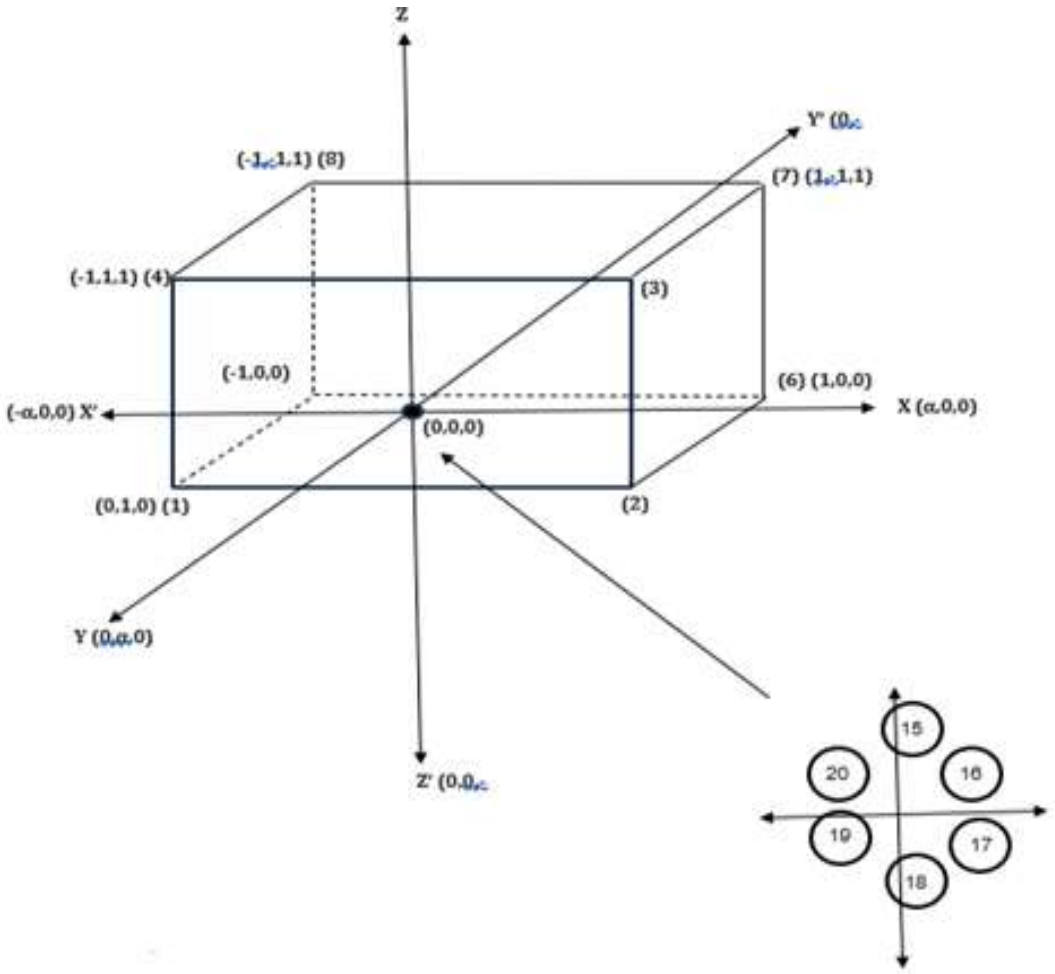

Fig.5.8 Central composite rotatable design plan for three factors

Table 5.10 Distribution of Experiment runs based on CCD

Nos. of X- variables	Total no. of observations (N)	No. of points in			Value of α
		Factorial 2^k	Star	Centre	
3	20	8	6	6	1.682

The actual and coded values of the process parameters at various levels in this set of investigation are listed in the Table 5.11.

Table 5.11 Actual value of different process parameters with level codes

	Actual value at different coded values				
Level	1	2	3	4	5
Coded Value	-1.682	-1	0	+1	+1.682
Peak Current (Ip), (A)	5	6	8	9	10
Pule-on duration (T_{on}), (μs)	5	10	20	30	40
Servo Voltage (SV), (V)	30	40	50	60	70

Each experiment's machining criteria—material removal rate (MRR) and radial overcut (OC)—have been noted, and Table 5.12 displays the outcomes of a series of tests for different sets of parametric combinations as intended. Following the determination of the observed response value, the values of the various regression coefficients of the second order polynomial mathematical Eq. 5.9 were calculated, and mathematical models based on the response surface methodology (RSM) were created for each response.

Table 5.12 Experimental Parametric Combinations

		Coded Value			Uncoded/Actual Value		
	Expt. No.	X_1	X_2	X_3	X_1	X_2	X_3
CUBIC POINTS	1	1	1	1	9	30	60
	2	1	1	-1	9	30	40
	3	-1	1	1	6	30	60
	4	-1	1	-1	6	30	40
	5	1	-1	1	9	10	60
	6	1	-1	-1	9	10	40
	7	-1	-1	1	6	10	60
	8	-1	-1	-1	6	10	40
STAR / FACE POINTS	9	-1.682	0	0	5	20	50
	10	0	-1.682	0	8	30	50
	11	0	0	-1.682	8	20	30
	12	1.682	0	0	10	20	50
	13	0	1.682	0	8	40	50
	14	0	0	1.682	8	20	70
CENTRE POINTS	15	0	0	0	8	20	50
	16	0	0	0	8	20	50
	17	0	0	0	8	20	50
	18	0	0	0	8	20	50
	19	0	0	0	8	20	50
	20	0	0	0	8	20	50

To determine whether the established mathematical models are enough for establishing the mathematical relationship between the answers and the machining parameters of the EDM process, the analysis of variance (ANOVA) is performed. A first order (linear) equation, the additional contribution from second order (quadric) terms, a lack of fit component that measures the deviation of the responses from the fitted surface, and, finally, an estimation of the experimental errors, which is derived from the central points of the designed experimental plan, are the reasons why the analysis of variance (ANOVA) test module is designed to separate the sum of squares of the responses into the contribution.

So, the mathematical formulation of ANOVA to test the adequacy of the model is obtained from first order, second order terms and lack of fit. In the ANOVA, the sum of responses (SS) and degree of freedom for different source of variation are expressed as follows:

(i) SS for the first order terms = $\sum_{U=1}^{k} b(iy)$ (5.12)

(ii) Degree of freedom for the first order terms = K

(iii) SS for second order terms = $b_0(o_y) + \sum_{U=1}^{k} b_{ii}(iiy) - G^2/N$ (5.13)

(iv) Degree of freedom for second order terms = k(k+1)/2 (5.14)

(v) SS for lack of fit is evaluated by subtraction of the value predicted by the model from the actual experimental value obtained.

(vi) Degree of freedom for lack of fit = n_2- k(k+3)/2 (5.15)

(vi) SS for Experimental Error = $\sum (Y_iu - \bar{Y}_1)^2$ (5.16)

(vii) Degree of freedom for lack of fit = (n_1-1) (5.17)

(ix) SS for Total = $\sum (Y_u^2) - G^2 / N$ (5.18)

(x) Degree of freedom for Total = (n_1+ n_2 -1) (5.19)

Where,

G, represents Grand Total.

N, represents total number of points

n_1, represents the number of central points

Y_u, is is the central points with mean $\bar{Y}$.

K, is the number of factors

n_2, represents number of non-central points.

By dividing their sum of squares by their corresponding degree of freedom (DOF), the ANOVA calculates the mean sum of squares for the first order terms, second order terms, lack of fit, and experimental error. The mean sum of the squares of lack fit (MSL) divided by the mean sum of experimental error (MSE) yields the F-ratio value, which can be written as follows:

$$F-\text{ratio}=\frac{\text{Mean sum of the squares of the Lack of Fit}}{\text{Mean sum of the Experimental Error}} \tag{5.20}$$

The determined F-ratio is contrasted with the F-ratio standard value. The test will support the suitability of the produced mathematical second order model at the confidence level for the selected parametric consideration and other related assumptions if the computed F-ratio is less than the corresponding standard value of a certain confidence level.

5.3.2. Experimental Procedure and Performances Characteristics

Procedural steps are necessary to follow, for conducting the planned set of experiments efficiently. The detailed steps are listed below:

(i) To prepare the tool of desired dimension by turning for EDM operation.

(ii) To clean the workpiece properly with phosphoric acid to remove dirt and grease.

(iii) To mount the tool in the tool holder of EDM machine.

(iv) To place the workpiece on the work holding platform.

(v) To switch on the power supply and then the pump for dielectric.

(vi) To adjust the flow control knobs to keep the rate of inlet flow and outlet flow of dielectric at constant level.

(vii) To keep the flushing pressure of the dielectric at the desired value by adjusting the knob.

(viii) To set the values for peak current, pulse-on duration and gap voltage at desired levels as planned by design of experimentation with other parameters remaining at constant values.

(ix) To set the value of depth of the through hole to be drilled.

(x) To note the initial reading of the time counter. To switch on the sparking after auto positioning the tool.

(xi) At the end of the machining operation, to retrieve the tool to its original position.

(xii) To note the final reading of the time counter to calculate the machining time required in EDM drilling of the through hole and switch off the power supply.

(xiii) To close the inlet flow knob and to drain out the dielectric from the tank.

(xiv) To remove the workpiece from the fixture, clean it with cotton and dry it before further processing.

(xv) The drilled hole was then examined through an Olympus Leica measuring microscope at the magnification of 5x to observe and measure the overall diameter of hole to estimate radial overcut was measured by it.

(xvi) The material volume is calculated (volume of material removed) to obtain material removal rate (mm^3/min) as discussed in the previous section.

5.3.3. Experimental Results and Discussions

5.3.2.1 Experimental Results

The responses of electro-discharge machining (EDM) process are material removal rate (MRR) and radial overcut (OC) during drilling of NiTinol. Peak current (Ip), Pulse on-time (T_{on}) and Gap Voltage (SV) are considered as process parameters of electro-discharge Machining (EDM) process on NiTinol work samples using copper tools of diameter 2 mm. The experimentally observed values of all the responses have been shown in the Table 5.12.

Table 5.13 Different controlling parameter combinations and test results

Expt. No.	Original values of machining parameters			Output Parameters	
	I_p (A)	T_{on} (µs)	SV (V)	Material Removal rate (MRR), (mm^3/min)	Radial Overcut (OC) (mm)
1	6	10	40	0.05707	0.20625
2	9	10	40	0.128163	0.1995
3	6	30	40	0.131664	0.08725
4	9	30	40	0.176283	0.15775
5	6	10	60	0.043995	0.129
6	9	10	60	0.108968	0.154
7	6	30	60	0.130354	0.0375
8	9	30	60	0.124779	0.0885
9	5	20	50	0.152131	0.016
10	10	20	50	0.391762	0.174

11	8	5	50	0.051441	0.131
12	8	40	50	0.129084	0.2125
13	8	20	30	0.119748	0.18575
14	8	20	70	0.093501	0.003
15	8	20	50	0.154599	0.154
16	8	20	50	0.129891	0.14925
17	8	20	50	0.309591	0.1905
18	8	20	50	0.331507	0.1355
19	8	20	50	0.167951	0.11
20	8	20	50	0.441945	0.199

5.3.2.2. Analysis on the Effect of Process Parameters for Different Machining Performances

5.3.2.2.1 Effect of process parameters on MRR

Fig 5.9 shows the influences of peak current on MRR for different pulse on-time. MRR increases with the increase of peak current. MRR decreases from 0.2 to 0.1 mm^3/min with increase in pulse on-time from 30 to 40 μs. This is due to the reason that with increase in peak current and pulse on time, current density in the discharge gap increases causing increasing sparking thereby increasing material removal rate. After a particular level of pulse on-time, abnormal sparking on debris particles causes decreasing MRR.

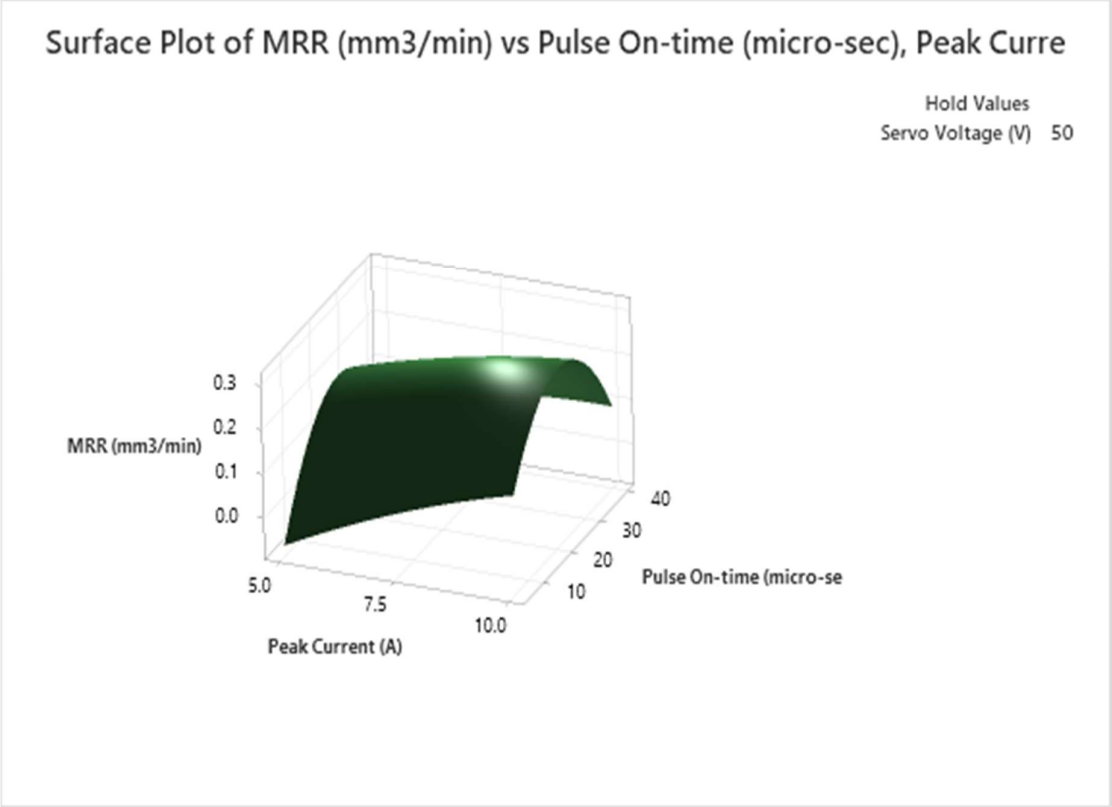

Fig.5.9 Effects of peak current and pulse on-time on MRR

Fig 5.10 shows the effects of pulse on-time and servo voltage on MRR for fixed value of peak current i.e. 7.5 A. MRR increases up to 0.2 mm^3/min with the increase of pulse on-time from 10 to 30 A. With increase in servo voltage from 30 to 45V MRR increases up to a certain level (0.2 mm^3/min) and then decreases when servo voltage increases from 45 to 75V. MRR decreases because of secondary sparking of accumulated debris particles in the machining gap. Original removal of material from the parent workpiece surface is very low due to a disordered alignment of debris particles.

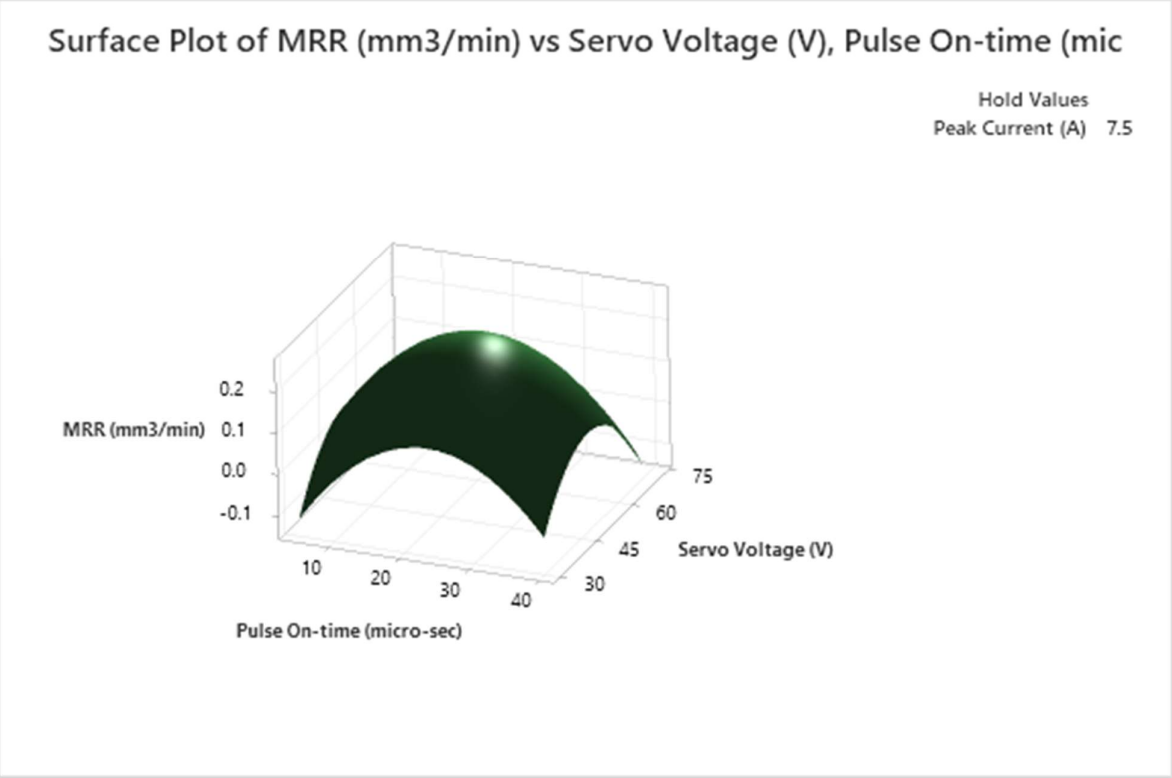

Fig.5.10 Effects of pulse on-time and Servo Voltage on MRR

5.3.2.2.2 Effects of process parameters on Overcut

Overcut is a significant performance characteristic, which determines the dimensional accuracy of the machined hole during EDMing of NiTiNOL and is referred to as hole enlargement or clearance, indicates the difference between the diameter of the EDM-drilled hole and that of the electrode. **Fig 5.11** shows the effect of peak current on overcut for different Pulse on-time. The variation of overcut with peak current increases from 5 to 7.5A, with increase in pulse on-time from 0 to 20μs up to a certain level of 0.15 mm and then increases skewedly, when peak current increases from 7.5 to 10 A and pulse on-time increases from 20 to 40 V. With increase in peak current, current density in the discharge zone increases causing high melting temperature, which is responsible for erosion of materials from the periphery of workpiece surface increasing the diameter of holes on NiTiNOL.

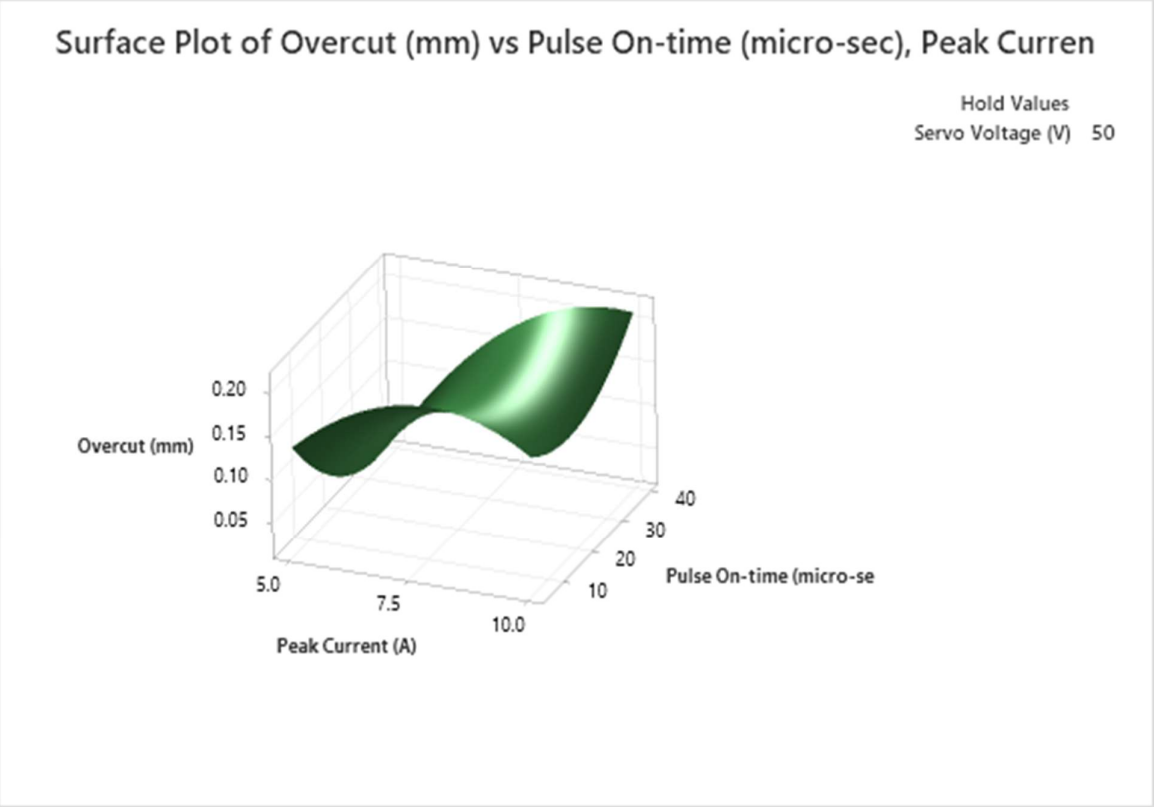

Fig. 5.11 Effects of peak current and pulse on-time on OC

Fig 5.12 shows the effect of pulse on-time on overcut (OC) for different servo voltage. OC decreases from 0.25 to 0.15 mm when the pulse on-time increases from 0 to 20 μs. Overcut increase up to 0.25 mm, when pulse on-time increases from 20 to 40 μs since all debris particles get re-melted and vaporized, material removal takes place from the parent material. With increase in servo voltage OC increases for all pulse on-time since the current density in the discharge gap increases causing increasing sparking thereby increasing OC. This leads to the formation of more free electrons and positive ions not only from the tip of tool-electrode but also from its side-wall. As this ionization cycle continues, the density of charged particles rises, eventually forming a high-concentrated plasma channel in the gap between the tool and workpiece. This plasma is low in electrical resistance. Hence, more electrons and ions developed at the side-wall of the tool-electrode strike the surfaces of the workpiece with high-velocity and their kinetic energy is transformed into intense, localized heat causing an increase in hole size.

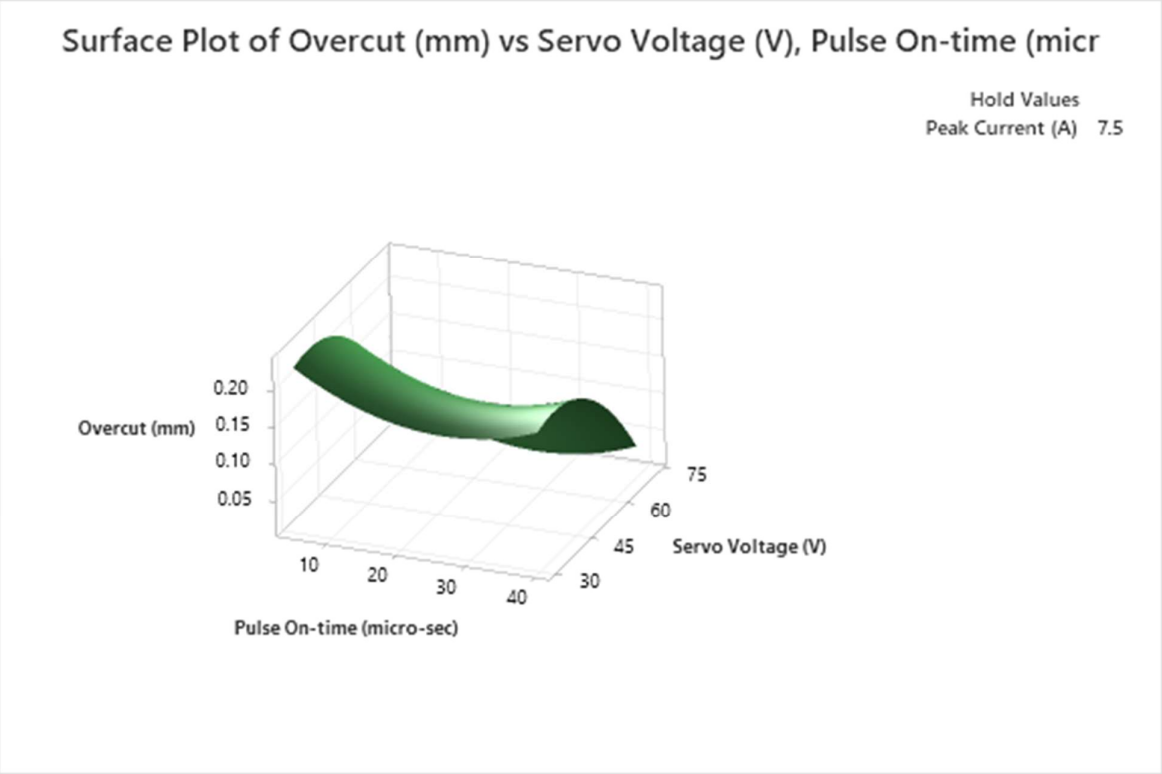

Fig. 5.12 Effects of pulse on-time and servo voltage on OC

5.3.2.3 Development of Mathematical Models for Different Machining Performances

Once the observed response values are known, the values of the various regression coefficients of the second order polynomial mathematical equation, i.e., Eq. 5.9, are assessed. Then, using test results of various responses gathered from the full set of experiments, mathematical models based on the response surface methodology (RSM) are created.

$B_0 = 0.2(oy) - 0.1 \sum (iiy)$ (5.21)

$B_i = 0.125(iy)$ (5.22)

$B_{ii} = 0.125(iiy) + 0.01875 \sum (iiy) - 0.1(oy)$ (5.23)

$B_{ij} = 0.25\ (ijy$ (5.24)

where,

(oy) = the summation of the response value

$$= \sum_{U=1}^{N} Y_u$$

(iy) = the effects of x_i^{th} variable on the response

$$= \sum_{U=1}^{N} Y_u$$

= summation of products of i^{th} column (Xiu) with response, Yu

(iiy) = the effect of higher order terms on the response

$$= \sum_{U=1}^{N} x^2_{iu} Y_u$$

= sum of products of the square of i^{th} column (x^2_{iu}) with response, Yu

(ijy) = the effect of x_i^{th} and x_j^{th} variable on the response

$$= \sum_{U=1}^{N} (x_{iu} * x_{ju})\, Y_u$$

= Sum of the product of the i^{th} column (x_{iu}), j^{th} column (x_{ju}) and the response Yu

$\sum$ (iiy) = sum of effect of higher order terms on response

$$= \sum_{U=1}^{N} \{\sum_{U=1}^{N} x^2_{iu} Y_u\}$$

= Sum of sum of products of the square of i^{th} column (x^2_{iu}) and response, Yu

A computer program called MINITAB is used to determine the values of the various coefficients of Eq. 5.9 based on the MRR and overcut test results from the planned tests, which are displayed in Table 5.12. The following are the mathematical correlations between the machining parameters under consideration and the MRR and OC phenomena:

$$Y_u\,(MRR) = 0.257093 + 0.0655X_1 + 0.015X_2 - 0.018481X_3 - 0.0185X_1^2 - 0.194X_2^2 - 0.171X_3^2 - 0.0354X_1X_2 - 0.0235X_1X_3 - 0.009X_2X_3 \quad (5.25)$$

$$Y_u\,(OC) = 0.148038 + 0.054861X_1 - 0.016127X_2 - 0.075672X_3 + 0.053630X_1^2 + 0.041060X_2^2 - 0.055693X_3^2 + 0.037643X_1X_2 + 0.005104X_1X_3 + 0.001641X_2X_3 \quad (5.26)$$

These mathematical models have been obtained to reflect the independent, quadratic and interactive effects of the various machining parameters on MRR and OC in EDM process.

5.3.2.3.1 Analysis of Variance (ANOVA) test of developed models

A computer program called MINITAB has been used to verify the adequacy of the generated mathematical model for Material Removal Rate (MRR) based on the mathematical formulation of the analysis of variance test module, which is provided by Eqn. 5.25. Table 5.14 is a list of the outcomes thus far.

From the analysis of variance (ANOVA), the F-ratio test procedure is applied to justify the goodness of fit of the developed mathematical. Since the value of F-ratio corresponding to lack of fit i.e. 0.29, obtained by using MINITAB software, is less than standard value of F-ratio for MRR i.e. 1.51 (corresponding to 75% confidence level) the developed model is adequate to 75% confidence level to represent the relationship between MRR and the considered machining parameters of the EDM process.

Table 5.14: ANOVA test results for MRR

Source	DF	Adj SS	Adj MS	F-Value	P-Value
Model	9	0.134976	0.014997	1.51	0.264
Linear	3	0.02128	0.007093	0.72	0.565
Peak Current (A)	1	0.019059	0.019059	1.92	0.196
Pulse On-time (µs)	1	0.001006	0.001006	0.10	0.757
Servo Voltage (V)	1	0.001214	0.001214	0.12	0.734
Square	3	0.100433	0.033478	3.37	0.063
Peak Current (A)*Peak Current (A)	1	0.000478	0.000478	0.05	0.831
Pulse On-time (µs) *Pulse On-time (µs)	1	0.068071	0.068071	6.86	0.026
Servo Voltage (V)*Servo Voltage (V)	1	0.047156	0.047156	4.75	0.054
2-Way Interaction	3	0.001626	0.000542	0.05	0.982
Peak Current (A)*Pulse On-time (µs)	1	0.001177	0.001177	0.12	0.738
Peak Current (A)*Servo Voltage (V)	1	0.000396	0.000396	0.04	0.846
Pulse On-time (µs) *Servo Voltage (V)	1	0.000053	0.000053	0.01	0.943
Lack-of-Fit	5	0.022116	0.004423	0.29	0.902
Pure Error	5	0.077087	0.015417		
Total	19	0.234179			

The adequacy of the mathematical model developed for overcut, i.e. Eq. 5.26, a computer software MINITAB has been used and the results thus obtained have been listed in Table.5.15. In ANOVA, the F-ratio test ratio is applied to justify the adequacy of the developed mathematical model. The developed model is adequate to 97.5% confidence level to represent the relationship between OC and the considered machining parameters of the EDM process as the value of F-ratio corresponding to lack of fit i.e. 2.71 obtained by using MINITAB software, is less than the standard value of F-ratio i.e. 2.84 (corresponding to 97.5 % confidence level).

Table 5.15: ANOVA test results for OC

Source	DF	Adj SS	Adj MS	F-Value	P-Value
Model	9	0.052572	0.005841	2.71	0.068
Linear	3	0.034896	0.011632	5.39	0.018
Peak Current (A)	1	0.013371	0.013371	6.2	0.032
Pulse On-time (micro-sec)	1	0.001166	0.001166	0.54	0.479
Servo Voltage (V)	1	0.02036	0.02036	9.44	0.012
Square	3	0.014396	0.004799	2.22	0.148
Peak Current (A)*Peak Current (A)	1	0.005264	0.005264	2.44	0.149
Pulse On-time (μs)*Pulse On-time (μs)	1	0.003049	0.003049	1.41	0.262
Servo Voltage (V)*Servo Voltage (V)	1	0.005012	0.005012	2.32	0.158
2-Way Interaction	3	0.001353	0.000451	0.21	0.888
Peak Current (A)*Pulse On-time (μs)	1	0.001333	0.001333	0.62	0.45
Peak Current (A)*Servo Voltage (V)	1	0.000019	0.000019	0.01	0.928
Lack-of-Fit	5	0.015953	0.003191	2.84	0.139
Pure Error	5	0.005624	0.001125		
Total	19	0.074149			

5.3.2.4 Determination of Optimal Parametric Combination

The Steepest Ascent optimisation approach of RSM allows the experimental region to be moved to a different set of machining parameter levels based on the central composite second order rotatable design plan. In this case, the machining parameters are selected to produce the best possible results. Along the path of steepest accent, or in the direction of the replies' optimal values, the Steepest Ascent optimisation approach is applied successively. Usually, the path of

Steepest Ascent is the line through the centre of region of interest and normal to the fitted response surface.

The optimal machining parametric combinations of EDM process to maximise material removal rate and minimise radial overcut can be determined with the help of response surface methodology. Here, both the single-objective and multi-objective optimum conditions have been determined based on the Eqns. 5.25 and 5.26.

5.3.2.4.1 Determination of single-objective optimal parametric combination

The single-objective optimal parametric combination has been performed for maximised MRR and minimised OC based on the developed models i.e. Eqs. 5.25 and 5.26 respectively using MINITAB software. The parametric combinations thus obtained are shown in the Fig. 5.13 and 5.14. The optical images of holes machined under the optimal parametric combinations for maximum MRR and minimum OC are also exhibited in Fig. 5.15 (a) and 5.15(b) respectively. MRR is recorded experimentally as 0.3078 mm^3/min under the optimal parametric settings, *i.e.* peak current 10A, pulse on-time 22 µs and servo voltage of 45V to attain the maximum MRR. OC is recorded experimentally as 1.9 µm at the optimal parametric settings of peak current 6A, pulse on-time 30 µs and servo voltage of 65V to achieving minimal radial overcut.

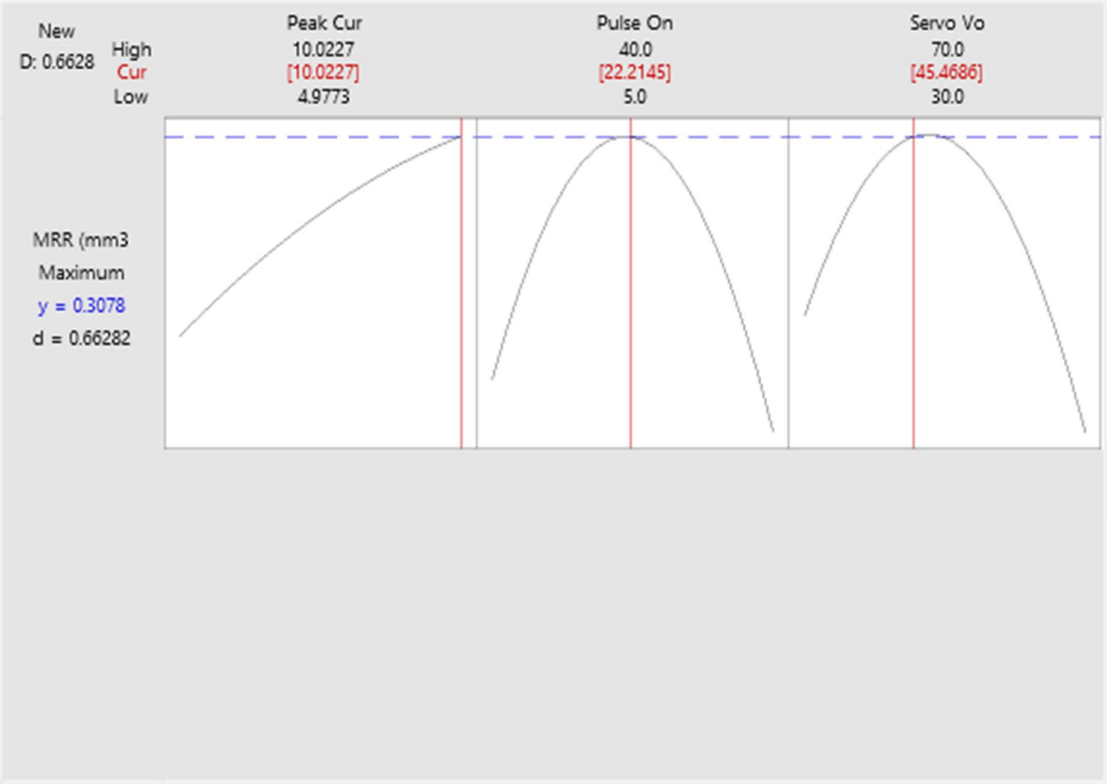

Fig. 5.13 Optimal parametric combination for maximized MRR

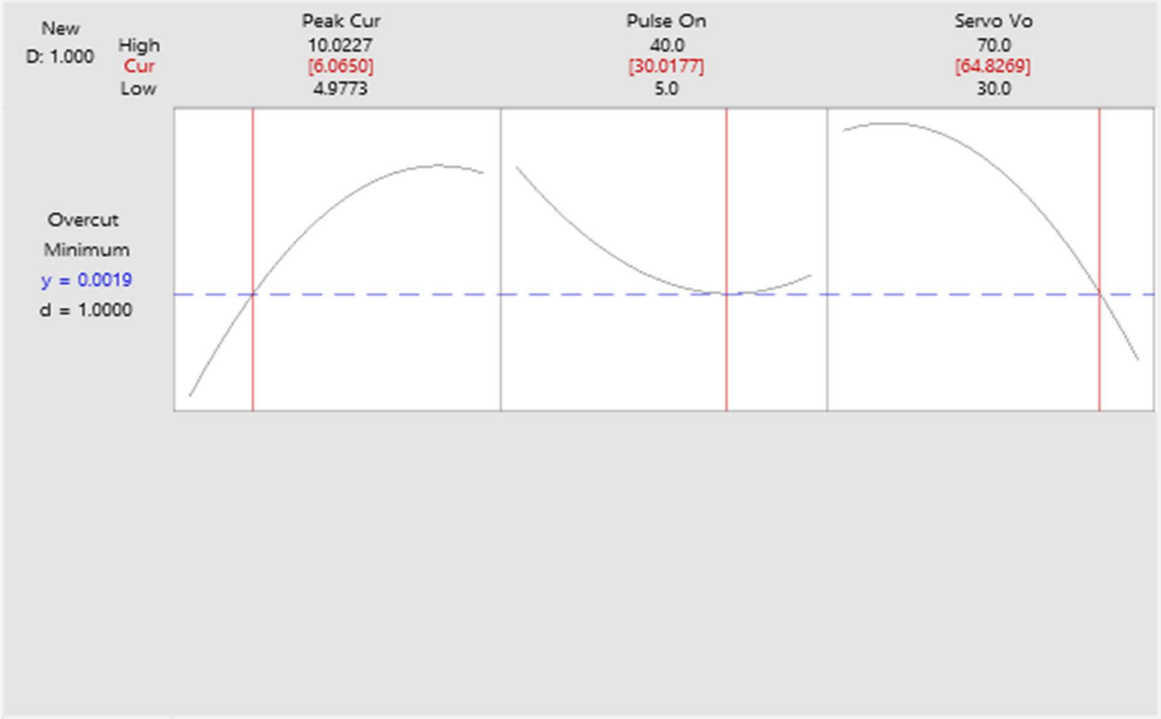

Fig. 5.14 Optimal parametric combination for minimisd OC

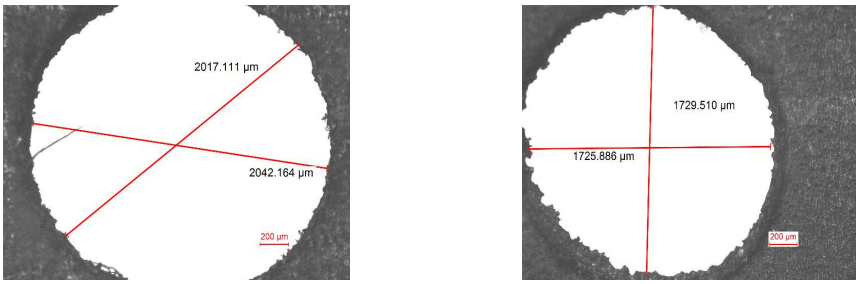

(a) at 10A/22µs/45V for maximized MRR **(b) at 6A/30µs/65V for maximized OC**

Fig. 5.15: Holes machined on NiTinol at optimal parametric combinations

5.3.2.4.2 Determination of multi-objective optimal parametric combination

Multi-objective optimisation has been performed in order to obtain maximum material removal rate and minimum radial overcut. The condition for maximum MRR and minimum OC has been found out with help of MINITAB software, which shows that at 4.98A of peak current, 25.86 µs and 53.83 V of servo voltage the above goal can be obtained. The Fig. 5.16 presents the optimum condition.

Further, a verification experiment has been conducted for multi-objective optimal condition *i.e.* at 4.98A of peak current, 25.88 µs and 53.83 V of. Fig 5.17 exhibits the hole at the above multi-objective optimal condition. MRR is measured as 0.1715 mm^3/min whereas OC is

measured as 11.7 µm. Fig. 5.18 exhibits the optical images of tool electrode at optimal parametric combination. Therefore, the performance characteristics of electro-discharge machining for drilling on NiTinol cab be analysed through the developed models and the multi-objective optimal results will help the manufacturers to explore optimal parametric setting.

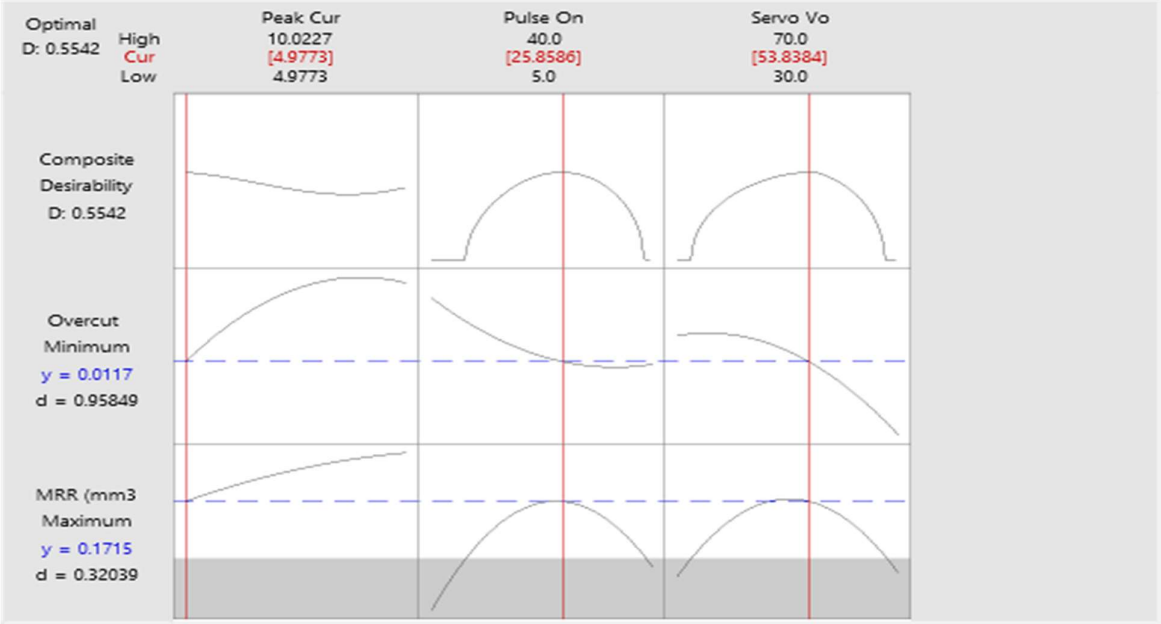

Fig. 5.16 Optimal parametric combination for maximized MRR and minimized OC

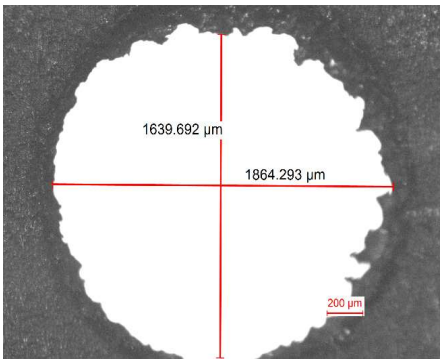

Fig. 5.17 Optical image of hole at 5A/25µs/55V

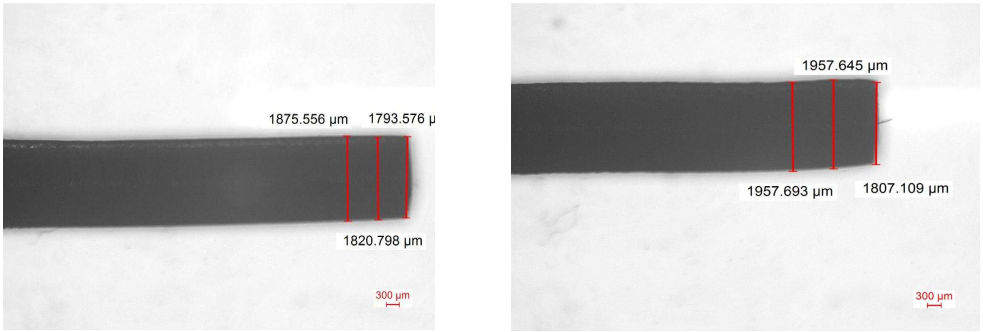

Fig. 5.18 Optical image of tool electrode at 5A/25µs/55V

6. GENERAL CONCLUSIONS AND FUTURE SCOPE

From the experimental test results, analysis and effects of various process parameters on machining characteristics, outcomes have been summarized for EDMing of advanced engineering materials such as ceramics and NiTinol. However, within the limitation of time and resources, the following conclusions may be drawn as below:

(i) EDM process can be used for cutting as well as drilling advanced engineering materials such as electrically non-conducting materials e.g. Alumina and shape memory alloy e.g. NiTinol.

(ii) As far as material of assisted electrode is concerned, copper is found best suited for EDM drilling of Al_2O_3. In comparison to cylindrical tool, drill bit is appropriate for machining of Al_2O_3 because of better flushing as well as removal of the machined byproducts through the flute of drill bit. EDM oil is best suited for machining of Al_2O_3 due to it‘s ability to dissociate into hydro-carbons, which helps in formation of pyrolytic carbon layer for carrying out the further machining.

(iii) Peak current (Ip), on time (Ton) and flushing pressure are the most influencing parameters on the performance characteristics e.g. material removal rate (MRR), tool wear rate (TWR) and overcut (OC). From the experimentation, it has been observed that increasing peak current (Ip) decreases MRR and TWR but increases overcut (OC), similarly increasing on time (Ton) decreases MRR and TWR but increases overcut (OC). In case of flushing pressure all the three responses i.e. MRR, TWR and overcut (OC) decreases with increase in flushing pressure value.

(iv) In straight polarity both MRR and taper angle are found more compared to reverse polarity during EDMing of NiTinol. Peak current increases MRR because it produces more intense sparks that erode the material faster. MRR increase with pulse on-time and sparking time whereas peak current and sparking time increase taper angle.

(v) According to the ANOVA test of Taguchi method polarity and pulse on-time are significantly most influential process parameters during drilling on NiTinol by EDM process.

(vi) MRR increases with the increase of peak current but decreases with increase in pulse on-time from 30 to 40 μs due to abnormal sparking on debris particles during machining of NiTinol by EDM process based on response surface methodology

(RSM). With increase in servo voltage from 30 to 45V MRR increases up to a certain level (0.2 mm^3/min) and then decreases when servo voltage increases from 45 to 75V.

(vii) After analyzing thoroughly various graphs as plotted for overcut, it is evident that overcut increases with corresponding rise in peak current while other parameters remaining fixed at constant level. In the lower ranges of pulse on-time overcut goes on increasing while other machining parameters including peak current are maintained at fixed value. With increase in servo voltage OC increases for all pulse on-time and peak current.

(viii) From the acquired test results, it is obvious that peak current and pulse on-time influence significantly MRR and overcut phenomenon while drilling of NiTinol by EDM process based on RSM. The developed models for MRR and OC applying experimental data have been proved to be accurate as well as collaborative at 75% confidence level.

(ix) From the MCDMs results it has been observed that peak current (I_p) of 1 A, on-time (T_{on}) of 3 µs and 5 kg/cm^2 of flushing pressure is the best parametric combination for maximum MRR and minimum OC and TWR when machining of Alumina (Al_2O_3) in EDM process.

(x) The Taguchi method-based experimentation will assist in determining the best machining parametric combinations to meet the maximum fulfilment of the objective requirement of EDM for shape memory alloy part manufacturing practice, in addition to analysing the significance of the various process parameters on the various machining criteria. Based on S/N ratio, maximum MRR and minimum taper angle are found at 12A/20µs/6s and 12A/30µs/4s respectively during machining of NiTinol by EDM process.

(xi) From the single-objective optimization results it is clear that maximized MRR is found at 10 A/ 22 µs/45V and minimized OC is obtained at 6 A/ 30 µs/ 64 V while drilling of NiTinol by EDM process based on RSM.

(xii) Also, according to the multi-objective optimization result, both maximized MRR and minimized OC are found simultaneously at the parametric combination of 5 A peak current, 26 µs pulse on-time and 54 V servo voltage.

The outcomes of the present research work have also been exhibited graphically as follows:

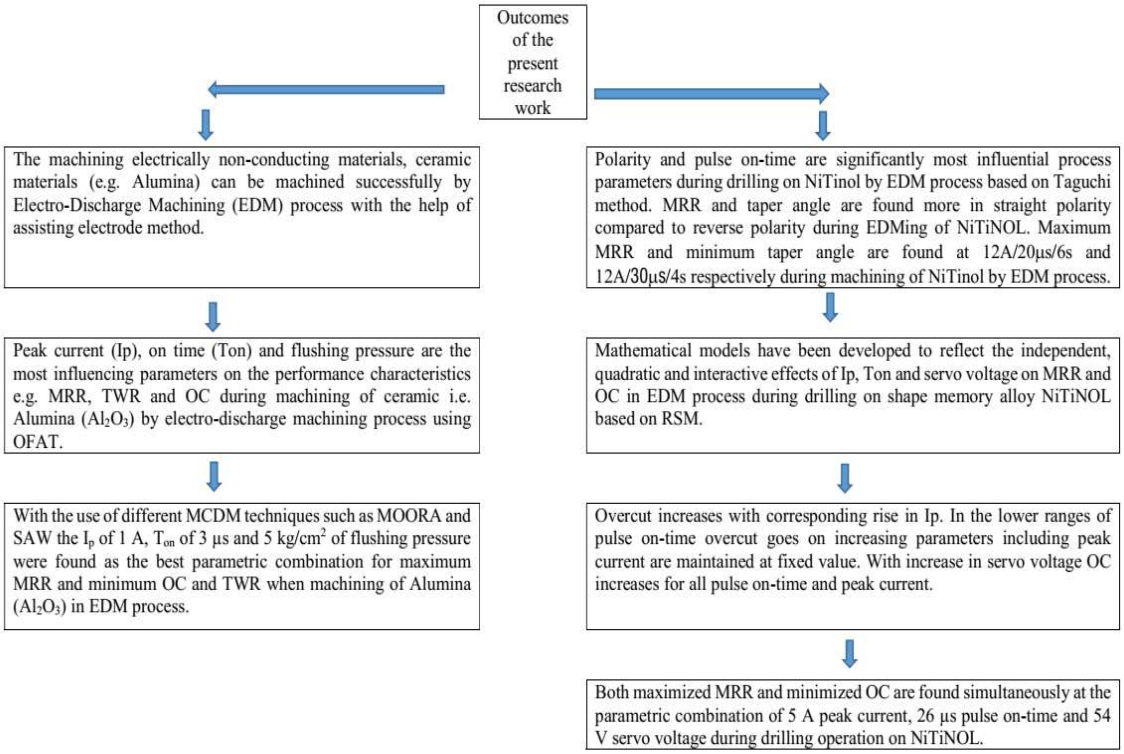

Hence, it is evident that various stages of experimentations based on different design of experiment (DOE) and analyses on the present research work will be quite worthwhile to explain the influence of various process parameters for achieving favourable control over electro-discharge machining of advanced engineering materials e.g. Alumina and NiTinol. The research outcomes will provide valuable guidance to the applied researchers and manufacturing scientists for setting up unique platform for machining advanced engineering materials such as ceramics and shape memory alloy with desired machining rate and accuracy.

However, author believes that few areas still need to be considered for improvement of the electro-discharge machining (EDM) process for machining of advanced engineering materials for wide acceptance in modern manufacturing industries. Therefore, some of the areas of EDM have further scope of research for successful utilisation, which include:

(i) To carry out investigation on the machining of electrically non-conducting ceramic materials by EDM process with the help of electrically conducting surface coating on workpiece sample.

(ii) To increase depth of hole on ceramic materials while machining by EDM process.

(iii) To develop complex profiles, 3D features on advanced engineering materials such ceramics, SMA by EDM process.

(iv) To find out suitable parametric combination with the help of advanced optimisation technique during machining of SMA by EDM process.

REFERENCES

References for EDM of ceramics workpiece

1. Sabur A, Ali M.Y., Maleque M.A., Khan A.A., ―Investigation of material removal characteristics in EDM of nonconductive ZrO2 ceramic‖ , Procedia Engineering (2013), 56, 696 -701
2. Lee T.C. and Lau W.S., ―Some characteristics of electrical discharge machining of conductive ceramics‖ , Materials and manufacturing processes (2007), 64, 635 – 648
3. Mohri N., Fukhuzawa Y., Tani T., Saito N., Furutani K., ―Assisting electrode method for machining insulating ceramics‖ , Annals of the CIRP (1996), 45, 201 – 204
4. Schubert A., Zeidler H., Kuhn R., Oschatzchen M.H. ―Microelectrical discharge machining: A suitable process for machining ceramics‖ , Procedia CIRP (2013), 6, 297 – 302
5. Abbas N.M., Solomon D.G., Bahari M.F., ―A review on current research trends in electric discharge machining (EDM)‖ , International Journal of Machine Tools & Manufacture (2007), 47, 1214 – 1228
6. Hanaoka D., Fukuzawa Y., Ramirez C., Miranzo P., Osendi M. I., Belmonte M., ―Electrical discharge machining of ceramic/ carbon nanostructure composites‖ , Procedia CIRP, (2013), 6, 95–100
7. Petrofes N.F. Gadalla A.M. ―Electric discharge machining of advanced ceramics‖ , American Ceramic Society Bulletin, (1988), 67, 1047 – 1052
8. Mohri N., Fukuzawa Y., Tani T., Sata T., ―Some considerations to machining characteristics of insulating ceramics – towards practical use in industry‖ ,CIRP Annals— Manufacturing Technology, (2002), 51, 161–164
9. Kalajahi M.H., Ahmadi S.R., Bavil Oliaei S.N., ―Experimental and finite element analysis of EDM process and investigation of material removal rate by response surface methodology, International Journal of Advanced Manufacturing Technology, (2013), 69, 687 - 704
10. Mohri N., Fukusima Y., Fukuzawa Y., Tani T., Saito N., ―Layer generation process on work-piece in electrical discharge machining‖ ,CIRP Annals—Manufacturing Technology, (2003), 52, 157–160
11. Vishwakarma U., Dvivedi A., Kumar P., ―FEA modelling of material removal rate in electrical discharge machining of Al6063/SiC composites‖, World Academic Science of Engineering Technology, (2012), 6, 148 – 153

12. Ho K.H. and Newman S.T., ―State of the art electrical discharge machining (EDM)‖ , International Journal of Machine Tools and Manufacture, (2003), 43, 1287 – 1300
13. Lauwers B., Kruth J.P., Brans K., ―Development of Technology and Strategies for the Machining of Ceramic Components by Sinking and Milling EDM‖, Annals of the CIRP, (2007), 56, 225 - 228
14. Schubert A., Zeidler H., Oschatzchen M. H., Schneider J., Hahn M., ―Enhancing micro-EDM using ultrasonic vibration and approaches for machining of nonconducting ceramics‖ , Journal of Mechanical Engineering, (2013), 59, 156–164
15. Fukuzawa Y. Mohri N., Gotoh H., Tani T., ―Three dimensional machining of insulating ceramics materials with electrical discharge machining‖ ,Transactions of Nonferrous Metals Society of China (English Edition), (2009), 19, 150 – 156
16. Pandey A. and Singh, S.―Current research trends in variants of Electrical discharge machining‖, International Journal of Machine Tools and Manufacture, (2010), 2(6), 2172 – 2191
17. Chandramouli S, Bodukuri A.K., Eswaraiah K., Laxman, J. ―Experimental investigation and optimization of EDM process parameters on Alumina metal matrix composites‖ Annals of the CIRP , (2018), 5, 24731 – 24740
18. Rajmohan T., Prabhu R., Subba Rao G. Palanikumar K., ―Optimization of machining parameters in Electrical discharge machining of 304 stainless steel‖, International Journal of Engineering and Technology, (2012), 38, 1030 – 1036
19. Darji S. and Pillai B. ―Estimation of MRR for micro-edm machining of HASTELLOY C 276 using Taguchi method‖, Journal of Materials Processing Technology, (2012), 1, 261 – 267
20. Yadav V., Jain V.K., Dixit P.M., ―Thermal stresses due to electrical discharge machining‖, International Journal of Machine Tools and Manufacture, (2002), 42, 877 – 888
21. Lauwers B., Kruth J. P., Liu W. Eeraerts W., Schacht, B. Bleys P., ―Investigation of material removal mechanisms in EDM of composite ceramic materials‖, Journal of Materials Processing Technology, (2004), 149, 347–352
22. Keskin Y., Kalkaci H.S., Kizil M., ―An experimental study for determination of effects of machining parameters on surface roughness in EDM‖, International Journal of Advance Manufacturing Technology, (2006), 28, 1118– 1121

23. Patel, V. D. Patel C. P., Patel, U. J. ―Analysis of different tool material on MRR and surface roughness of mild steel in EDM‖ , International Journal of Engineering Research and Applications, (2011), 1(3), 394-397
24. Singh, J., Kumar V., ―Investigation on the Material Removal Mechanism and the Thermal Aspects in the Electrical Discharge Machining Process‖, International Journal of Engineering and Technology, (2012), 2, 9 – 16
25. Pachaury V, Tandon P., ―An overview of electric discharge machining of ceramics and ceramic based composites‖ , Journal of Manufacturing Processes, (2017), 25, 369 – 390
26. Pie Jingyu, Zhang Lenan, Du Jianyi, Zhuang Xiaoshun, Zhou Zhaowei, Wu Shunkun, Zhu Yetian, ―A model of tool wear in electrical discharge machining process based on electromagnetic theory‖, International Journal of Machine Tools & Manufacture, (2017), 117, 31-41
27. Pham D.T., Dimov S.S., Bigot S., Ivanov A. Popov K., ―Micro-EDM - recent developments and research issues‖ , Journal of Materials Processing Technology (2004), 149, 50–57
28. Murray J., Zdebski D., Clare A.T., ―Work piece debris deposition on tool electrodes and secondary discharge phenomena in micro-EDM‖ , Journal of Materials Processing Technology (2012), 212, 1537– 1547
29. Trych A., ―Further study of carbon fibers electrodes in micro electrical discharge machining‖ , Procedia CIRP (2013), 6, 309 – 313
30. Urso G. D,, Maccarini G., Ravasio C., ―Process performance of micro-EDM drilling of stainless steel , International Journal of Advance Manufacturing Technology, (2014), 72, 1287–1298
31. Hosel T., Muller C., Reinecke H. ―Spark erosive structuring of electrically nonconductive zirconia with an assisting electrode‖ , CIRP Journal of Manufacturing Science and Technology, 2011, 4 , 357 – 361
32. Chen Y.F. Lin Y.J., Lin Y.C., Chen S.L., Hsu L-R, ―Optimization of electro-discharge machining parameters on ZrO2 ceramic using the Taguchi method‖ , Proc. Instituite of Mechanical Engineers, Journal Engineering Manufacture, Part:B (2012), 224, 195 – 205
33. Chevalier J,, Gremillard,L ―Ceramics for medical applications: A picture for the next 20 years‖ , Journal of the European Ceramic Society, (2009), 29, 1245 – 1255

34. Kucukturka G., Cogun C., ―A new method for machining of electrically nonconductive workpiece using electric discharge machining technique‖, International Journal Machining Science & Technology, (2010), 14, 189 – 207
35. Liu Y.H., Li X.P., Ji R.J., Yu L.L., Zhang H.F., Li Q.Y. ―Effect of technological parameter on the process performance for electric discharge milling of insulating Al2O3 ceramic‖, Journal of Materials Processing Technology, (2008), 208, 245 – 250
36. Ferraris E., Reynaerts D., Lauwers B., ―Micro-EDM process investigation and comparison performance of Al_2O_3 and ZrO_2 based ceramic composites‖, CIRP Annals - Manufacturing Technology, (2011), 60, 235 – 238
37. Mehta S., Rajurkar A., Chauhan J., ―A Review on Current Research Trends in Die-Sinking Electrical Discharge Machining of Conductive Ceramics‖, International Journal of Recent Trends in Engineering, (2009), 1, 100 – 104
38. Lajis M.A., Radzi M.,Amin N, ―The Implementation of Taguchi Method on EDM Process of Tungsten Carbide‖, European Journal of Scientific Research, (2009), 26 , 609 – 617
39. Lee S.H., Li X.P. ―Study of the effect of machining parameters on the machining characteristics in electrical discharge machining of tungsten carbide‖, Journals of Materials Processing technology, (2001), 115, 344 – 358
40. Liu K., Lauwers B., Reynaerts D., ―Crossing barriers in structuring ceramics‖, Microniek, (2010), 50, 28 – 34
41. Yoo H.K., Ko, J.H., Lim K.Y., Kwon W.T., Kim Y.W., ―Micro-electrical discharge machining characteristics of newly developed conductive SiC ceramic‖, Ceramics International, (2015), 41, 3490 – 3496
42. Schubert A., Zeidler H., Oschatzchen M.H., Schneider J., Hahn M., ―Enhancing micro-EDM using ultrasonic vibration and approaches for machining of nonconducting ceramics‖, Journal of Mechanical Engineering, (2013), 59, 156 – 164
43. Mishra, K,, Mukhopadhyay P., Sarkar B. R., Doloi B, Bhattacharyya B., ―Improvement of micro-EDM performances with aid of vibration‖, International Journal of Precision Technology, (2018), 8, 38 – 65
44. Zhou, J. M. , Anderson M., Ståhl J. E., ―Identification of cutting errors in precision hard turning process‖, Journal of Materials. Processing Technology, (2004), 153-154, 746-750
45. Charnes A.,Cooper W. W., Rhodes E., ―Measuring the efficiency of decision-making units, European Journal of Operational Research‖, (1978), 2, 429-444

46. Thompson, R. G.' Singleton Junior F. D., Thrall R. M., Smith B. A., ―Comparative evaluation for locating a high-energy physics lab in Texas‖, Interfaces, 1986, 16, 35-49

References for EDM of NiTiNOL workpiece

1. Kremer D, Lebrun J.L, Hosari B., Moisan A : Effects of Ultrasonic Vibrations on the Performances in EDM; E.N.S.A.M. Paris.
2. Alidoosti A, Ghafari-Nazari A, Moztarzadeh F, Jalali N,, Moztarzadeh S and Mozafari M 2013: Electrical discharge machining characteristics of nickel–titanium shape memory alloy based on full factorial design. Journal of intelligent Material systems and Structures 24: 1546–1556.
3. Chen S L, Hsieh S F, Lin H C, Lin M H and Huang J S 2007: Electrical discharge machining of TiNiCr and TiNiZr ternary shape memory alloys. Materials Science and Engineering: A 445: 486–492.
4. Zinelis S 2007: Surface and elemental alterations of dental alloys induced by electro discharge machining (EDM). Dental Materials 23: 601–607.
5. Velmurugan C, Senthilkumar V, Dinesh S and Arulkirubakaran D 2018: Machining of NiTi-shape memory alloys: A review. Machining Science and Technology 22: 355–401.
6. Manjaiah M, Narendranath S and Basavarajappa S 2014: Review on non-conventional machining of shape memory alloys. Transactions of Nonferrous Metals Society of China 24: 12–21.
7. Majumder H and Maity K 2018 : Prediction and optimization of surface roughness and micro-hardness using grnn and MOORA-fuzzy-a MCDM approach for nitinol in WEDM. Measurement 118: 1–13.
8. Garg M P, Jain A and Bhushan G 2014: Multi-objective optimization of process parameters in wire electric discharge machining of Ti-6-2-4-2 alloy. Arabian Journal for Science and Engineering 39: 1465–1476.
9. Gokler M I˙ and Ozano¨zgu¨ A M 2000: Experimental investigation of effects of cutting parameters on surface roughness in the WEDM process. International Journal of Machine Tools and Manufacture 40: 1831–1848.
10. Zhang Z, Ming W, Huang H, Chen Z, Xu Z and HuangZhang Y G 2015: Optimization of process parameters on surface integrity in wire electrical discharge machining of tungsten tool YG15. The International Journal of Advanced Manufacturing Technology 81: 1303–1317.

tungsten tool YG15. The International Journal of Advanced Manufacturing Technology 81: 1303–1317.

11. Gopal P M 2019 Wire electric discharge machining of silica rich E-waste CRT and BN reinforced hybrid magnesium MMC. Silicon 11: 1429–1440.
12. Goyal A 2017: Investigation of material removal rate and surface roughness during wire electrical discharge machining (WEDM) of Inconel 625 super alloy by cryogenic treated tool electrode. Journal of King Saud University-Science 29: 528–535.
13. Huang H, Zheng H Y and Liu Y 2005: Experimental investigations of the machinability of Ni50.6Ti49.4 alloy. Smart Materials and Structures 14: S297.
14. Mahapatra S S and Patnaik A 2007: Optimization of wire electrical discharge machining (WEDM) process parameters using Taguchi method. International journal of Advanced Manufacturing Technology 34: 911–925.
15. Soni H, Narendranath S and Ramesh M R 2018: Experimental investigation on effects of wire electro discharge machining of Ti50Ni45Co5 shape memory alloys. Silicon 10: 2483–2490.
16. Narendranath S, Manjaiah M, Basavarajappa S and Gaitonde V N 2013: Experimental investigations on performance characteristics in wire electro discharge machining of Ti50Ni42.4Cu7.6 shape memory alloy. Proceedings of the Institution of Mechanical Engineers, Part B: Journal of Engineering Manufacture 227: 1180–1187.
17. Magabe R, Sharma N, Gupta K and Davim J P 2019: Modeling and optimization of Wire-EDM parameters for machining of Ni 55.8 Ti shape memory alloy using hybrid approach of Taguchi and NSGA-II. The International Journal of Advanced Manufacturing Technology 102:1703–1717.
18. Bisaria H and Shandilya P 2018 Experimental studies on electrical discharge wire cutting of Ni-rich NiTi shape memory alloy. Materials and Manufacturing Processes 33.

Ex-Professor
Production Engineering Department
Jadavpur University
Kolkata - 700 032

Professor
Production Engineering Department
Jadavpur University
Kolkata - 700 032